Analyzing pan-Arctic 1982–2006 trends in temperature and bioclimatological indicators (productivity, phenology and vegetation indices) using remote sensing, model and field data

by

Kristina A. Luus

A thesis
presented to the University of Waterloo
in fulfillment of the
thesis requirement for the degree of
Master of Science
in
Geography

Waterloo, Ontario, Canada, 2009

I hereby declare that I am the sole author of this thesis. This is a true copy of the thesis, including any required final revisions, as accepted by my examiners.

I understand that my thesis may be made electronically available to the public.

Abstract

Warming induced changes in Arctic vegetation have to date been studied through observational and experimental field studies, leaving significant uncertainty about the representativeness of selected field sites as well as how these field scale findings scale up to the entire pan-Arctic. The purposes of this thesis were therefore to 1) analyze remotely-sensed/modeled temperature, Normalized Difference Vegetation Indices (NDVI) and plant Net Primary Productivity (NPP) to assess coarse-scale changes (1982–2006) in vegetation; and 2) compare field, remote sensing and model outputs to estimate limitations, challenges and disagreements between data formats. The following data sources were used:

- Advanced Very High Resolution Radiometer Polar Pathfinder Extended (APP-x, temperature & albedo)
- Moderate Resolution Imaging Spectroradiometer (MODIS, Normalized Difference Vegetation Index (NDVI) & Enhanced Vegetation Index (EVI))
- Landsat Enhanced Thematic Mapper (Landsat ETM, NDVI)
- Global Inventory Modeling and Mapping Studies (GIMMS, NDVI)
- Global Productivity Efficiency Model (GloPEM, Net Primary Productivity (NPP))

Over the pan-Arctic (1982-2007), increases in temperature, total annual NPP and maximum annual NDVI were observed. Increases in NDVI and NPP were found to be closely related to increases in temperature according to non-parametric Sen' slope and Mann Kendall tau tests. Variations in phenology were largely non-significant but related to increases in growing season temperature.

Snow melt onset and spring onset correspond closely. MODIS, Landsat and GIMMS NDVI data sets agree well, and MODIS EVI and NDVI are very similar for spring and summer at Fosheim Peninsula. GloPEM NPP and field estimates of NPP are poorly correlated, whereas GIMMS NDVI and GloPEM NPP are well correlated, indicating a need for better calibration of model NPP to field data.

In summary, increases in pan-Arctic biological productivity indicators were observed, and were found to be closely related to recent circumpolar warming. However, these changes appear to be focused in regions from which recent field studies have found significant ecological changes (Alaska), and coarse resolution remote sensing estimates of ecological changes have been less marked in other regions. Discrepancies between results from model, field data and remote sensing, as well as central questions remaining about the impact of increases in productivity on soil-vegetation-atmosphere feedbacks, indicate a clear need for continued research into warming induced changes in pan-Arctic vegetation.

Acknowledgements

This thesis could not have been completed without the assistance, generosity and support of many individuals.

I'd like to thank Dr. Richard Kelly for sharing his insights into theoretical aspects of remote sensing, suggesting interesting directions to take and providing the opportunity to work on this project. I would like to thank Dr. Alexander Brenning for his help with the statistical aspects of this thesis, discussion of results, and final corrections. Finally, I would like to acknowledge Dr. Claude Duguay for his assistance regarding Arctic vegetation, and Dr. John Lin for his support regarding the interpretation of remote sensing and model outputs.

I would like to thank Dr. Robert Jefferies and Emma Horrington for their provision of a great time series of field net primary productivity data, which proved to be crucial to my research project as a whole but would have impossible to collect. I would also like to thank Libo Wang and Chris Derckson for providing Quick Scat snow melt end and onset data as well as assistance in data interpretation. Finally, I would like to thank National Oceanic and Atmospheric Administration for providing APP-x data, Global Land Cover Facility for GloPEM and GIMMS products, and NASA for MODIS and Landsat images.

I would also like to thank Dr. Peter Deadman for his generosity in supervising my Master's progress for the first year, and for his ongoing support in my transition from tropical to arctic research. I am very thankful also to Dr. Lawrence Plug (Dalhousie) for teaching me about remote sensing, and how to use Matlab and LaTeX, and to Patrick Nicholson for helping me learn Unix. Thank you also to Drs. Merrin Macrae, Peter Deadman, Richard Kelly, Alexander Brenning, William Annable, and Keith Hipel for teaching excellent courses.

Friends and family have also been invaluable in helping me have fun and stay focused while working on my thesis. A special thank you goes to fellow geographers Josh King, Ray Cabrera, Ryan Sim, Lisa Hansen, Daniel Dong, Steve Howell, Grant Gunn, Alec Casey, Miranda Lewis, Mike Neilly, Andy Snowdon, Michelle Rutty and Kathy Mulroy. Thank you also to Patrick Nicholson, Sarah Beckerman, Marianne Schelew, Adam Grosberg and Monique Woolnough for their many years of close friendship, and support throughout my Master's. I am also grateful for the financial support of the Ontario Graduate Scholarship Program.

Dedication

Aili Lüüs (1911–2008) and Elisabeth Averil Tremblay (1985–2003)

Contents

List of Tables

List of Figures

Chapter 1

Introduction

Arctic warming is predicted to continue over the next century with simultaneous increases in precipitation (*Christensen et al.*, 2007). To date, ecological changes have been noted at the field scale in the earlier onset of spring snow melt in northern Alaska (*Stone et al.*, 2002) and bud burst in Greenland (*Høye et al.*, 2007). Repeat photography has indicated increasing shrub prevalence in Alaskan tundra (*Sturm et al.*, 2005). Remote sensing has shown northward movement of the Arctic tree line (*Grace et al.*, 2002) and small changes in the greeness and quantity of Arctic vegetation, as indicated by the Normalized Difference Vegetation Index (*Neigh et al.*, 2007). In order to establish whether the Arctic has changed from a carbon sink to source under a warming and wetting climate, it is important to quantify changes in the annual sequestration of carbon by vegetation and to compare this to the rate at which carbon is released from Arctic soils (*Oechel et al.*, 1993; *Wu and Lynch*, 2000; *Thompson et al.*, 2006; *Sitch et al.*, 2007). With rising levels of CO_2, plant stomates can ingest neccessary quantities of CO_2 while remaining less open, which decreases the quantity of plant evapotranspiration, thus increasing the quantity of soil moisture (*Beerling*, 2007). Increases in soil moisture induce higher levels of anaerobic respiration, thus increasing the release of methane (CH_4), a potent

greenhouse gas, from thawing permafrost.

The complexity of the ecological response to climate change, as well as the significant role of Arctic vegetation on global nutrient and atmospheric cycling, mean that there are many positive and negative feedbacks involved in the response of vegetation to climate change [Figure 1.1]. It is therefore vital that recent climate induced changes in Arctic vegetation be accurately quantified and analyzed over the entire pan-Arctic.

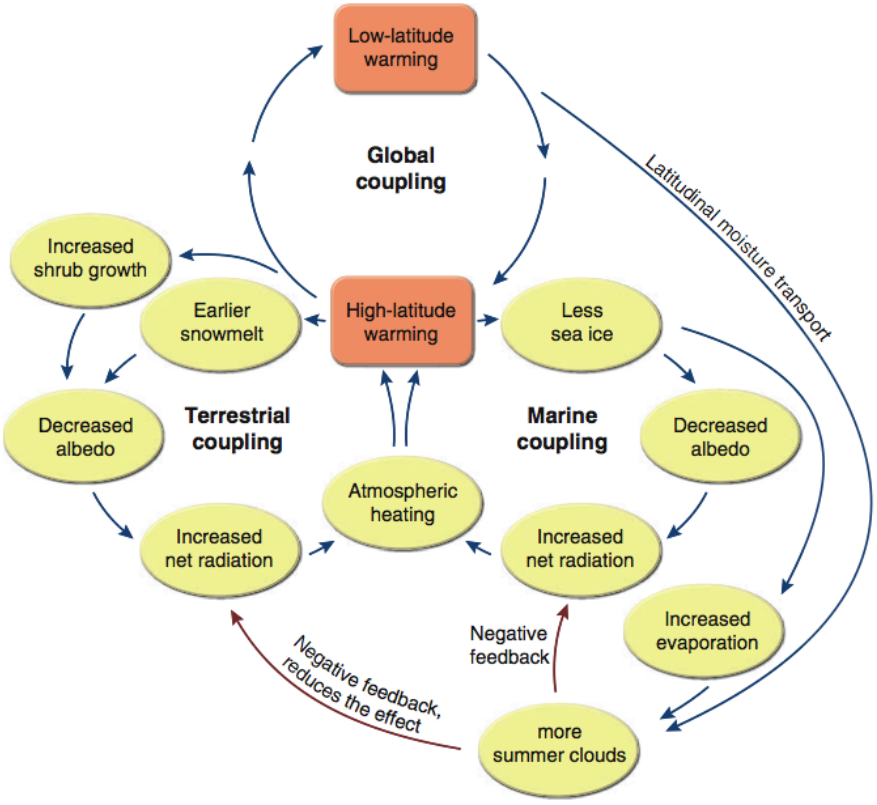

Figure 1.1: Snow, vegetation and temperature feedbacks (*Eamer*, 2009)

The vegetation indicators chosen for this thesis (productivity, phenology, NDVI) are established bioclimatological indicators (*Roerink et al.*, 2003). Each indicator can be assessed using a combination of modeling and remote sensing, but is more commonly assessed in field studies. Productivity refers to the net carbon uptake of vegetation, phenology refers to the seasonal timing of biological processes (specif-

ically, of spring bud-burst and autumn senescence), biomass refers to the total amount of aboveground plant matter and bioclimate subzones refers to standardized characterization of Arctic vegetation according to climate and plant species present.

The scarcity of carbon flux towers and field measurement data in the vast and heterogeneous Arctic have so far prevented the extensive validation of model productivity estimates. Furthermore, the ecophysiological parametrizations of productivity models for Arctic biomes is also problematic (*White et al.*, 2000; *Liu et al.*, 2002; *Thornton*, 2009). Changes in productivity of Arctic vegetation, as well as the errors introduced by different estimation methods, remain poorly understood. Current methods of estimating productivity have indicated little net change, with small seasonal changes attributed to Arctic Oscillations and El Niño/La Niña (*Zhang et al.*, 2007).

Biomass estimation and bioclimate subzone classification have both been conducted using three years of data by the International Association of Vegetation Science (*Walker et al.*, 2005). A recent paper by *Raynolds et al.* (2008) analyzed changes in NDVI and vegetation distributions using the aforementioned classifications according to changes in temperature.

1.1 Aims and objectives

Responses of Arctic vegetation to experimental in-situ warming and nutrient enrichment have been well documented, most notably as part of the International Tundra Experiment (*Henry and Elmendorf*, 2008). Furthermore, recent studies have observed climate-induced shifts in Arctic vegetation (*Snyder*, 2008; *Levesque et al.*, 2008; *Tape et al.*, 2006). Despite these changes, NDVI has been found to decrease slightly in tundra regions by *Snyder* (2008), change slightly across the

Arctic by *Neigh et al.* (2007), and found to increase in tundra regions by *Raynolds et al.* (2008) and *Jia et al.* (2007). The aims of this thesis were therefore to 1) understand how recent changes in pan-Arctic vegetation (1982–2006) bioclimatological indicators (phenology, NDVI and productivity) are reflected in satellite and remote sensing records; 2) analyze the relationship between trends in temperature and trends in the aforementioned indicators; and 3) compare findings from remote sensing, model outputs and field studies.

1.1.1 Objectives

The objectives of this thesis are to:

- Estimate phenology, net primary productivity and normalized difference vegetation index over time (1982-2000) over the pan-Arctic (north of 60N) using remote sensing and model outputs.
- Analyze the aforementioned vegetation indicators to understand the response of the pan-Arctic to recent climate change, potential implications and how results fit with recent findings and debates in literature.
- Statistically assess changes over time in temperature and bioclimatological variables, and whether they are related.
- Conduct comparisons of remote sensing, model and field observations of changes in Arctic vegetation in order to elucidate potential data assimilation and scaling challenges which arise when studying Arctic vegetation.

1.2 Thesis significance

Establishing historical estimates of bioclimatological indicators in Arctic vegetation is of theoretical significance; comparing various sensors with one another and field data is of practical significance.

1.2.1 Practical

Comparing readings from multiple resolutions of NDVI for the Arctic (AVHRR at 8×8km, MODIS at 500×500m and Landsat at 30×30m) is important for shedding light on the scale at which processes can be tracked in these ecosystems. Very high resolution imagery such as IKONOS (1-4×1-4m) has been found to adequately represent ecological changes observed in field studies (*Laidler et al.*, 2008); however, the majority of net primary productivity models occur over much larger spatial resolutions (*Cramer and Field*, 1999). It is therefore important to understand whether coarser resolutions adequately capture field scale processes.

1.2.2 Theoretical

Phenology and productivity are both reliable biophysical indicators of changes occuring in the Arctic and NDVI is an established indicator of climate variability (*Roerink et al.*, 2003). Understanding when and where changes are taking place is important for understanding the underlying system dynamics and establishing remote sensing based estimates to enable further research in this area. Monitoring Northern vegetation is also important because it affects albedo, vegetation-atmosphere gas exchange and permafrost (*Olthof et al.*, 2008). Arctic remote sensing phenological studies have so far been limited to regions of tundra (*Delbart and Picard*, 2007), Eurasia (*Karlsen et al.*, 2006; *Picard et al.*, 2005; *Ebata and Tateishi*,

2001), or North America (*White et al.*, 2008; *Reed*, 2006; *Vierling et al.*, 1997), or have been limited to spring onset studies (*Bunn and Goetz*, 2006). The major theoretical contribution of this thesis is therefore in assessing circumpolar spring and autumn phenology.

Understanding the NPP dynamics of the High Arctic is important both for understanding whether, where, and how Arctic vegetation has changed, and also for understanding both regional and global carbon dynamics (*Hobbie et al.*, 2000). Temperature is main driver of GPP in wetlands, but both precipitation and temperature drive evergreen coniferous forest GPP (*Migliavacca et al.*, 2008). It therefore important that the parameter set used for estimating productivity is geographically appropriate, and that the fit with field data is properly assessed.Since NPP products are calibrated globally using eddy flux covariance measurements, and there are very few eddy flux towers in the Arctic, it is possible that the modeled results of NPP are not entirely accurate.

1.3 Structure of thesis

The following thesis begins with a literature review focusing on the response of Arctic ecosystems to recent climate warming, comparisons of field, remote sensing and model findings, and Arctic-specific research challenges. Methodology follows with a description of study sites, data products used and techniques for data handling and statistical analysis. Results are then presented for 1) changes in temperature, albedo, NPP, and NDVI over time, as well as the response of NPP and NDVI to changes in mean May–September temperature; 2) comparison of data products, and remote sensing vs field data; and 3) pan-Arctic comparison of changes in bioclimatological indicators (NDVI, phenology and NPP) over time and their relation to changes in mean May–September temperature. Discussion focuses on conceptual

linkages between the aforementioned indicators, as well as a critical examination of what is indicated by the multi-faceted perspectives on warming-induced changes in Arctic vegetation provided by various technologies. Conclusions focus on implications of findings and suggestions for future work.

Chapter 2

Literature Review

The purpose of the literature review is to first assess the current state of research regarding Arctic ecosystem responses to a changing climate, and linkages between findings from field, model and remote sensing approaches. Site specific challenges are then described in context. For an in depth review of remote sensing and modeling tools that can be used to estimate the productivity of vegetation, please refer to *Luus and Kelly* (2008). Conclusions focus on pertinent research gaps, and their significance.

2.1 Arctic ecosystem response to climate change

Changes in vegetation are predicted to occur under a warmer and wetter climate in the Arctic (*Christensen et al.*, 2007) due to multiple interactions between temperature, hydrology, soil nutrient levels, vegetative reproduction and rates of predation which are complex and difficult to quantify. Because of the complexity involved, the majority of studies conducted on changes in Arctic vegetation have been conducted at a small scale using field experimentation. Traditional ecological knowledge indicates the following changes in Arctic vegetation: earlier blooming, increase in

prevalence of birch, increased shrubiness, longer shoots and lower berry productivity, increase in tree productivity (supported up by tree ring studies), larch spread to new locations and deepening of the soil active layer which results in softer soil (*Levesque et al.*, 2008). However, these claims are often based on subjective experiences, and are therefore difficult to verify quantitatively especially since they result from field-scale observations which are not necessarily representative of large regions of the Arctic. It is therefore important to establish documented and consistent remote sensing based estimates. Also, even if there is no net change, ecosystem dynamics can be rapidly altered by shifts in the timing of vegetation (*Høye et al.*, 2007). Therefore, the following sections focus on in-situ field scale and remote sensing experiments on changes in Arctic species composition, productivity, phenology, nutrient cycling and carbon cycling.

2.1.1 Species composition/ NDVI

Arctic vegetation is highly heterogeneous (*Stow et al.*, 2004). The main environmental factors determining species prevalence being soil moisture, elevation, soil type and surface temperature regime, depending on the region sampled. Land cover changes are influenced indirectly and broadly by human contact, with few areas of intensive impact (*Stow et al.*, 2004). The majority of the Arctic contains non-vascular plants such as bryophytes and lichens. Non-vascular plants can only outcompete vascular plants in conditions where water table stability and where both nutrient (N and P) levels and temperature are low. Under the aforementioned conditions, lichens and bryophytes can form extensive groundcover and can dominate non-vascular plants by decomposing slowly and capturing available N and C (*Vitt*, 2007).

Plant growth tends to be limited more by nutrient levels than temperature in

areas of low elevation (*Nadelhoffer et al.*, 1997); however, across the entire Arctic, temperature is the main limiting factor (*Raynolds et al.*, 2008). Regions of high elevation tend to be water-limited, and vegetation type in these areas depends most closely on soil moisture (*Laidler et al.*, 2008; *Vitt*, 2007).

One method of detecting species composition changes over time and relationship to environmental variables has been through the extraction of the Normalized Difference Vegetation Index (NDVI) from remotely sensed images. NDVI calculates a normalized ratio between near- infrared ($\tau_N IR$) and red ($\tau_R ED$) surface reflectance as follows (*Tucker*, 1979):

$$NDVI = \frac{\rho_{NIR} - \rho_{RED}}{\rho_{NIR} + \rho_{RED}} \tag{2.1}$$

The ratio between red (0.63-0.69 μm) and near-infrared (0.76-0.90 μm) radiation is a useful indicator of the presence of vegetation because whereas non-vegetated regions reflect red and infrared light equally, vegetated surfaces reflect much more infrared radiation than red radiation [Figure 2.1]. The discrepancy in light reflection by vegetation is due to the propensity of leaf mesophyll to reflect near-infrared rays and for chlorophyll to absorb red light. NDVI is therefore highest (≈ 1) in the presence of dense vegetation and lowest (≈ 0) in the presence of snow, bare soil or clouds. NDVI is widely recognized as an excellent way to estimate the fraction of ground covered by vegetation, quantity of biomass and health of vegetation (*Pettorelli et al.*, 2005). Additionally, NDVI has been found to be strongly correlated with productivity in the Arctic (*Laidler et al.*, 2008), and to be moderately positively correlated with land surface temperature (*Raynolds et al.*, 2008).

Analyses of bimonthly NDVI data have also indicated little change over the past two decades in terms of productivity (*Neigh et al.*, 2007; *Bunn and Goetz*, 2006), with tundra regions showing increases in productivity and forested areas showing

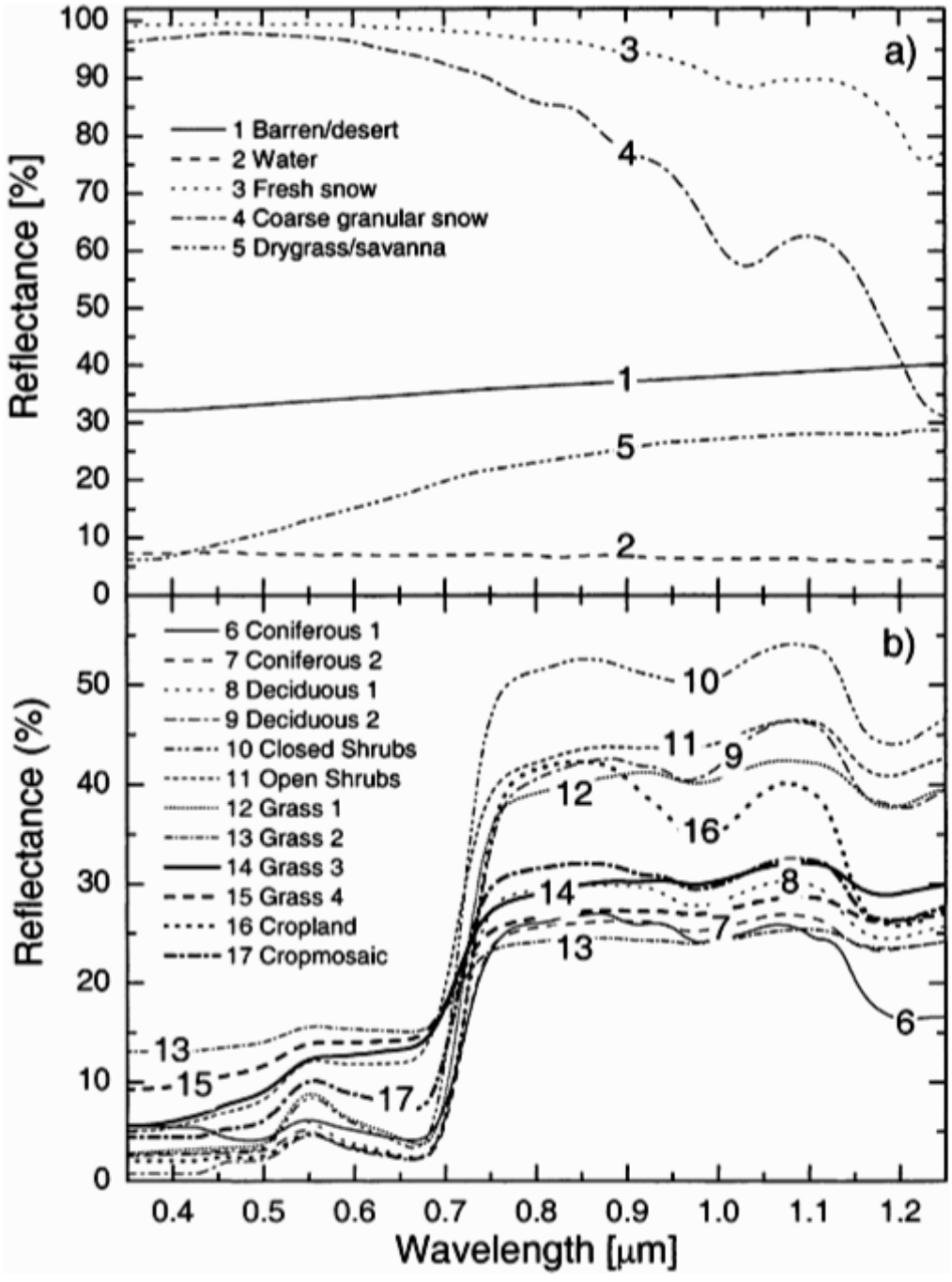

Figure 2.1: Surface target spectra for regions with (below) and without (above) live vegetation cover from *Trishchenko et al.* (2002)

decreases in productivity (*Bunn and Goetz*, 2006). This finding was confirmed by a similar study of 60-70^o N tundra NDVI by *Jia et al.* (2007), which found increases in NDVI of 0.64%/y over North America and 0.44%/y over Eurasia. The

difference between these studies is explained by *Jia et al.* (2007) as being due to the restriction of Arctic study sites to tundra regions, and the application of a homogenous vegetation approach to remove noise caused by bare ground and lakes.

Several recent studies have focused on the key controls on the NDVI response of Arctic vegetation. Studies in Nunavut have shown that NDVI has been found to be positively correlated to the percentage of vegetative landcover and surface moisture (*Laidler et al.*, 2008). Field comparisons of IKONOS and Landsat-derived NDVI indicated that Landsat-derived NDVI showed the closest relationship with environmental factors (*Laidler et al.*, 2008). In a similar study, *Raynolds et al.* (2006) used AVHRR-derived NDVI composites of the circumpolar Arctic to establish theoretical relationships between environmental variables and NDVI. Growth was almost exclusively temperature-limited in the coldest regions, defined as those which were dominated by mosses, lichens and liverworts. Intermediate regions dominated by forbs and dwarf-shrubs were influenced by substrate and elevation. Warmest Arctic regions with tussock vegetation were mostly influenced by geologic history (*Raynolds et al.*, 2006). The divergent conclusions reached by *Laidler et al.* (2008) and *Raynolds et al.* (2006) may be explained in part by the propensity of water to pool in regions of low elevation, leaving higher elevations drier. Thus, elevation and surface moisture tend to be positively correlated, and may present as confounding factors.

Regardless, the complex interactions between environmental variables and how they influence spectral response, species composition and productivity remains an open question in Arctic research. This question becomes even more pertinent when considered in context of a changing climate, whereby warming, drying and increased plant productivity (*Sitch et al.*, 2007) as well as warming. Both drying (44%) and wetting (53%) in different areas (*Thompson et al.*, 2006) have been observed. With a changing climate come changes in limiting factors which lead to changes in the

phenology, productivity and species composition of vegetation.

Climate change is known to bring about changes in interspecific competition which are most likely to be observed at ecotone boundaries (*Stow et al.*, 2004). Repeat large format photography in 1999-2002 of areas photographed in 1945-1953 by *Tape et al.* (2006) indicated an increase in shrub abundance in pan-Arctic regions. Similarly, *Stow et al.* (2004) has observed increases in the number of shrubs in Northern Alaska using repeated oblique-aerial photographs taken at a high resolution. Experimental warming and N fertilization have transformed acidic tundra ecotones into tall, shrub-dominated ecotones (*Thompson et al.*, 2006).

Increased shrubiness has been found to be associated with faster snow melt in spring because shrubs provide greater surface insulation, thereby advancing the date of snow melt (*Wang and Overland*, 2004). Another positive feedback of increased shrubiness is a reduction in albedo which is hypothesized to lead to surface and low atmospheric warming, resulting in an increase in shrub prevalence (*Wang and Overland*, 2004). However, positive feedbacks hypothesized to exist between shrubification, warming and CO_2 release by *Chapin III et al.* (1995) were recently disproved in an experimental field study conducted by *Myers-Smith and Hik* (2008).

2.1.2 Nutrient cycling

The limiting nutrient in the majority of the Arctic is nitrogen (N), which has been closely linked to LAI in studies of a variety of ecotones in Northern Alaska (*Williams and Ratsetter*, 1999), whereas wet sedge environments are phosphorous (P) limited (*Nadelhoffer et al.*, 1997). In an experiment that increased nutrient levels, deciduous shrub biomass increased "at the expense of nonvascular plants, graminoids, and evergreen shrubs" (*Nadelhoffer et al.*, 1997). In an experiment with increased temperature, vascular plants increased in prevalence while non-vascular

plants became rarer (*Nadelhoffer et al.*, 1997).

Deepening of the active layer is predicted to occur as a result of increasing surface temperatures, and has the result of decreasing soil N (*Thompson et al.*, 2006). Perhaps as a result of the N limitation of drier regions, there are predictions that moist regions will show a greater response to climate change than drier regions, and ecosystem change will be determined more by storage, than mineralization, of N (*Nadelhoffer et al.*, 1997). Methane emissions from lakes and permafrost have been growing recently as temperatures have been rising, and this increase is expected to rise even as water tables rise because methanogenesis is more sensitive to temperature than saturation (*Sitch et al.*, 2007).

Disturbance history and N cycle control ecosystem response to CO_2 (*Thornton*, 2008). Model results indicate increase in CO_2 increases NPP and the existence of a strong disturbance interaction related to N availability (*Thornton*, 2008). However, N limitation is reducing the extent of NPP enhancement instigated by elevated CO_2 (*Norby et al.*, 2008). Moderate Resolution Imaging Spectroradiometer (MODIS) is a NASA instrument on Terra and Aqua satellites which measures reflected and emitted visible and infrared light in 36 discrete wavebands over 1-2 days. Many products with a wide range of scientific applicationshave been developed using MODIS observations (*NASA*, 2009). One MODIS product, MODIS Land Surface Albedo, estimates Earth radiation and was not designed for biophysical applications. Recently, however, a strong correlation was found to exist between percentage canopy foliar nitrogen and MODIS albedo (r=0.88) (*Ollinger et al.*, 2008a). This is significant because neither MODIS Albedo nor foliar N are related to the Leaf Area Index (ratio of leaf to ground unit, LAI) (*Ollinger et al.*, 2008a), and because foliar N is directly related to ecosystem CO_2 uptake (*Ollinger et al.*, 2008b). The correlation between CO_2 uptake, foliar N and albedo may offer an interesting way to both assess changes in productivity over time, and to estimate the accuracy of remotely

sensed CO_2 uptake (Net Primary Productivity) model outputs.

Eight Mile Lake near Healy, Alaska contains discontinuous permafrost undergoing thawing (*Schuur et al.*, 2008). Repeated observations at this site have revealed positive feedbacks to exist between permafrost thawing and nutrient enrichment. Thawing of permafrost leads to release of old carbon (as measured using carbon isotope 14C02) which increases respiration, NPP and GPP. Although this region of the Arctic continues to function as a C sink, *Schuur et al.* (2008) hypothesizes that continued warming may lead to the loss of 77-106 Pg of C from Arctic permafrost along with C cycle destabilization and increased growth of vegetation.

Concerns regarding positive feedbacks between warming and permafrost thawing are heightened by the prevalence of methane in permafrost which is formed through the anerobic decomposition of vegetation. Methane is a greenhouse gas with twenty-five times greenhouse gas warming potency of CO_2 (*Freedman*, 2007). Under recent warming (1970-2000), methane emissions from permafrost have increased 20-60% at Stordalen mine in subarctic Sweden (*Christensen et al.*, 2004).

2.1.3 Phenology

Phenology is defined as the "science of natural recurring events", and is studied extensively in Europe using a continuous and well maintained data set exists for mean onset dates and temperatures (*Menzel et al.*, 2006). Within the context of this thesis, 'phenology' is used to refer specifically to the seasonal timing of biological processes in vegetation.

Although the impacts of climate change can be seen both in the net biomass produced by vegetation as well as the seasonal timing of this growth, vegetation phenology has tended to be frequently overlooked (*Roerink et al.*, 2003). To date, field studies of phenology in the High Arctic have been limited to a single field

study by *Høye et al.* (2007) which found >30 day advances in emergence dates for arthropods, birds and six plant species in Zackenberg, Northeast Greenland from 1996-2005. Studies have also found that a herbaceous alpine pioneer species, *Ranunculus glacialis*, does not display changes in phenology under experimental warming (*Totland and Alatalo*, 2002). Phenological changes in the High Arctic "may weaken or even disrupt trophic interactions among species that are crucial to successful reproduction in this highly seasonal environment" (*Høye et al.*, 2007).

The impact of changes in phenology on carbon sequestration, however, is less well understood. Whereas *Stow et al.* (2004) suggested that total carbon uptake is independent of phenological dates, *Baldocchi et al.* (2005) found that every additional day of growing season increased C sequestration by 5gC/day in a decidious forest. To date, spring onset in vegetation has been independent of autumn onset (*White et al.*, 2008), meaning that earlier spring onset is not correlated with either late or early autumn onset. It is therefore reasonable to hypothesize that little change in pan-Arctic productivity will be directly linked to alterations in phenology, though it remains an interesting research question of pertinence to this thesis.

There has also been some disagreement over which remote sensing strategies are best suited to estimating phenology. The majority of remote sensing studies of phenology have relied on NDVI data extracted from AVHRR, yet AVHRR is poorly calibrated to terrestrial surfaces and has difficulties with geometric registration and cloud screening (*Zhang et al.*, 2003). Conversely, MODIS was validated with good results for deriving phenology over New England (*Zhang et al.*, 2003). Another option is to use GIMMS, which is an AVHRR-derived product created by the Global Land Cover Facility (www.landcover.org) that is geometrically, atmospherically and cloud corrected and has been used in previous studies of Alaskan phenology (*Verbyla*, 2008).

Products such as GIMMS have been used both for assessing phenology as well

as productivity. *Verbyla* (2008) used GIMMS AVHRR-derived NDVI, and found decreases in net maximum NDVI over boreal Alaska and an increase in NDVI along the northern coast of Alaska. In order to extract phenology from a time series of NDVI for a site, the most popular method is to use a Fast Fourier Transform to change the 15-day composite images into a continuous data set, and then choose points of inflection to determine the start and end of both spring bud-burst and autumn senescence (*Loyarte et al.*, 2008).

Once a continuous remote sensing record is established, there are several other methods of estimating important dates for phenology. These methods include setting global thresholds for an entire study site, or setting locally tuned NDVI thresholds (ex: estimating start of spring as the date when NDVI>0.3). More complex methods of estimating phenology are either conceptual-mathematical, or are a hybrid of previously mentioned methods (*White et al.*, 2008). Therefore, significant uncertainty exists regarding both which date should be regarded as the start of season, problems arise in the comparison of data from studies using different methods, and a clear need exists to look at the timing of specific biological processes rather than estimating a single date (*White et al.*, 2008).

Currently, the largest retrieval uncertainty is faced by studies in the tropics and high latitudes (*White et al.*, 2008). A recent study by *White et al.* (2008) has indicated an earlier start of season in central/southern Alaska with no trend detected in the rest of the North American Arctic (1982-2006) (*White et al.*, 2008).

2.1.4 Productivity

Primary productivity refers to "the rate at which energy is stored in the organic matter of plants per unit area of the Earth's surface. It is often expressed in units of dry matter (e.g., grams of dry mass/ m^2 y) rather than energy because of the

ease of determining mass and the relative constancy of the conversion from mass to energy (caloric) units for plant tissues" (*Fahey and Knapp*, 2007).

Gross Primary Productivity (GPP) is the "amount of carbon photosynthesized by plants" (*Myneni et al.*, 1995). Net Primary Productivity (NPP) is calculated by subtracting autotrophic respiration from GPP, which corresponds to roughly 50% of net canopy photosynthesis (*Gower et al.*, 1999). Net Ecosystem Productivity (NEP) is NPP minus soil respiration (*Maisongrande et al.*, 1995). Gross Ecosystem Productivity (GEP) can thus either be calculated by adding NEP and autotrophic respiration, or by subtracting soil respiration from GPP. Autotrophic respiration (R_A) refers to respiration by plants, and heterotrophic respiration (R_H)refers to respiration by organic matter decomposers. For a brief comparison of these terms, please refer to Table 2.1.

From a field sampling perspective, productivity can be expressed either as a mass or energy flux. If assessed as a mass flux, productivity can be described either through C mass or as dry weight (with or without ash). C mass accounts for 50% (47%–55%) of total dry weight. Alternatively, annual growth can be estimated using measurements in shrub diameter multiplied using species-specific allometric biomass equations (*Young*, 2007). Annual non-vascular growth can be estimated using innate (leaf, frond or stem, patterns) or surrogate (neighbour or wire/net) markers, which can then be multipled by bulk density to estimate annual production (*Vitt*, 2007).

	Primary Productivity	Ecosystem Productivity
Gross	*GPP:*rate of plant energy storage	*GEP:*GPP-heterotrophic respiration
Net	*NPP:* GPP -autotrophic respiration	*NEP:* NPP-heterotrophic respiration

Table 2.1: Definitions of productivity terms.

Of all the aforementioned variables, NPP is most widely used for resource management, studies of the terrestrial carbon sink and analyses of ecosystem health

(*Cao et al.*, 2004). NPP is usually modeled either using remote sensing-based models such as GloPEM or ecosystem simulation models such as 3-PGS. N and P fertilization of a wet sedge tundra by *Boelman et al.* (2003) over 13 years resulted in a four-fold increase in aboveground biomass and Gross Ecosystem Production (GEP) with corresponding increases in NDVI ($R^2 = 0.84$). However, Net Ecosystem Production (NEP) was not found to vary between treatments. This is because NEP is calculated by subtracting Ecosystem Respiration (ER) from GEP, and treatments increased GEP and ER equally (*Boelman et al.*, 2003). This finding suggests that changes in biomass could be assessed remotely using NDVI as a proxy for GEP. Furthermore, recent studies by *Williams et al.* (2008) have shown LAI and NDVI to be closely related in Arctic ecosystems. NDVI is therefore a proven proxy for GEP and LAI. Furthermore, because of the low ratio of aboveground vegetation per unit of ground (LAI<3) of biomass in the Arctic, no issues exist with NDVI saturation (*Haboudane et al.*, 2004).

Since 2004, NPP has been decreasing in deciduous forest control and experimental plots (*Norby et al.*, 2008). Some of the changes in NPP can be explained by the leaf area day (total days for which leaves are present) (*Norby et al.*, 2008). Although climate change has been predicted to bring about increased productivity in the Arctic (*Stow et al.*, 2004), NPP has increased in tundra biomes while decreasing in shrub and tree biomes (*Thompson et al.*, 2006). Experimental studies conducted as part of the International Tundra Experiment (ITEX) have indicated strong response of vegetation to warming and fertilization, with smaller increases found with fertilization along but no significant increase due to warming alone (*Chapin III et al.*, 1995; *Grogan*, 2008). Experimental nitrogen enhancement in a bog led to increase in photosynthesis, and a decrease in respiration (*Juutinen et al.*, 2008)

A recent increase in temperature was found to suppress lichen productivity

and increases vascular plant productivity, and that replacing lichen with vascular plants causes increases in NDVI (*Olthof et al.*, 2008). These changes in NDVI were detected using robust trend detection. Changes in vegetation composition were observed using spectral mixture analysis (*Olthof et al.*, 2008). Wang and Overlander 2004 observed significant decreases (1982-2000) in NDVI area of Arctic tundra (*Henry and Elmendorf*, 2008). *Goetz et al.* (1999) observed a 10% increase in NDVI over the past 20 years (*Grogan*, 2008).

2.1.5 Carbon cycling

Northern regions are an important source and sink of Carbon (C), and contain between 25-33% of the world's C pool (*Oechel and Vourlitis*, 1997). The impacts of climate change are predicted to be most significant in the Arctic, which release C at a greater rate at rising temperatures (*Oelbermann et al.*, 2008). Recent research has indicated that current warming trends in Alaska are leading to significant increases in the rate of Alaskan permafrost thaw, with older carbon being released preferentially (according to $^{1}4CO_2$:$^{1}2CO_2$ ratios) (*Schuur et al.*, 2008).

Process-based models have been used to assess CO_2 exchange in the Arctic under climatic changes. These models use either eddy flux covariance data or experimental field data for parametrization (*Sitch et al.*, 2007).

Plants store C because their C:N ratio is greater than that of the soil (*Sitch et al.*, 2007), although they were earlier thought to have equal C:N ratios (*Nadelhoffer et al.*, 1997). C emissions occur as a result of nutrient increase following warming (*Mack et al.*, 2004). With increasing nutrient release and uptake, plants were found to undergo twice as much growth which increased their storage of C but also increased by an equivalent amount the emission of C from deeper soil levels (*Mack et al.*, 2004). In a similar experiment, experimental warming and N fertil-

ization simulating expected impacts of climate change resulted in decreases in soil C (*Thompson et al.*, 2006).

Under a regime of increased CO_2, earlier experiments found increases in plant productivity instigated by higher CO_2 levels would return to normal within 3 weeks, but at the time, a hypothesis was stated that synergistic effects might cause more long-lasting changes in productivity (*Oechel and Vourlitis*, 1997).

An often-debated research gap in the study of Arctic remains regarding how climate change will impact C cycling in the Arctic (*Wu and Lynch*, 2000), since the rate of C storage is based on NPP and decomposition (*Thompson et al.*, 2006). Climatic warming is predicted to increase plant productivity, thus sequestering carbon at a greater rate and increasing microbial respiration in soils, which will increase atmospheric C (*Stieglitz et al.*, 2000; *Boelman et al.*, 2003). Whether increased emissions of C are counterbalanced by increased C sequestration therefore remains an often discussed issue. With increased temperature in the Arctic, heterotrophic respiration (R_H) is thought to increase more rapidly than NPP over the short-term, and NPP more than R_H over the long-term. The growth in R_H is especially prevalent if soils dry, according to model predictions (*Sitch et al.*, 2007) since R_H is inversely proportional to soil moisture (*Thompson et al.*, 2006). Since leaf stomates can ingest CO_2 more easily during higher CO_2 periods, their stomates remain closed more often, thus decreasing the quantity of evapotranspiration and raising soil moisture levels (*Beerling*, 2007). Higher CO_2 conditions therefore lead to increased soil moisture, which may lead to decreases in R_H, thus leading the Arctic to act more as a sink than source of C.

One method of assessing this question has been to collect field measurements of CO_2 release and NPP under experimental warming, as in *Boelman et al.* (2003). Another approach has been to couple a Terrestrial Ecosystem Model (TEM) with a soil thermal model to assess carbon cycling (*Thompson et al.*, 2006), and calibrate

the model using field-derived measurements of aboveground NPP.

2.2 Site-specific challenges

Arctic vegetation poses significant accuracy challenges for both remote sensing and modeling. The classification accuracy of remote sensing at visible and infra-red wavelengths is complicated by cloud cover and low spatial resolution.

2.2.1 Field studies

Field studies are sparse for Arctic regions because study sites are remote, difficult and expensive to access. Vegetation is characterized by a short growing season and harsh winter which complicates the installation of year-round fixtures. Of benefit to researchers studying net primary production is the relatively small size of vegetation, which allows destructive sampling that would not be possible in regions with very large trees. Samples can also be dried more easily because of their size. Vegetation is diverse across the Arctic, but each individual study site is likely to have smaller biodiversity than an equivalently sized plot in a temperate or tropical region.

2.2.2 Remote sensing of Arctic vegetation

Of the many challenges posed by remote sensing in Arctic environments, the most notable problem is that of cloud cover. In some parts of the Arctic, there is persistent cloud cover for up to weeks at a time (*Stow et al.*, 2004). Many Arctic studies therefore use passive microwave sensors, since passive microwave readings are independent of solar illumination and cloud cover. If passive microwave can be used, the L band is better suited to assessing changes in vegetation than the Ku and C

bands (*Sitch et al.*, 2007). However, extraction of vegetation indices such as NDVI require cloud-free optical data (*Jensen*, 2007). Because of long-lasting Arctic cloud cover, it is possible that changes requiring the use of optical satellite instruments can be missed completely (*Stow et al.*, 2004). Finally, NDVI measurements are heavily sensitive to changes in illumination levels caused by varying cloud cover (*Hope*, 1999). Most commonly, researchers therefore select images according to a maximum cloud cover threshold to reduce errors associated with cloud cover (*Hope*, 1999).

When possible, a high temporal resolution of observations should be used to enhance the ability to catch phenological changes (*Stow et al.*, 2004). Another approach is to create composite images of maximum values of NDVI which then effectively removes the effect of clouds, which have a lower NDVI than vegetation. This method is used to create the GIMMS product, which has been found to be reliable in a study of Alaskan vegetation by *Verbyla* (2008).

Another challenge of Arctic remote sensing is that of large quantities of surface water, as well as snow and ice cover, which can bias measurements of vegetation (*Stow et al.*, 2004). The challenges posed by surface water are especially problematic in regions of Hudson's Bay lowlands such as near Churchill. Also, because the incident sun angles are so low at Arctic latitudes, shade contributes to solar radiance which results in a great deal of noise (*Stow et al.*, 2004). Fortunately, the low height of vegetation mitigates the size of shadows (*Laidler et al.*, 2008). Soil also has a high reflectance (0.3 for red and NIR) (*Laidler et al.*, 2008) which complicates the differentiation of soil from vegetation.

2.3 Conclusions

Changes in the productivity, phenology and species composition of vegetation, as well as in nutrient and carbon cycling are currently observed in in situ studies of the Arctic (*Stone et al.*, 2002; *Høye et al.*, 2007; *Christensen et al.*, 2007). Yet, the sparse distribution of Arctic field sites requires these field studies to be compared to remotely sensed historical datasets in order to assess whether the sample sites are representative of pan-Arctic changes, and to analyze challenges that occur in scaling and assimilating findings from field, model and remote sensing data sets. The cumulative impacts of these changes on Arctic ecosystem dynamics and global carbon cycling remain poorly understood due to their complexity and the challenges involved in conducting field, modeling and remote sensing studies in this region (*Sitch et al.*, 2007; *Stow et al.*, 2004).

Although the processes leading to changes in vegetation are complex, analyzing remote sensing estimates of these changes over time will enable further research into the factors associated with these changes (soil moisture, surface temperature, soil nutrients), and can thereby provide insights into changes in Arctic ecosystem dynamics occurring under an ever-changing climate.

Many important questions remain regarding the response of pan-Arctic vegetation to climate change. Combining remote sensing with models enables pan-Arctic comparisons over time that can yield important insights. However, issues related to scaling, reliability and interconnections between data products need to first be analyzed. It is therefore hoped that the following thesis will analyze pan-Arctic vegetation changes over time using the aforementioned products, and also assess the reliability, interconnections and challenges of using remote sensing and modeling to estimate biophysical vegetation changes over time.

Chapter 3

Methodology

Methodology is described first according to the acquisition and characteristics data sets (GloPEM, GIMMS, MODIS EVI, MODIS NDVI, Landsat and APP-x). Each data set was analyzed both over the pan-Arctic, within 5^o latitudinal bands and 20^o longitudinal, as well as for three study sites in the Canadian Arctic. The second section of methodology therefore describes Canadian Arctic study sites in detail with associated high resolution images. The next methodology sections focus on technical aspects of data processing, and the visual and statistical analysis of results.

3.1 Data products

The data products used for this thesis are described in table 3.1 below in terms of their technical specifications, pertinent recent applications, and the extent to which these products are likely to be of benefit in this study according to both how well they perform in Arctic vegetation biomes as well as how well they estimate the specified indices. One challenge of AVHRR-derived GIMMS NDVI and GloPEM NPP is that there is an artefact causing a strong horizontal line to appear in north-

central Russia. Emails to providers of GIMMS and GloPEM products regarding this artefact have gone unanswered.

Product	Spatial	Temporal resolution	Inputs	Description
APP-x	25×25km	30 day (1982–2004)	AVHRR	Temp/Albedo
GIMMS	8×8km	15 day (1981–2006)	AVHRR	NDVI
GloPEM	8×8km	10 day (1981–2000)	AVHRR,met,field	NPP
Landsat 4-5 TM	30×30m	≈weekly (1982–)	–	Multispectral
MOD13A1	500×500m	16 days (2000–)	Terra & Aqua	NDVI & EVI

Table 3.1: Data product key characteristics. For key acronyms, please refer to text below or Table B.1

3.1.1 AVHRR Polar Pathfinder-Extended (APP-x)

APP-x products provide estimates of a variety of radiation, cloud cover and surface properties for the pan-Arctic using AVHRR readings upscaled from 1.1×1.1km to 25×25km in addition to ozone and atmospheric profile data. APP-x products are calculated by the Cooperative Institute for Meteorological Satellite Studies at the University of Wisconsin Madison, and are calibrated to 41 Arctic meteorological stations. APP-x monthly mean temperature and albedo were used for this study, although higher temporal resolution data is available (*Wang and Key*, 2003).

3.1.2 GIMMS (NDVI)

GIMMS, Landsat and MODIS NDVI are calculated using the same standard equation NDVI equation(*Tucker*, 1979):

$$NDVI = \frac{\rho_{NIR} - \rho_{RED}}{\rho_{NIR} + \rho_{RED}} \tag{3.1}$$

Global Inventory Modeling and Mapping Studies (GIMMS) is a Normalized Difference Vegetation Index (NDVI) product calculated from 1.1×1.1km Advanced

Very High Resolution Radiometer (AVHRR) data, and resampled to 8×8km composites. GIMMS NDVI is geometrically and atmospherically corrected, and conveys maximum NDVI observed over 15 day periods in order to filter out clouds, which have a low NDVI. GIMMS is an established indicator of phenology (*Yoccoz*, 2008; *Reed*, 2006; *Stow et al.*, 2001) and biomass in low Leaf Area Index (LAI) regions such as the Arctic (*Williams et al.*, 2008; *Boelman et al.*, 2003; *Raynolds et al.*, 2006).

3.1.3 Landsat (NDVI)

Landsat is a multispectral sensor with a very long hisorical record (1982–) and a finer resolution than GIMMS (30x30m), which is now offered for free by the US Geological Survey (USGS). Although free data sets are not corrected, resampled or composited to remove noise, the availability of this data set as well as its historical record makes it desirable for long term dynamical studies of land cover. Landsat Thematic Mapper 4-5 contains 7 bands, where bands 3 and 4 are red and infra-red radiation respectively. NDVI can therefore be calculated directly from Landsat images using a simple equation (*Global Land Cover Facility*).

3.1.4 Field net primary production estimates

Net primary productivity is assessed in situ by extracting aboveground vegetation samples, oven drying them and then determining NPP based on the weight of dry plant matter. Carbon accounts for 47–55% of dry plant weight, with a mean value of 50% for the majority of species. NPP is much more difficult to measure than dry plant weight, the robust and well-accepted conversion of NPP=50% of dry weight is widely used (*Fahey and Knapp*, 2007). The main challenges in field sampling are in determining how many plots to sample, and whether to use randomized or selective

sampling (where samples are taken from regions with varying characteristics in one region). Another challenge is that field measurements are usually taken with the idea of characterizing a larger region using many measurements. However, there can be a great deal of heterogeneity in the distribution of NPP, over a typical (1 ha) sampling region (*Fahey and Knapp*, 2007).

Two challenges are posed in field sampling of moss and lichen vegetation which cover a majority of the Arctic. Firstly, both decay more slowly than vascular plants, and it can therefore be difficult to differentiate live and decomposing peat. A second issue arises in the classification of aboveground biomass, since much of the non-shrub biomass in tundra ecosystems lies along the ground beneath the shrub canopy and the transition between growing and decomposing sections of a biomass is gradual (*Vitt*, 2007). *Vitt* (2007) therefore recommended that non-vascular biomass estimates should be based on samples of the top 5cm and 10cm to enable consistency in the way in which 'aboveground' is defined. Shrub dominated regions are also difficult to characterize in terms of NPP because shrubs tend to propagate widely into dense communities and contain numerous stems (*Young*, 2007). Furthermore, the rate of herbivory is difficult to quantify for any ecological region (*Young*, 2007).

3.1.5 MODIS EVI and NDVI

MODIS NDVI has been compared with GIMMS and Landsat for the high Arctic because MODIS NDVI has a 500×500m resolution which offers a medium resolution in comparison to GIMMS (8×8km) and Landsat (30×30m) (*Jensen*, 2005). Questions of the influence of scale on results can therefore be examined.

MODIS Enhanced Vegetation Index (EVI) and NDVI images are available as 16 day composites from NASA, both at the 500×500m resolution and from 2000

onwards. Also, MODIS NDVI and EVI have been found to outperform AVHRR in estimating percentage tree cover (*Hansen et al.*, 2002) so it will be interesting to see if this success holds over to Arctic vegetation estimation.

MODIS EVI is calculated as follows:

$$EVI = G\frac{\rho_{NIR} - \rho_{RED}}{\rho_{NIR} + C_1 \times \rho_{RED} - C_2 \times \rho_{BLUE} + L} \tag{3.2}$$

"where ρ are atmospherically corrected or partially atmosphere corrected (Rayleigh and ozone absorption) surface reflectances, L is the canopy background adjustment that addresses nonlinear, differential NIR and RED radiative transfer through the canopy, and C_1, C_2 are the coefficients of the aerosol resistance term, which uses the blue band to correct for aerosol influences in the red band. The coefficients adopted in the EVI algorithm are $L = 1$, $C_1 = 6$, $C_2 = 7.5$ and G(gain factor)=2.5" (*Huete et al.*, 2002). EVI is therefore designed for monitoring vegetation while removing atmospheric noise (*Huete et al.*, 2002). MODIS EVI has recently been found to be outperform AVHRR NDVI in estimating phenology, productivity and photosynthesis in temperate regions (*Mahadevan et al.*, 2008; *Sims et al.*, 2006; *Xiao et al.*, 2004). In a low Arctic (70^o north) sedge-shrub tundra, NDVI was conversely found to be more closely correlated to green phytomass (r=0.63) and leaf turnover (r=0.79) than EVI. The relationship between EVI, NDVI and productivity in the high Arctic has yet to be assessed.

3.1.6 GloPEM (NPP)

Net Primary Productivity (NPP) estimations can be conducted at the in situ using biomass sampling or eddy flux covariance data, or by modeling a combination of remote sensing, field and meteorological estimates (*Gower et al.*, 1999). Please refer to *Luus and Kelly* (2008) for a discussion of different approaches used to

estimate NPP using modeling and remote sensing. NPP estimates tend to be better calibrated in regions where extensive vegetation sampling has been conducted, and which contain numerous eddy flux covariance towers; conversely, the shortage of these inputs in Arctic regions limits the ability to assess the accuracy of NPP estimates.

NPP provides important input on the quantity of carbon taken up by vegetation. In the Arctic, NPP readings over time relate directly to both to the role of vegetation in global carbon cycling, and furthermore reflects changes in biomass induced by recent climate warming. GloPEM (Global Production Efficiency Model) derives 10-day estimates of NPP ($gC/m^2/10$ day) from 1981-2000 using USGS AVHRR data, resampled to an 8×8km resolution (*Goetz et al.*, 1999). GloPEM calculates NPP as a function of autotrophic respiration, and the utilization and absorption of canopy radiation. Remote sensing inputs are all derived from AVHRR, and consist of canopy air temperature, photosynthetically active radiation and fraction of photosynthetically active radiation absorbed by the canopy. Meteorological inputs include the quantity of aboveground biomass (kg/m^2), site latitude, optimal air temperature for photosynthesis, soil water holding capacity, monthly mean air temperature, daily surface vapor pressure, precipitation, mean fraction of sunshine, diurnal temperature range (K), net radiation and initial soil water content. To date, research has been conducted of comparing carbon estimates in China (*Pan et al.*, 2006) using GloPEM, but no studies have yet focused on GloPEM estimates of NPP for the Arctic, or on quantifying Arctic GloPEM NPP uncertainties.

3.2 Acquisition

Data product sources are summarized below in Table 3.2. Landsat images were selected on the basis of having <20% cloud cover, being free of snow and available

Product	Source of data	Website
APP-x	Polar Satellite Meteorology	stratus.ssec.wisc.edu/products/appx
GIMMS	Global Landcover Facility	glcf.umiacs.umd.edu/data/gimms
GloPEM	Global Landcover Facility	glcf.umiacs.umd.edu/data/glopem
Landsat	USGS Earth Explorer	edcsns17.cr.usgs.gov/EarthExplorer
MOD13	NASA Land Processes	lpdaac.usgs.gov/lpdaac/get_data

Table 3.2: Data product acquisition information. For key acronyms, please refer to text below or Table B.1, and for data product descriptions, refer to Table 3.2

for summer months June, July and August. Selecting images for NDVI analysis based on a maximum cloud cover threshold is an established unbiased method for dealing with cloud cover(*Hope*, 1999).

GIMMS, GloPEM and APP-x data sets were downloaded in their entirety for the Arctic. MOD13 EVI and NDVI will be downloaded for one site only, Fosheim peninsula, and for summer months May through September, to assess whether EVI is better at predicting snow on/off dates than NDVI.

3.3 Study site selection

Study sites were selected on the basis of availability of field data, which was found using the International Polar Year Polar Data Catalogue (www.polardata.ca). The location of study sites is indicated with square boxes in Figures 3.1 and 3.3, and site characteristics are summarized in Table 3.3. Field data were collected on

Study site	Northing	Easting	Ecotone
Churchill	58.80-58.27	-93.93- -92.95	Sedge, moss, low shrub wetland
Herschel	69.64-69.52	-139.27- -138.84	Sedge, moss, dwarf-shrub wetland
Fosheim	80.12-80.08	-85.67 - -85.50	Prostrate/hemiprostrate shrub tundra

Table 3.3: Study site characteristics

Cape Churchill from 1989 to August 2008 by R.L. Jefferies and E. Horrigan from the University of Toronto, and were generously shared for this thesis as part of International Polar Year.

The three study sites are located near the westernmost, easternmost and northernmost extents of the Canadian Arctic, and provide an interesting contrast. The northernmost site, Fosheim, has undergone the largest extent of warming [Figure 3.1] and is also predicted to undergo the largest increase in surface temperature in response to scenarios invoking a doubling in CO_2 levels, followed by Herschel and then Churchill (*Moritz et al.*, 2002). However, whereas Churchill and Herschel have both undergone increases in NDVI, NDVI has decreased in Fosheim between 1982–2005 [Figure 3.2] which indicates that there is something more complex driving patterns in NDVI than surface temperatures alone.

Herschel and Churchill provide an interesting basis of comparison because they have undergone different changes in surface temperature and NDVI [Figures 3.1 and 3.2], and are far apart geographically but they are both sedge and moss intertidal wetlands which remain dry in summer [Figure 3.3]. Another benefit of these three study sites is that they are all located relatively close to meteorological stations (YUB, YRB and YYQ), which are sparse in the Canadian Arctic but important for setting parameters for modeling net primary productivity. All three regions are characterized by Cryosolic (permafrost containing) soil type according to *Soil Classification Working Group* (1998).

True colour satellite images indicating the GIMMS 8×8km footprint are presented below for Churchill [Figure 3.4], Fosheim [Figure 3.5] and Herschel [Figure 3.4]. The Churchill site is part of La Perouse Bay, a saltwater intertidal marsh. It contains a large number of ponds and lakes, which are likely to diminish the NDVI signal because of the low NDVI of water in comparison to vegetation. The Churchill site contains low Arctic shrub wetland dominated by *Carex subpathacea* sedge, *Puccinellia phrynganodes* grass and willow (*Jefferies et al.*, 1979; *Jefferies*, 2008). An east-west gradient exists in the GIMMS pixel, where the western edge contains a higher proportion of shrubs and willows, and the remainder of the site is

of a lower elevation with smaller wetland vegetation and more ponds. Of the three sites, Churchill is the most heterogeneous in distribution of water and vegetation types.

Fosheim Peninsula, the study site which is furthest North, is also the most barren and rockiest [Figure 3.5]. Prostate/hemiprostrate shrub tundra is interspersed by unconsolidated gravel and sand on west- and northwest- facing slopes (*Young et al.*, 1997). Over 140 species of vascular plant are found at Fosheim Peninsula, whereas surrounding regions of Ellesmere Island are much colder and have lower plant diversity (*Young et al.*, 1997).

Herschel Island is a coastal salt marsh like Churchill [Figure 3.4]. However, unlike Churchill, Herschel Island is in the High Arctic. Herschel Island is covered mainly in *Puccinellia phryganodes* grass and *Carex ursina* sedge (*Jefferies*, 1977). The GIMMS pixel used for analysis of the Herschel study site contains a great deal of water. Due to the small size of Herschel Island in relation to GIMMS pixels, the pixel selected contains the highest proportion of land area possible. However, masking of water pixels will likely be easier for Herschel Island than for Churchill because of the smaller number of ponds and lakes, which vary seasonally much more than the coastline.

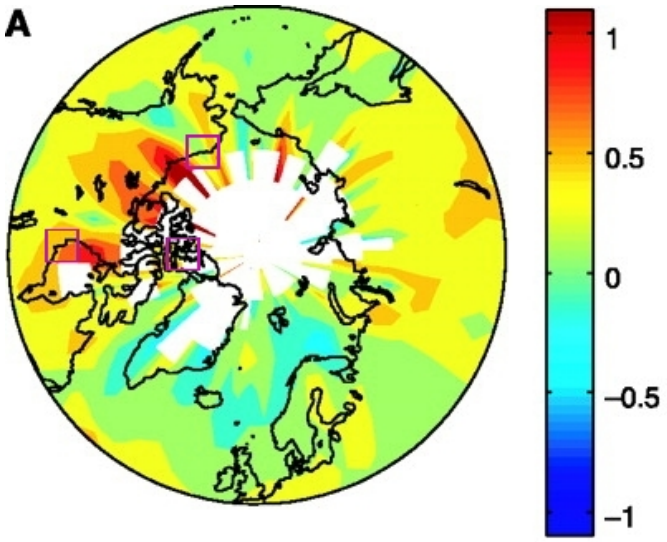

Figure 3.1: Changes in surface air temperature from 1970-2000 (*Moritz et al.*, 2002)

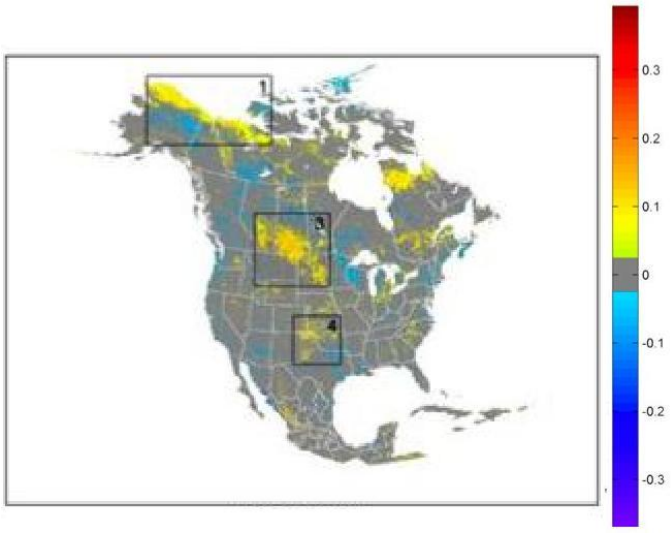

Figure 3.2: Changes in 1982–2005 North American AVHRR-derived NDVI according to *Neigh et al.* (2007)

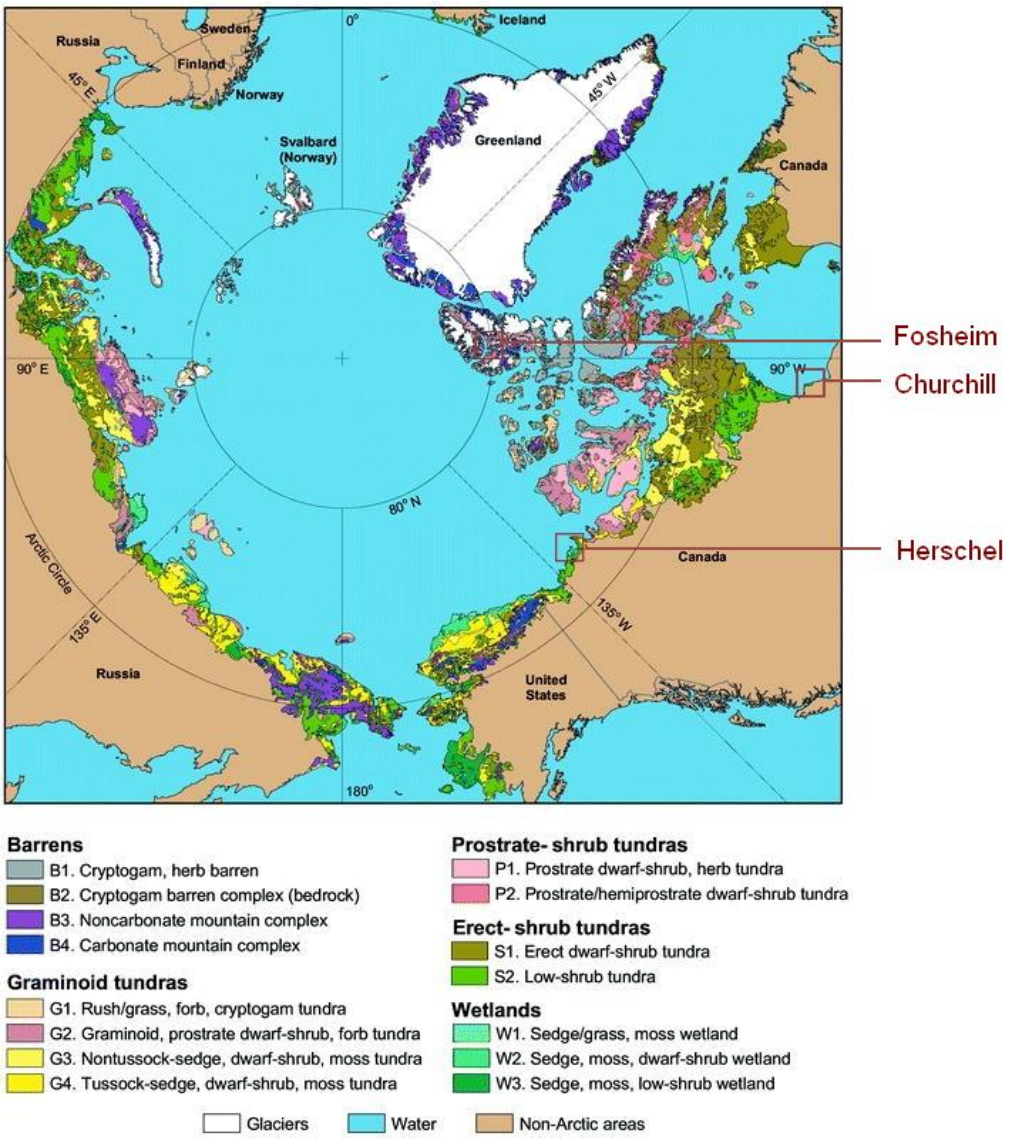

Figure 3.3: Map of circumpolar Arctic vegetation types classified by *Walker et al.* (2005)

Figure 3.4: Landsat (1990 composite) image of Churchill, with GIMMS 8×8km footprint in white

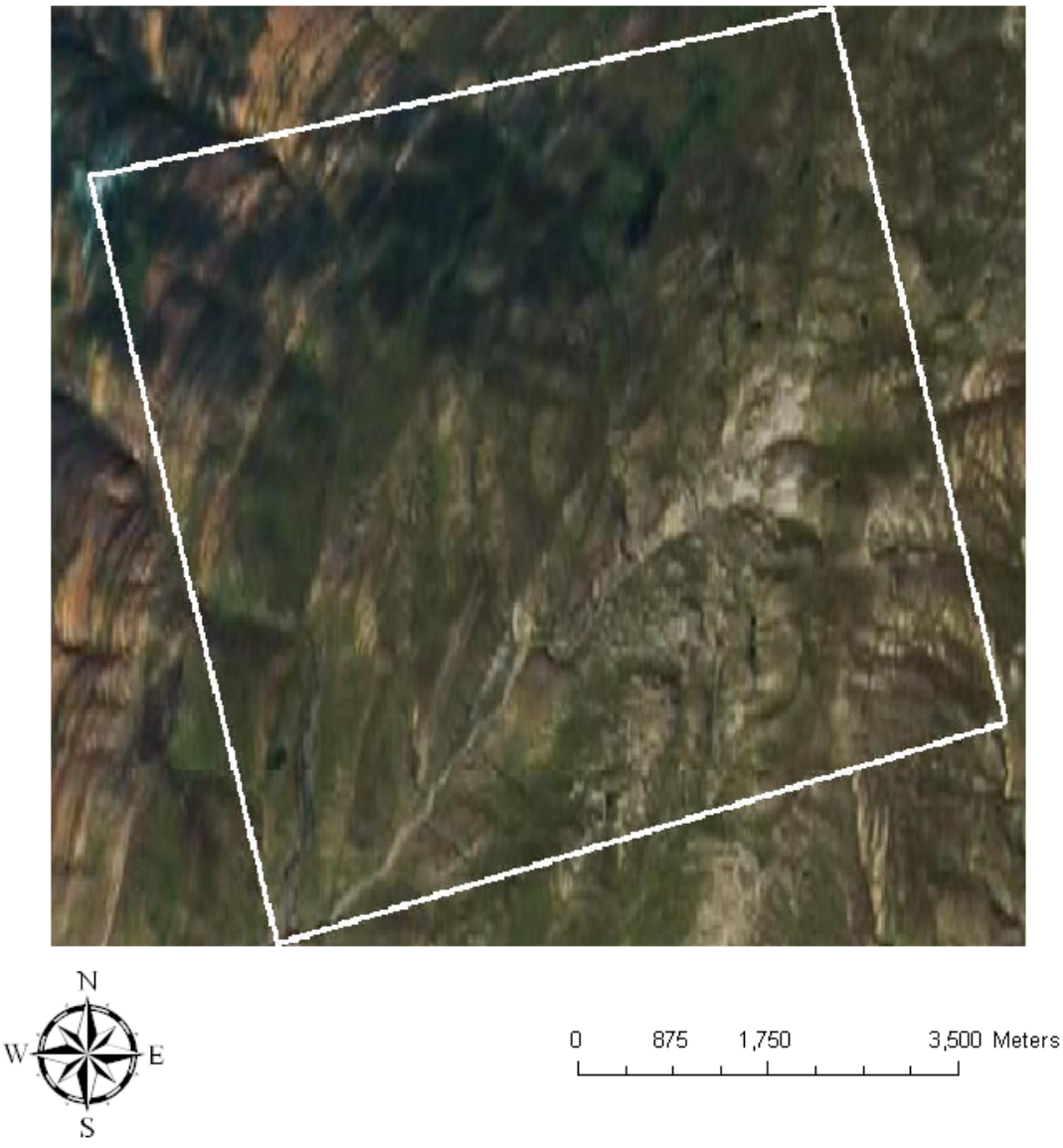

Figure 3.5: Google Earth image of Fosheim Peninsula, with GIMMS 8×8km footprint in white

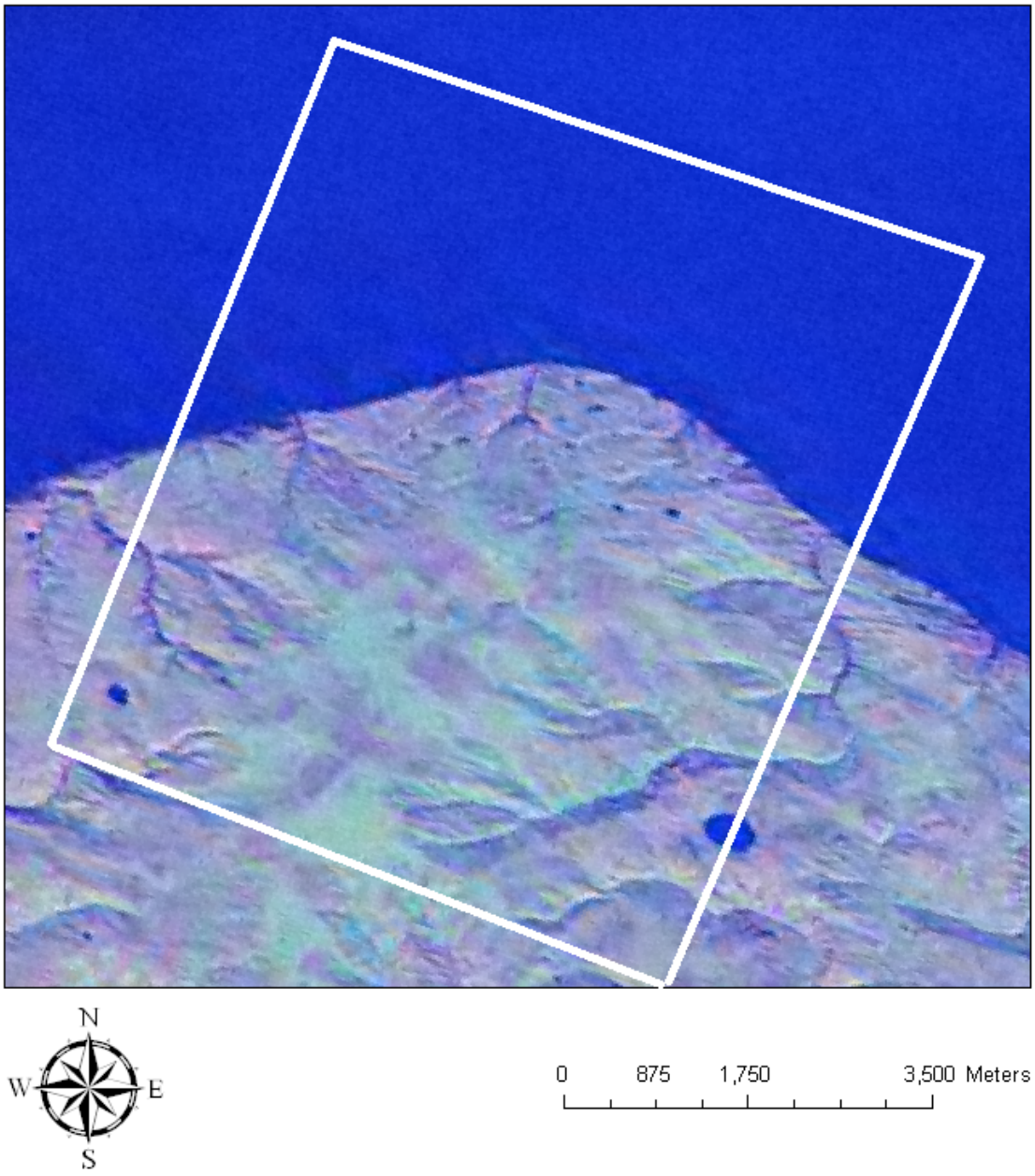

Figure 3.6: Landsat (1990 composite) image of Herschel Island, with GIMMS 8×8km footprint in white

3.4 Data processing

For all data sets, masking of pixels composed mostly of water was conducted according to the internal classifications of each data set. Within each product, if a pixel was labelled 'water' at any point throughout the time series, this pixel was then assigned a 'Not a Number' (NaN) in Matlab to ensure it is masked out for the entire duration of analysis. All calculations and analysis were conducted in Matlab 7.6 (R 2008a).

3.4.1 Temperature, productivity and NDVI

Surface temperature from APP-x, NDVI from GIMMS and NPP from GloPEM are available processed and georeferenced. GloPEM NPP estimates (grams of C per m^2 per 15 days) are available on a 15-day 8km×8km resolution from 1981-2000.

In addition to assessing NDVI over time for three study sites, estimates of maximum annual NDVI will be generated in order to assess changes in maximum greeness (as done for northern Alaska by *Jia et al.* (2003)). Maximum annual NDVI is additionally recognized as a reliable indicator of pan-Arctic aboveground phytomass (*Raynolds et al.*, 2006).

Pan-Arctic estimates of these characteristics were therefore drawn directly from these products, using coordinate data georeferenced in ArcGIS. The Matlab function `map2pix` was used to convert map coordinates of study sites to the appropriate pixels, and `imcrop` was used to extract the specified locations from the datasets. Programming loops were used in Matlab to batch crop, process, and plot data. In order for phenology and statistics to be estimated, data sets were split into time series matrices where each matrix would be composed of a single row over time. To save memory, each loop would load variables for one matrix, make calculations and then save all variables in a `.mat` file for further processing.

3.4.2 Phenology

GIMMS NDVI has already been atmospherically, cloud and geometrically corrected. GIMMS has also been successfully used in the past by *Yoccoz* (2008) to estimate Arctic phenology. Estimates of productivity will therefore be based directly on the GIMMS product for 1981-2006. Many methods exist for determining key phenological dates, with much variation resulting between methods (*Olthof et al.*, 2008). One of these established methods involves estimating the day at which NDVI=50% of mean maximum annual NDVI at each pixel for both spring (as NDVI is rising) and autumn (as NDVI is falling) [Figure 3.7]. The aforementioned method was used for estimating phenology in this thesis because it requires only remote sensing input (and no further model or field inputs), and is widely used in remote sensing studies of phenology. The shortcoming of this approach is that it doesn't relate closely to field derived measurements of key spring and autumn dates as the time at which buds open, and leaves begin to dessicate and fall. Each sequence of NDVI images was assessed to determine the threshold for each individual pixel, defined as half of the mean (1982–2006) maximum annual NDVI [Figure 3.8].

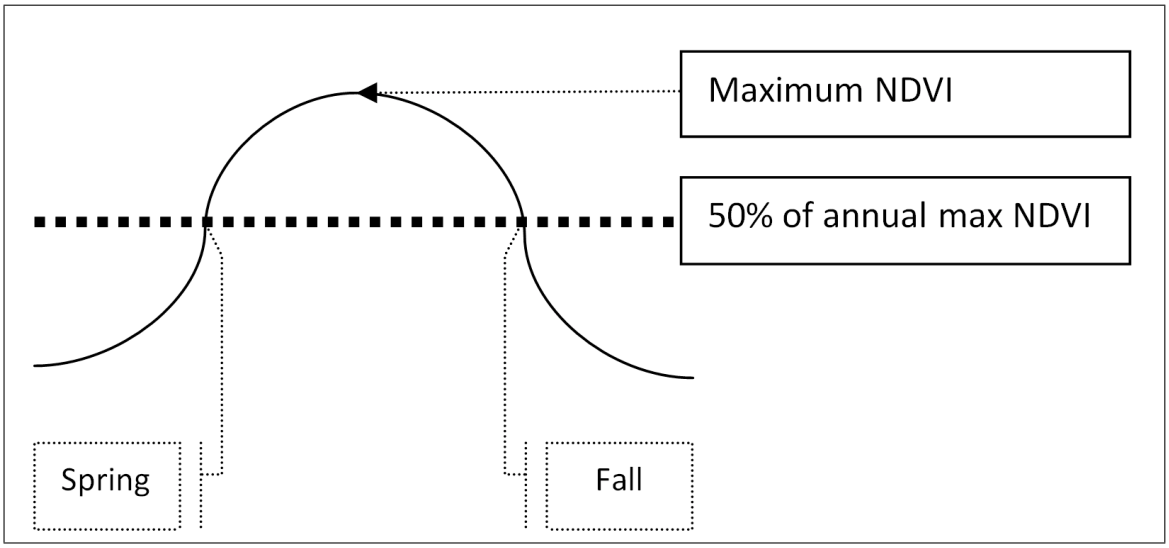

Figure 3.7: Illustration of interpolated GIMMS NDVI over time with identification of key spring and autumn dates as 50% of annual maximum NDVI

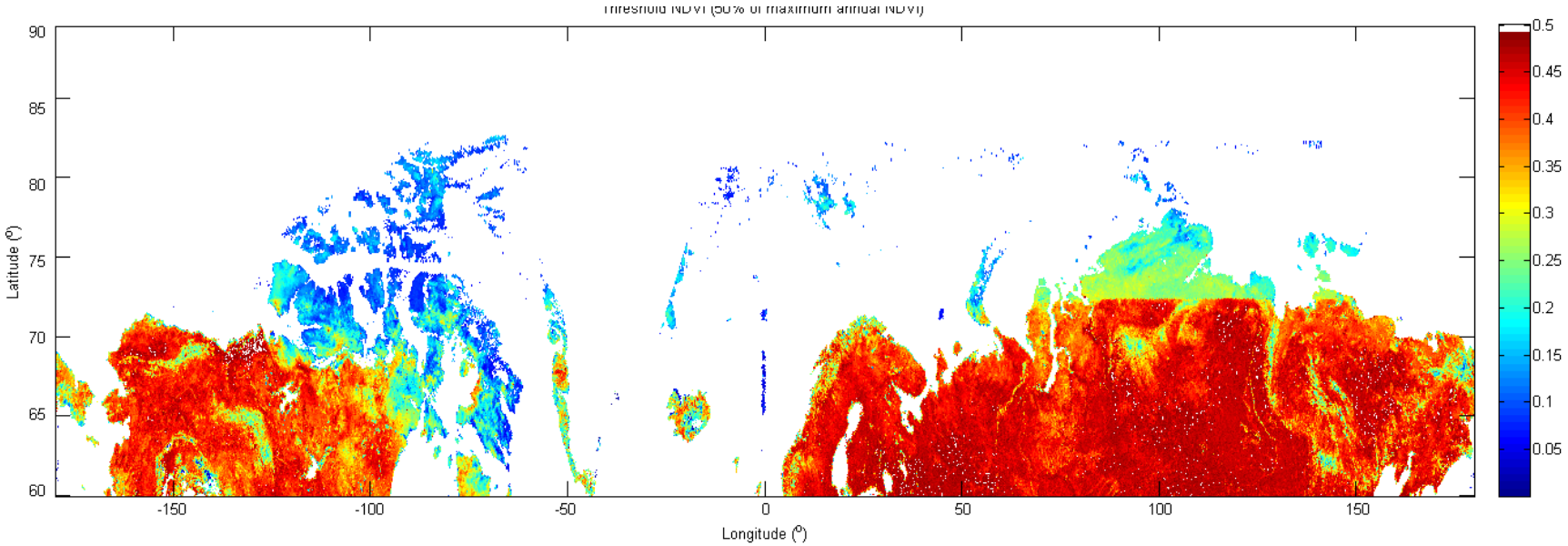

Figure 3.8: Pan-Arctic phenology threshold NDVI (half of mean (1982–2006) annual maximum NDVI)

NDVI was then interpolated linearly and in two-dimensions using the Matlab function `interp1` in order to have NDVI estimates for each day from 1982 to 2006. Key dates were defined as the date at which NDVI goes from below to above pixel-specific thresholds in spring, and vice versa in autumn. Processing pan-Arctic phenology was conducted column by column across the entire scene to minimize matrix size. Site level phenology was determined by following a single 8×8km pixel over time.

3.5 Net primary productivity (field)

Field net primary productivity readings were collected by Robert L. Jefferies, Emma Horrigan and other students/field assistants between 1989 and 2003 at two field sites in La Perouse Bay, east of Churchill named Randy's Flat and East Bay. In each year, biweekly samples of aboveground vegetation (g/m^2) were taken at 5-6 locations at each study site from May to August (*Jefferies*, 2008). For the purpose of comparing field to GloPEM NPP, samples from the 5-6 locations at each study site were averaged and compared directly to GloPEM.

3.6 Statistical analysis and plotting

All statistical tests were conducted at the nominal <0.05 level. No correction for multiple testing was applied, although limitations of this approach are described in the discussion section. Pearson parametric correlation was used for comparing fit between field NPP and GloPEM as well as between Landsat and GIMMS because relationships between these variables were expected to be linear.

Mann-Kendall test and Sen's slope were used to determine change over time in temperature and bioclimatological indicators, as well as to identify relationships be-

tween temperature and bioclimatological indicators. Sen's slope estimates the slope of a univariate time series non-parametrically based on the median slope of paired ordinal points. Mann-Kendall test determines whether decreases and increases in a data set are significant according to the sum of sign differences between observation pairs. Both statistics are considered to be the most useful trend analysis statistics for environmental time series (*Mahey*, 2008), and have been used in many papers such as *Duguay et al.* (2006). Pan-Arctic plots of statistical results were created by first building time series matrices for each column, then calculating statistics for each pixel over time then reconstructing the pan-Arctic scene. Trends in vegetation indices were analyzed both over time, and according to mean annual growing season (May–September) temperatures. Sen's non-parametric slope and Mann-Kendall test non-parametric coefficients were calculated in Matlab using Jeff Burkey's script downloaded from `www.mathworks.com/matlabcentral/fileexchange/11190`.

Bodies of water and ice were masked out in map plots by first assigning the value `NaN` to all water cells and then modifying the `colormap` to display all `NaN` values in white. Plotting was done in Matlab using `hist` for histograms, `plot` for dot plots, and `imagesc` for maps. Trend lines were inserted in plots according to Sen's slope value for time series which indicated significant (α <0.05) change over time according to Mann-Kendall. Because the intercept for these values is unknown, the median value was instead used to center the trend line.

Chapter 4

Results

Results and discussion are divided below according to the various aims of this thesis. Within each section, results are provided first for the three study sites with appropriate figures as well as Mann-Kendall test test results and Sen's slope to detect changes over time and relationship between changes in bioclimatological characteristics and mean May–September temperature. Results are then provided for changes over the pan-Arctic according to Mann-Kendall test and Sen's slope.

The first section focuses on findings regarding albedo and temperature using the AVHRR Polar Pathfinder Extended (APP-x), since these provide an important context for further discussions regarding climate-induced changes in pan-Arctic vegetation. The next section assesses NDVI, NPP and NDVI-derived phenology over time to look at the response of vegetation. The third section compares remote sensing products to one another (GloPEM NPP vs GIMMS NDVI, MODIS EVI/NDVI vs GIMMS NDVI, and GIMMS vs Landsat NDVI), and concludes with a comparison of field vs GloPEM NPP for a study site near Churchill. The final section provides a comparison of pan-Arctic changes over time and according to mean May–September temperature according to 5^o latitudinal bands, 20^o longitudinal bands and for the entire pan-Arctic.

4.1 APP-x temperature

The increase in temperature at Fosheim is significant at the mean annual, March–May and growing season (May–September) time periods [Table 4.1]. However, rises in temperature observed in March–May and June–August are not significant. In summary, rises in temperature at Herschel are not significant. Fosheim underwent an increase in mean annual and growing season temperature. Churchill temperatures in June–August rose significantly.

	Herschel	Churchill	Fosheim
Mean annual temperature	0.06	0.04	**0.17**
Mean May–Sept temperature	0.07	0.10	**0.26**
Mean March, April & May temperature	0.09	0.04	**0.09**
Mean June, July & August temperature	0.05	**0.09**	0.34

Table 4.1: Temporal trend in APP-x temperature variables in terms of Sen's slope ($^oC/year$) (1982–2004). Results considered significant according to Mann-Kendall test (α <0.05) appear in bold.

Pan-Arctic increases in mean seasonal land surface temperature of 1^oC per decade (1982–2004) are observed for spring, summer and fall months equally [Figure 4.1] from monthly AVHRR Polar Pathfinder Extended (APP-x) readings. These results are consistent with recent findings by *Wang and Key* (2003) of significant (α <0.1) increases in mean temperature for the entire pan-Arctic (land and ocean).

Significant increases in temperature are highest in south-eastern Alaska/Yukon and Novaya Zemlaya (Russia) [Figure 4.8]. Increases in temperature are also concentrated in northeastern Russia, north and south-west Alaska and Nunavut, Ellesmere Island and Baffin Island. Maximum decreases in temperature are smaller than maximum increases in temperature, and are only concentrated in coastal Iceland, Greenland and central Scandinavia.

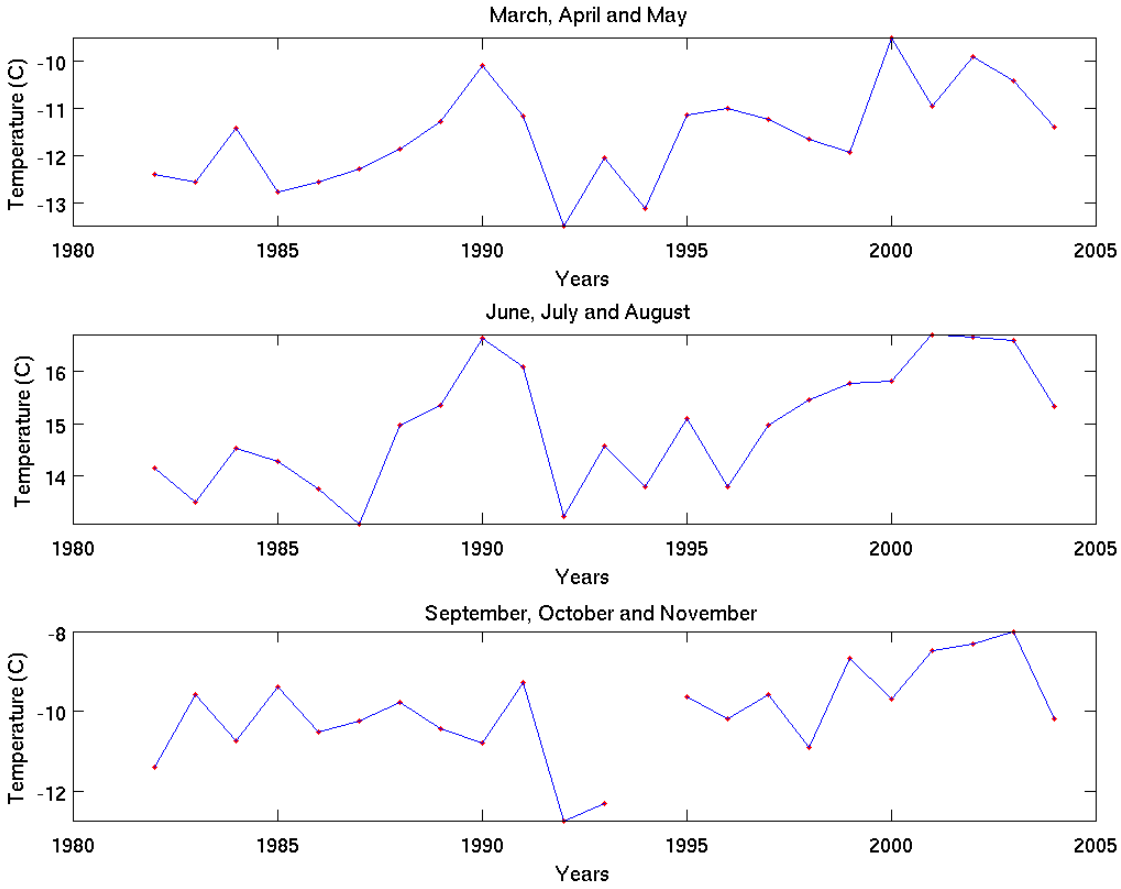

Figure 4.1: Mean pan-Arctic land surface temperature (C) 1982–2000, as divided per season (spring- top, summer- middle, and fall- bottom)

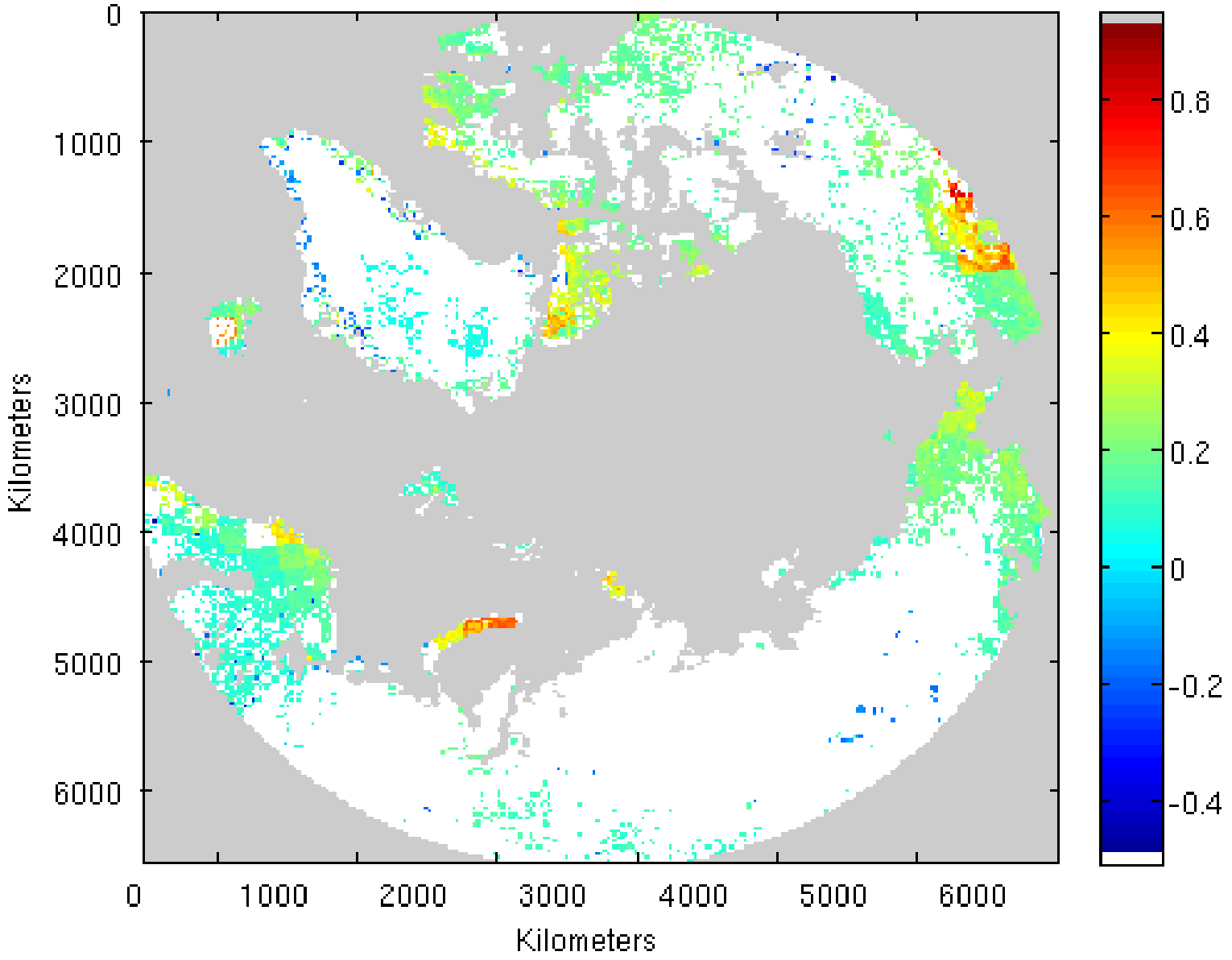

Figure 4.2: Pan-Arctic Sen's slope of significant (according to Mann-Kendall test) changes in mean summer (May–September) temperature

4.2 Vegetation indices

The following subsection describes changes over time in maximum annual NDVI over time. Phenology is estimated from GIMMS NDVI in section 4.2.3.

4.2.1 GIMMS NDVI

At the three study sites, NDVI displays regular, periodic and seasonal changes, with equal amplitude at maximum NDVI over time. NDVI is very low in winter due to the small difference between the quantity of red and infrared radiation reflected from snow. As the snow melts and aboveground biomass increases, NDVI rises because plant chlorophyll preferentially absorbs red radiation whereas plant mesophyll reflects infrared radiation (*Pettorelli et al.*, 2005). Senescence of vegetation in autumn again causes a drop in NDVI [Figure 4.3].

An increase in maximum annual NDVI (1982–2006) was observed at Herchel [Table 4.2]. However, maximum annual NDVI at the other two study sites does not vary significantly over time. No change was observed in the date of peak annual NDVI. Plots of maximum annual NDVI values and the percentage of anomaly of maximum NDVI to mean maximum NDVI (defined as maximum annual NDVI divided by the fraction of the long term average) can be found in Figures C.2 and C.3, respectively. Changes in the timing and size of maximum annual NDVI are not explained by mean annual growing season temperature [Table 4.3].

	Herschel	Churchill	Fosheim
Maximum annual NDVI	**0.01**	-0.00	-0.00
Date of maximum annual NDVI	0.00	0.00	0.00

Table 4.2: Temporal trend in GIMMS NDVI in terms of Sen's slope (NDVI/year and ordinal days/year) (1982–2006). Results considered significant according to Mann-Kendall test (α <0.05) appear in bold.

	Herschel	Churchill	Fosheim
Maximum annual NDVI	0.00	0.00	0.00
Date of maximum annual NDVI	0.00	-0.03	0.00

Table 4.3: Trend in GIMMS NDVI according to mean annual growing season temperature in terms of Sen's slope (NDVI/^{o}C) (1982–2004). No results are significant according to Mann-Kendall test (α <0.05).

At the pan-Arctic scale, variations in maximum annual NDVI were first tracked, and then classified according to Circumpolar Arctic Vegetation Map (CAVM) maximum NDVI ranges [Figure 4.4]. Plotting the surface area (km^2) covered by each vegetation classification over time, likewise, indicates that there are no significant net differences over time in relative maximum greenness [Figure 4.5].

However, the locations of differences in maximum annual NDVI does change over time [Figure 4.6]. Significant increases in peak annual NDVI were observed along the Arctic Circle in North America (northern Alaska, northern Yukon, northern Northwest Territories and southern Nunavut), western Greenland, Iceland, Scandinavia/western Russia and eastern Russia. Significant decreases in peak annual NDVI were observed in central Alaska and southern Northwest Territories, as well as north-central Russia. All in all, many regions experienced shifts in maximum annual NDVI although the average area covered by each CAVM categorization remains unchanged.

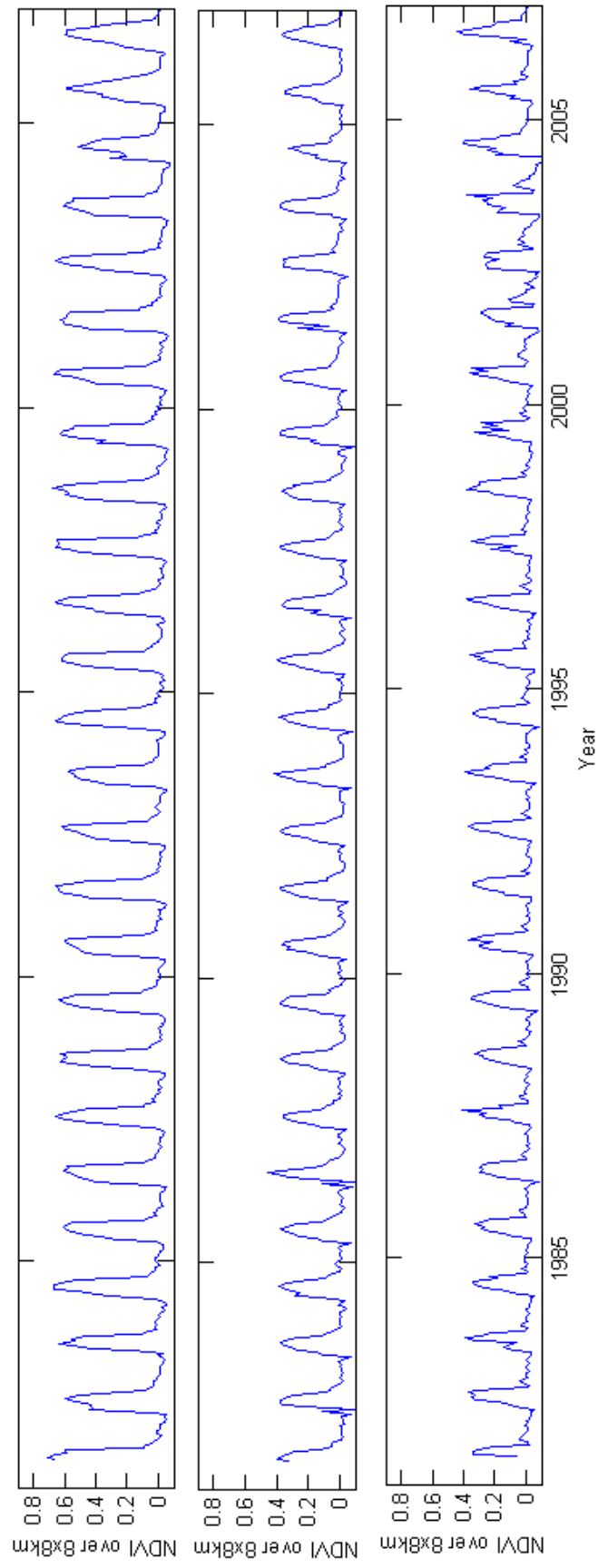

Figure 4.3: GIMMS biweekly NDVI 1981–2006 at Churchill (top), Fosheim (middle) and Herschel (bottom)

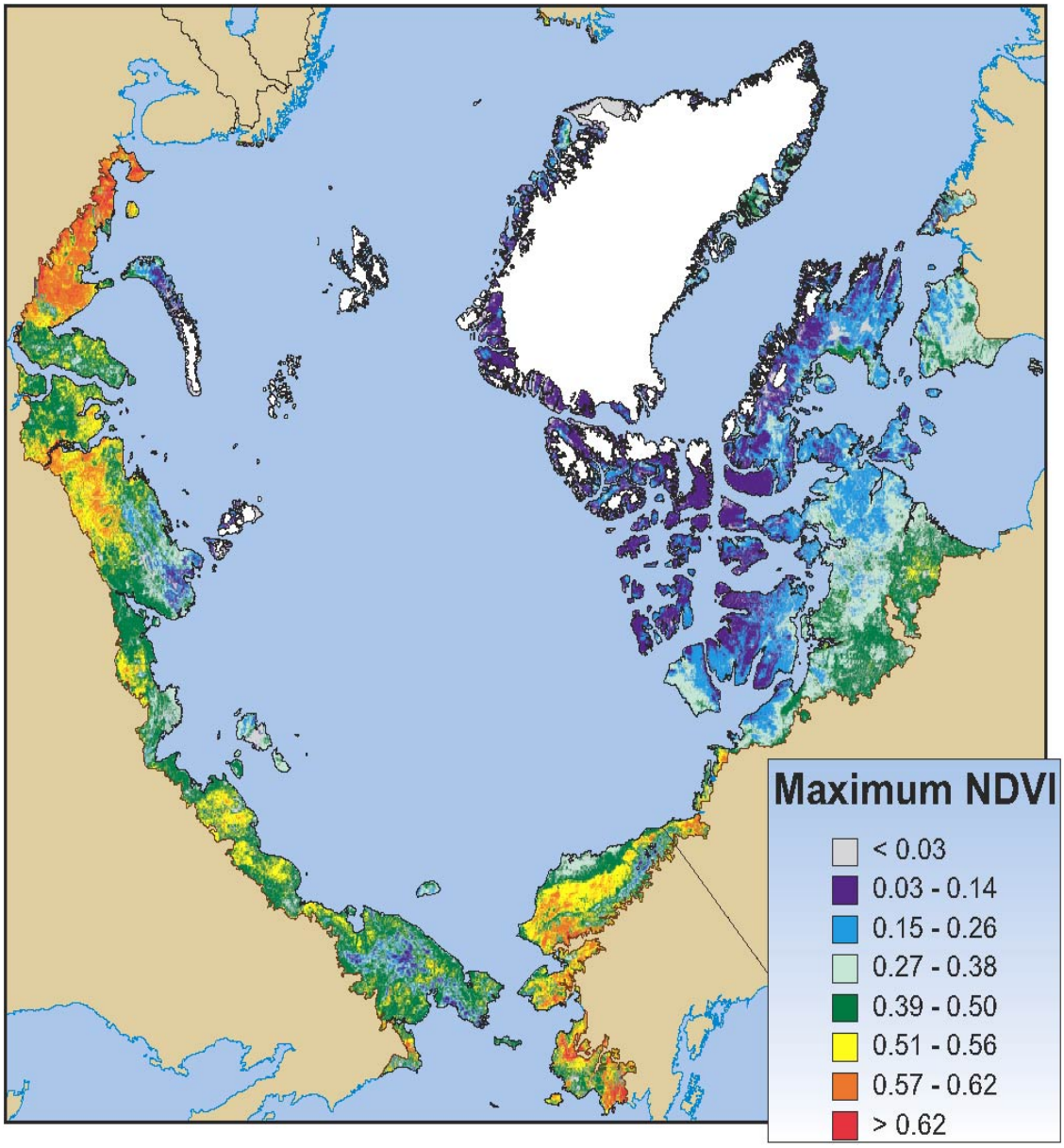

Figure 4.4: Circumpolar Arctic Vegetation Map mean annual maximum NDVI classifications from *Walker et al.* (2005)

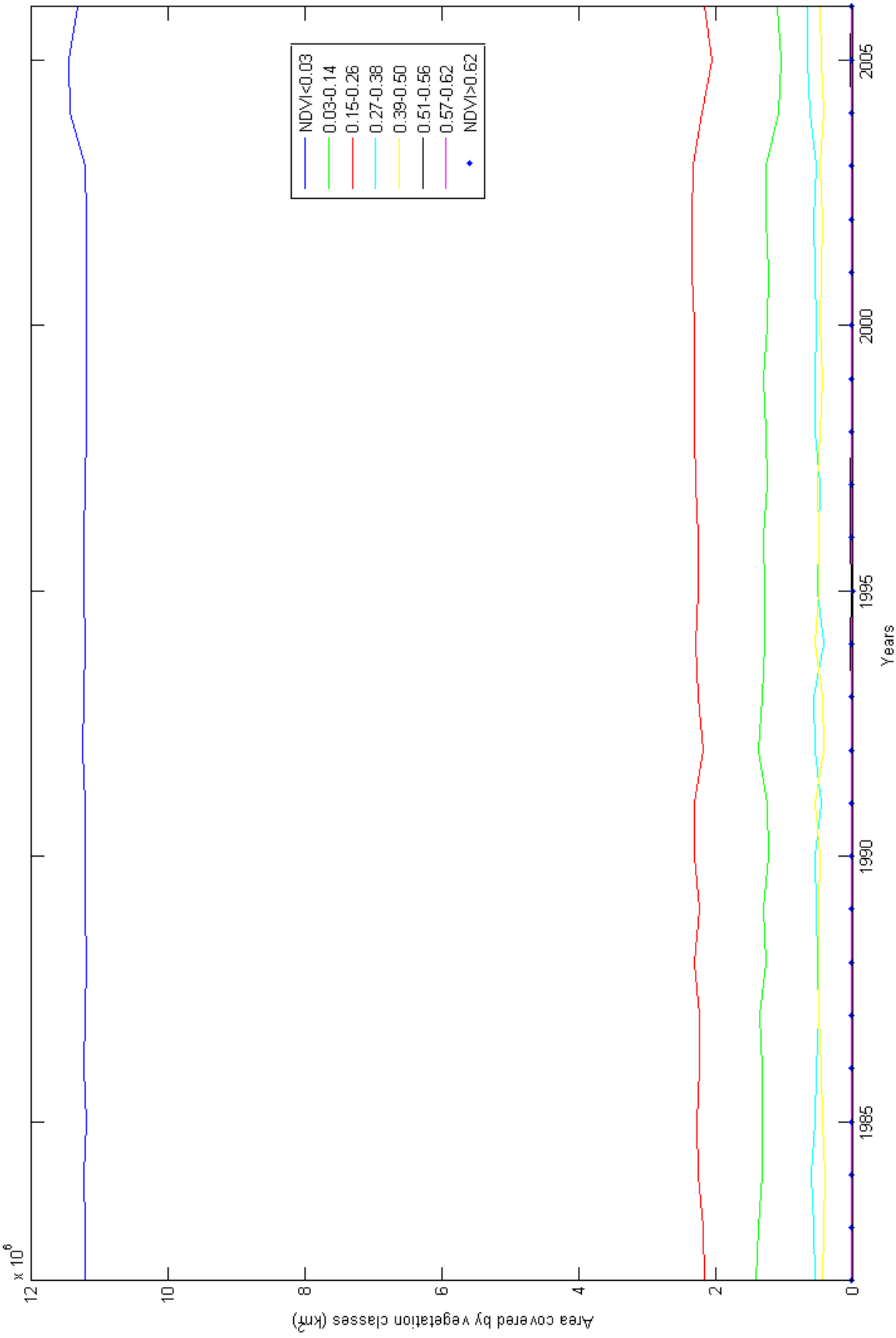

Figure 4.5: Pan-Arctic area (km^2) covered by eight maximum annual NDVI classifications

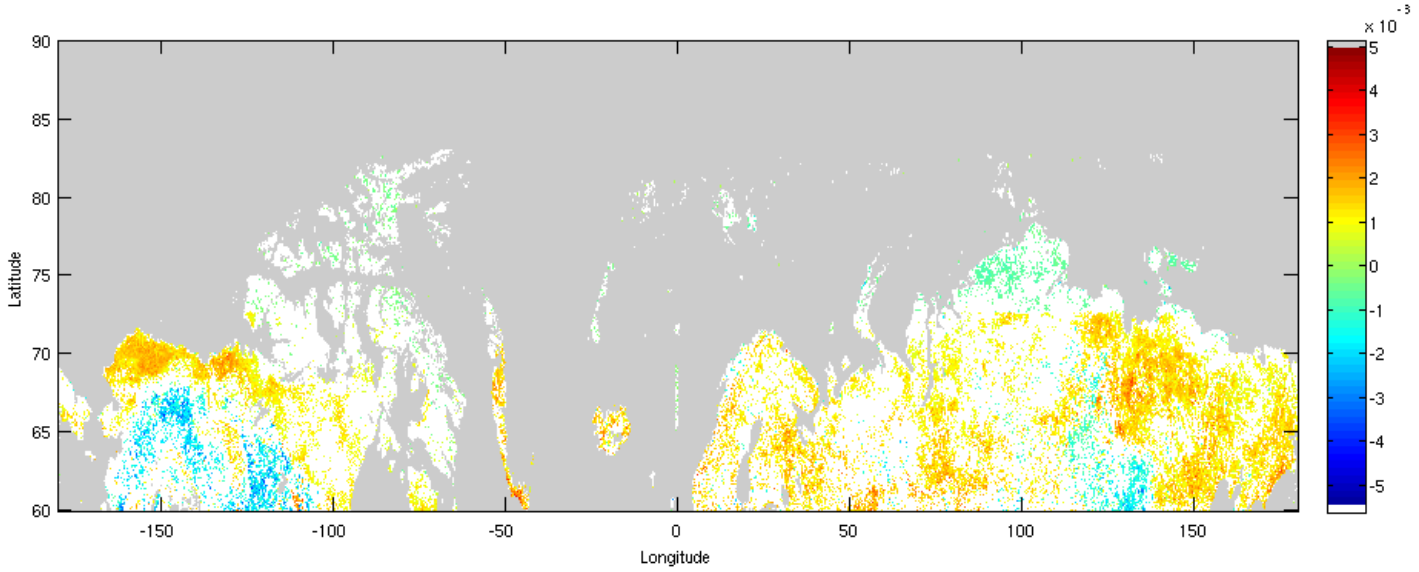

Figure 4.6: Pan-Arctic Sen's slope of significant changes in maximum annual NDVI (according to Mann-Kendall test)

4.2.2 GloPEM NPP

NPP has a similar seasonal cycle to NDVI, with no NPP in winter and peak NPP around the beginning of August, depending on site. At Herschel Island, Churchill and Fosheim Peninsula, no significant change is observed over time (1982–2000) in total annual NPP and maximum annual NPP. The date of maximum annual NPP does not change significantly at any site [Table 4.4]. However, it is interesting to note the magnitude of total annual NPP Sen's slope is quite large, despite the lack of slope significance according to Mann-Kendall. It is therefore likely that there are large outlying pairs of observations of total annual NPP, although the sum of all pairwise differences is not greater than that which would be expected due to chance.

However, although changes in NPP over time are not significant at Churchill, increases in total annual NPP and maximum annual NPP at Churchill can be explained by increases in mean growing season temperature [Table 4.5]. Changes in total annual NPP, maximum annual NPP and the timing of peak annual NDVI at the other study sites cannot be explained by changes in growing season temperature.

	Herschel	Churchill	Fosheim
Total annual NPP (gC/m^2/year)	-3.19	3.58	0.37
Maximum annual NPP (gC/m^2/10 days)	-1.14	0.53	0.07
Date of maximum annual NPP (ordinal days/year)	0.24	-0.10	0.20

Table 4.4: Temporal trend in GloPEM NPP in terms of Sen's slope (1982–2000). Results considered significant according to Mann-Kendall test (α <0.05) appear in bold.

	Herschel	Churchill	Fosheim
Total annual NPP	12.7	**27.1**	5.00
Maximum annual NPP	-0.43	**3.48**	1.53
Date of maximum annual NPP	0.00	0.00	0.00

Table 4.5: Trend in GloPEM NPP according to mean annual growing season temperature in terms of Sen's slope ($gC/m^2/^oC$) (1982–2000). Results considered significant according to Mann-Kendall test (α <0.05) appear in bold.

Mean annual pan-Arctic GloPEM NPP increases substantially (9%) between 1982 to 2000 by 25 gC/year/m^2. Grouping mean annual NPP according to 2.5^o latitudinal pan-Arctic bands indicates that the increase in NPP is greatest at 63.5-67.5^{o}N ($\approx$ 40 gC/year/m^2).

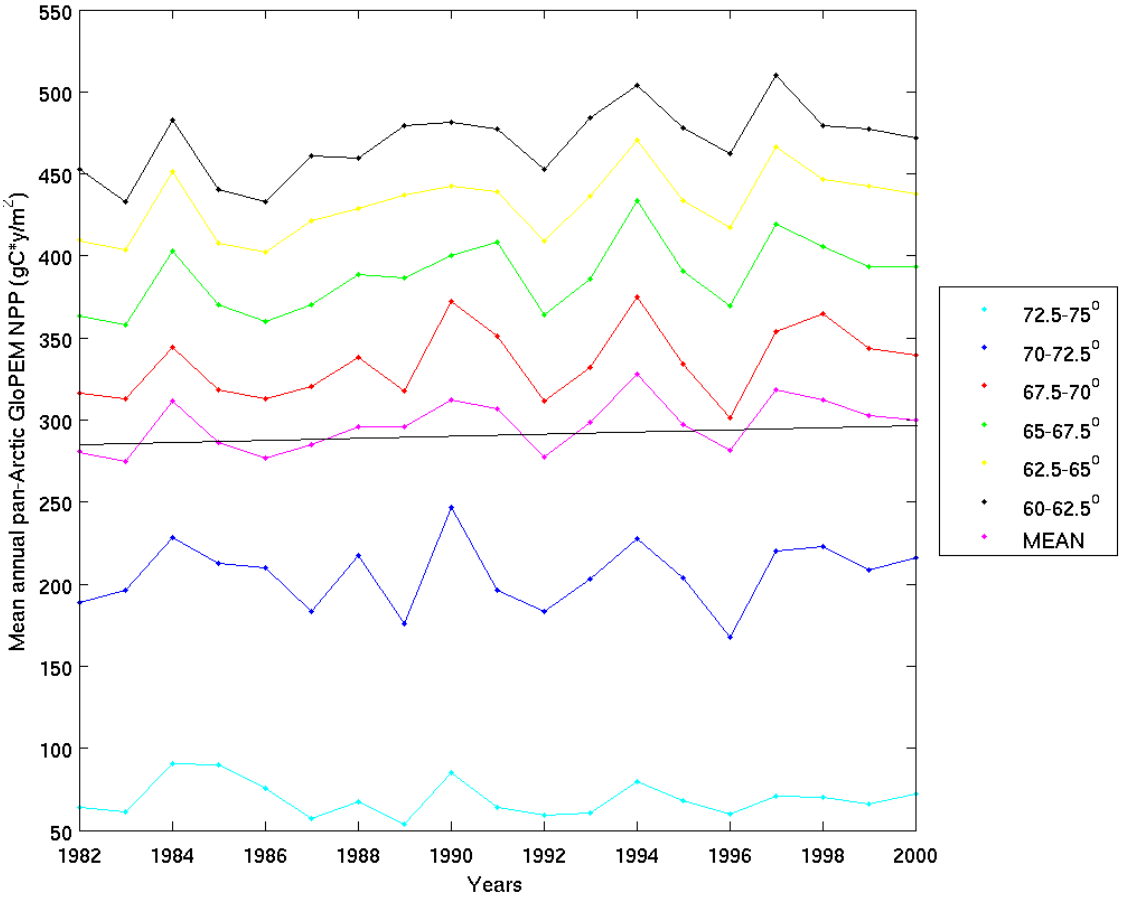

Figure 4.7: Pan-Arctic total annual NPP grouped according to 2.5 degree latitudinal bands (gC/m^2/year). Trend line according to Sen's slope indicated in black.

Significant increases in total annual NPP are observed in northern Yukon, southern Finland, western Norway and central Russia. Decreases are limited to small regions of northeast Alaska and Banks Island [Figure 4.8]. Churchill has a much higher reading for total annual NPP than readings within the pan-Arctic diagram; however, this is likely because Churchill is 2^o south of 60^{o}N, and is therefore outside the pan-Arctic range of this figure.

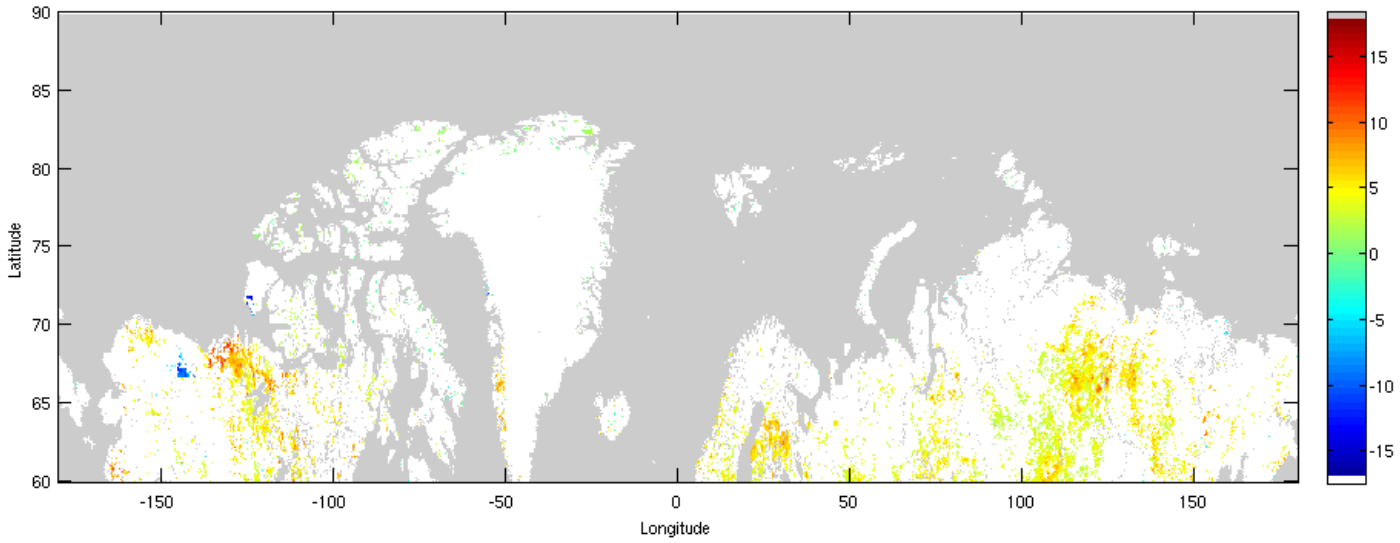

Figure 4.8: Pan-Arctic Sen's slope of significant changes in total annual NPP (according to Mann-Kendall test)

4.2.3 GIMMS NDVI-derived phenology

Phenology is an important indicator of climatic response of vegetation which has dramatic consequences for Arctic food webs that rely on synchronous timing of plant, insect and animal populations. Figure 4.9 shows autumn onset in Churchill over time. Key autumn phenology dates in Churchill are stable every year near day 250 within a small range of variation until 2004, when it begins rising dramatically up to day 294 in 2005. It appears that autumn onset has been delayed by about a month on average after 2004 [Figure 4.9]. Fosheim peninsula undergoes greater variability in autumn onset ($\pm$15 days), although 2006 is again the record high for the period [Figure 4.10]. Herschel Island [Figure 4.11] autumn onset dates vary slightly between day 254 and 258 until 2005–2006, where autumn onset is late by over 10 days.

Spring onset, likewise, is relatively similar every year near Churchill until 2005, with a range of variation of less than 30 days. In 2005, spring onset is $\approx$50 days later than over the previous years. 2006 and 2007 spring onset is later than during the period 1982-2004 [Figure 4.12]. The onset and end dates of snow melt onset for Churchill remain relatively stable (2000-2006) and agree well with the dates at which NDVI is equal to 50% of mean maximum annual NDVI, with snow melt [Figure 4.13]. Spring onset on Herschel varies greatly (>100 days) over the entire 1982-2007 period, with only a slight indication of earlier spring onset in 2005-2007 that is likely not significant [Figure 4.14]. As with Churchill, the date of spring onset in vegetation corresponds very closely to the dates of snow melt onset and end [Figure 4.15]. Fosheim Peninsula spring onset varies by >30 days throughout the study time period, with a slight shift to later spring onset from 2002 onwards [Figure 4.16]. Spring onset co-occurs with snow melt onset and end near Fosheim [Figure 4.17].

In summary, over 1982 to 2006, spring continues arriving at the same time at Herschel Island, and arrives later at Fosheim and Churchill. Autumn onset (1982–2006) becomes later at Churchill and Herschel Island. When comparing spring onset dates to snow on/off dates gathered by *Wang et al.* (2008), it appears that there is a very close fit between snow onset dates and the date at which vegetation reaches 50% of its annual maximum for all three study sites. However, years with double peaks in linearly interpolated NDVI cause mistakes in phenology estimates that prevent very good fit between snow melt end/onset and spring phenology. Filtering of noise caused by snow, snow sublimation and lakes would likely lead to improved accuracy in detecting spring phenology, and improved fit between snow melt and phenology estimates.

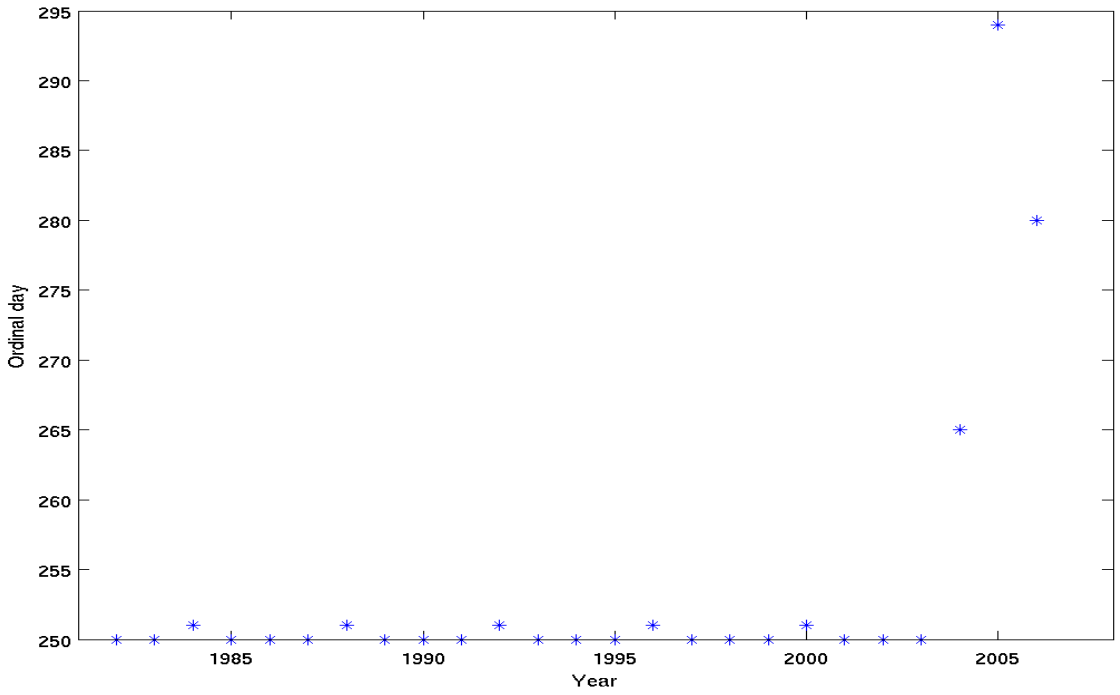

Figure 4.9: Fall phenology dates at Churchill

Despite many variations in year to year spring and fall onset dates observed in the Figures 4.9–4.17, these changes are not significant [Table 4.6]. These fluctuations over time have low Sen's slope values and do not indicate change according

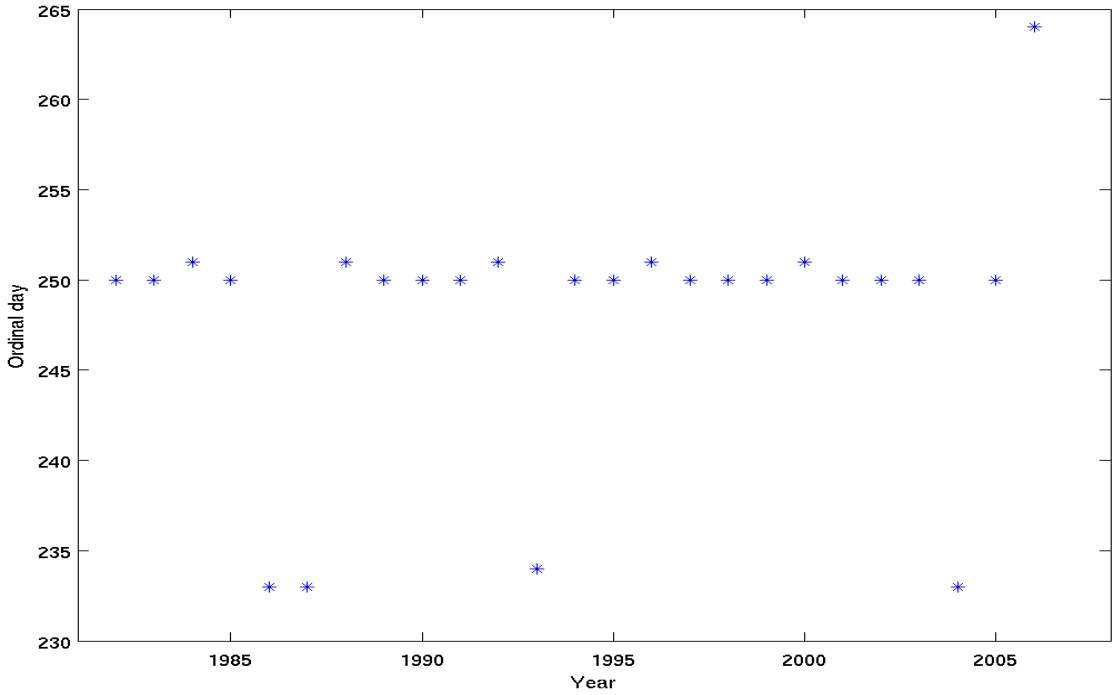

Figure 4.10: Fall phenology dates at Fosheim

to Mann-Kendall tests, and are therefore considered as noise.

When compared to changes in growing season temperature, however, increases in temperature appear to be related to earlier spring onset [Table 4.7]. However, the slope of these changes may be exaggerated for these three sites since Churchill and Herschel have both undergone non-significant and small (<=0.1 Sen's slope) increases in mean annual and mean growing season temperature. Fosheim, a site which has undergone significant increases in temperature, does not show a significant relationship between spring onset and growing season temperature. At all three sites, autumn onset is not related to changes in growing season temperature.

	Herschel	Churchill	Fosheim
Ordinal date of autumn onset	0.00	0.33	0.20
Ordinal date of spring onset	0.03	0.00	0.35

Table 4.6: Temporal trend in GIMMS NDVI-derived phenology in terms of Sen's slope (ordinal days/year) (1982–2006). Results considered significant according to Mann-Kendall test (α <0.05) appear in bold.

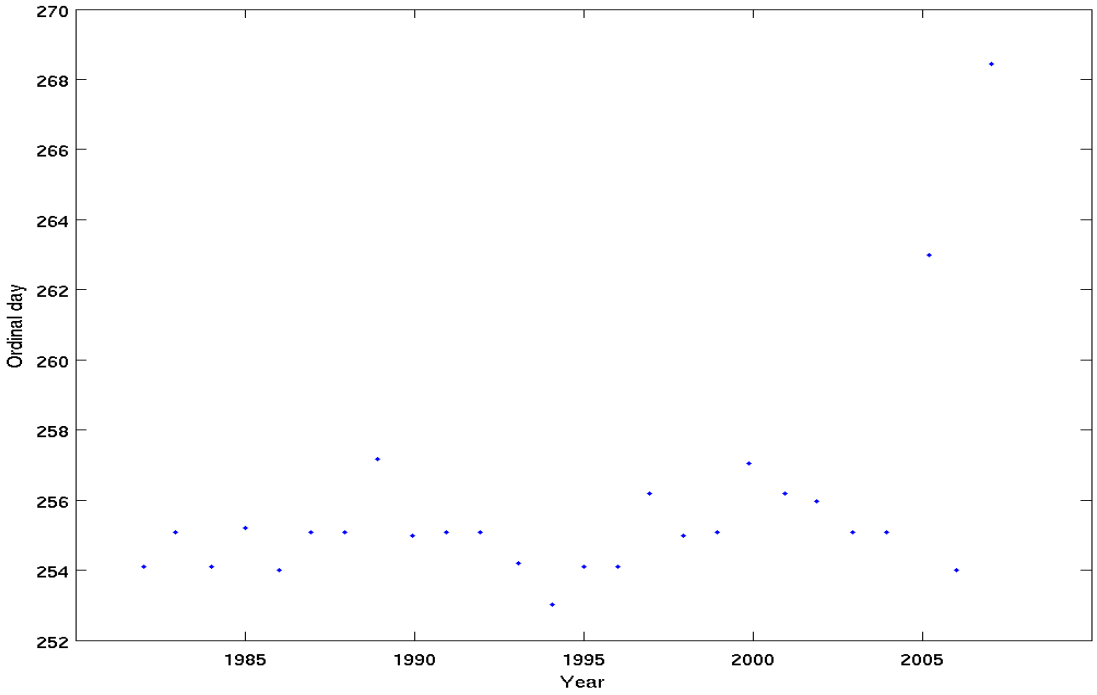

Figure 4.11: Fall phenology dates at Herschel

	Herschel	Churchill	Fosheim
Ordinal date of autumn onset	0.00	0.33	0.20
Ordinal date of spring onset	**-3.40**	**-2.38**	0.50

Table 4.7: Trend in GIMMS NDVI-derived phenology according to mean annual growing season temperature in terms of Sen's slope (ordinal days/^{o}C) (1982–2004). Results considered significant according to Mann-Kendall test (α <0.05) appear in bold.

Observations of later fall onset are thinly dispersed across southern Scandinavia and western Russia [Figure 4.18]. Delays in spring onset are observed on Ellesmere Island and northern Russia. Spring onset is slightly delayed in southern Scandinavia and central Russia [Figure 4.19].

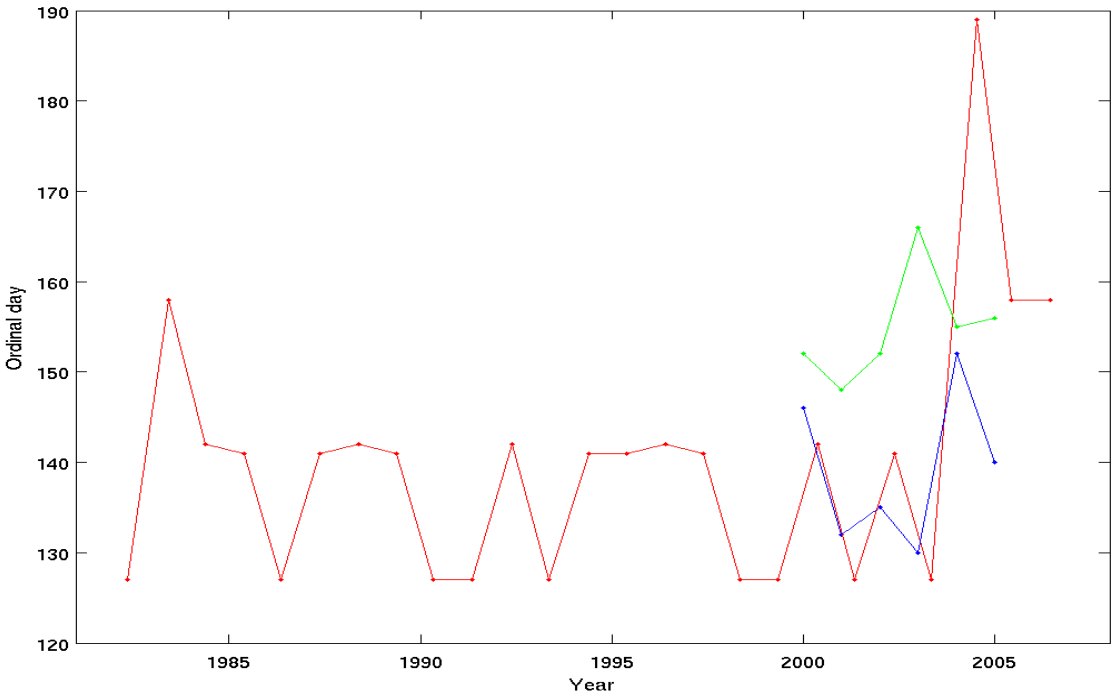

Figure 4.12: Spring phenology dates at Churchill (red) estimated from GIMMS NDVI compared to (*Wang et al.*, 2008) snow melt onset (blue) and end (green) dates.

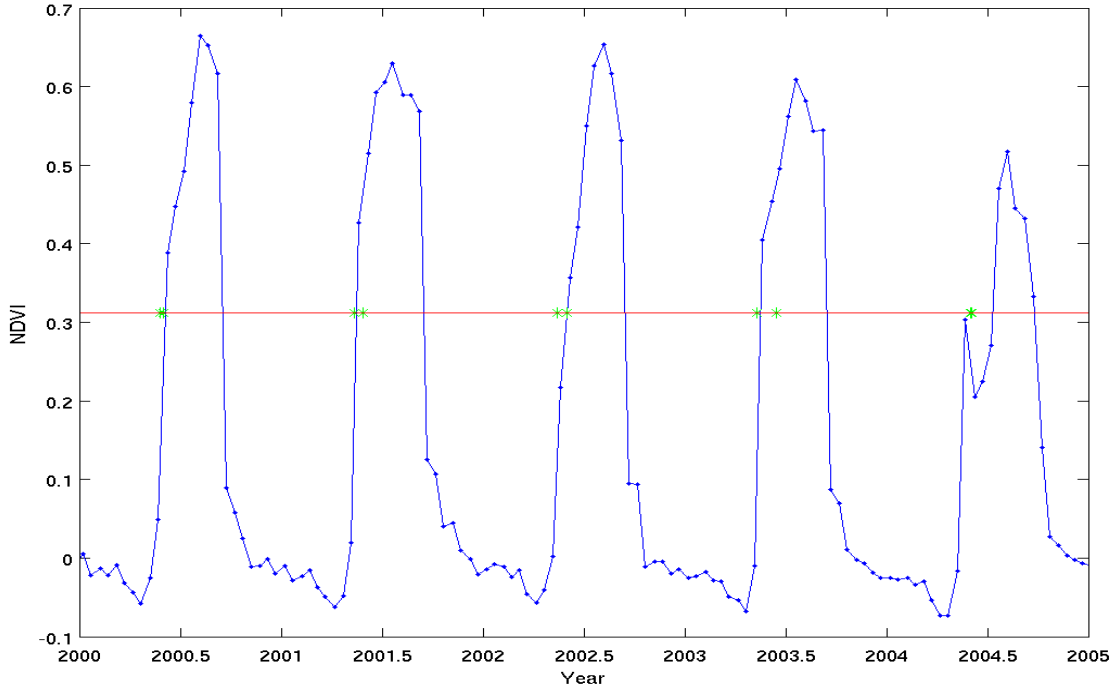

Figure 4.13: Spring phenology dates at Churchill (blue) compared to (*Wang et al.*, 2008) snow melt onset/end dates (green). Threshold NDVI indicated in red.

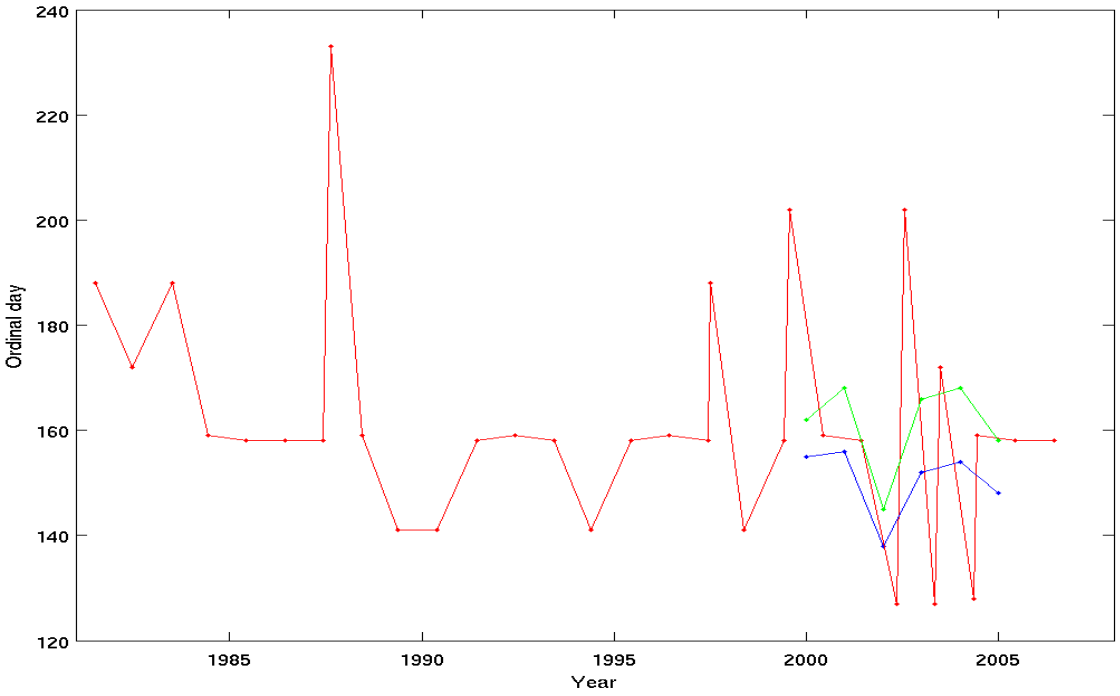

Figure 4.14: Spring phenology dates at Herschel (red) estimated from GIMMS NDVI compared to (*Wang et al.*, 2008) snow melt onset (blue) and end (green) dates.

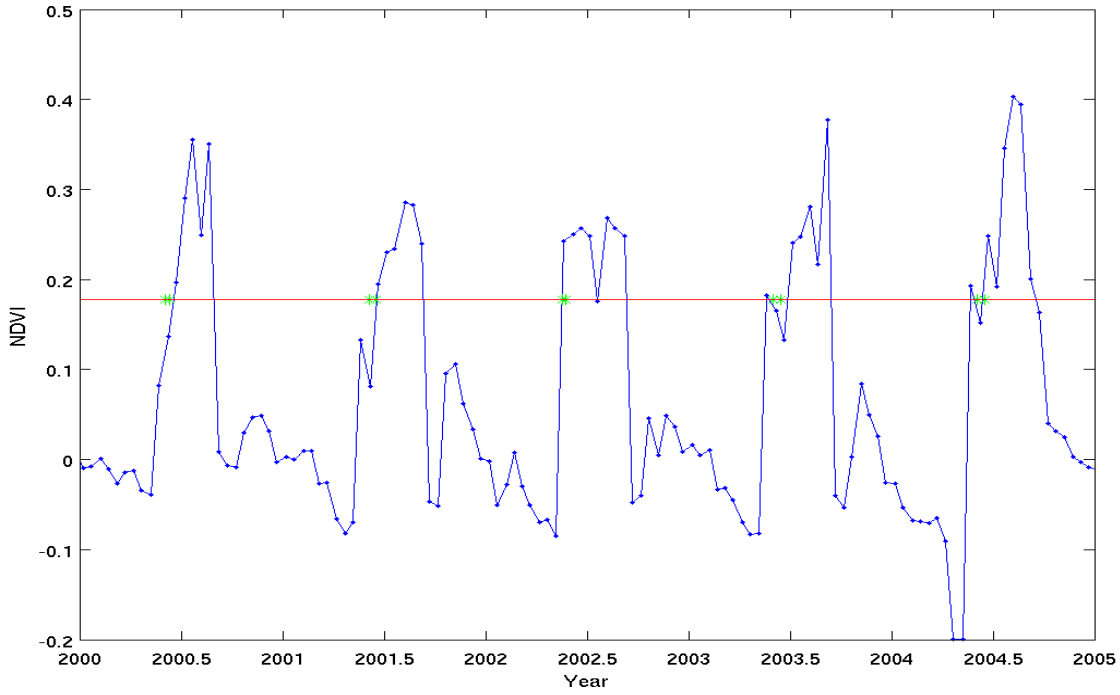

Figure 4.15: Spring phenology dates at Herschel (blue) compared to (*Wang et al.*, 2008) snow melt onset/end dates (green). Threshold NDVI indicated in red.

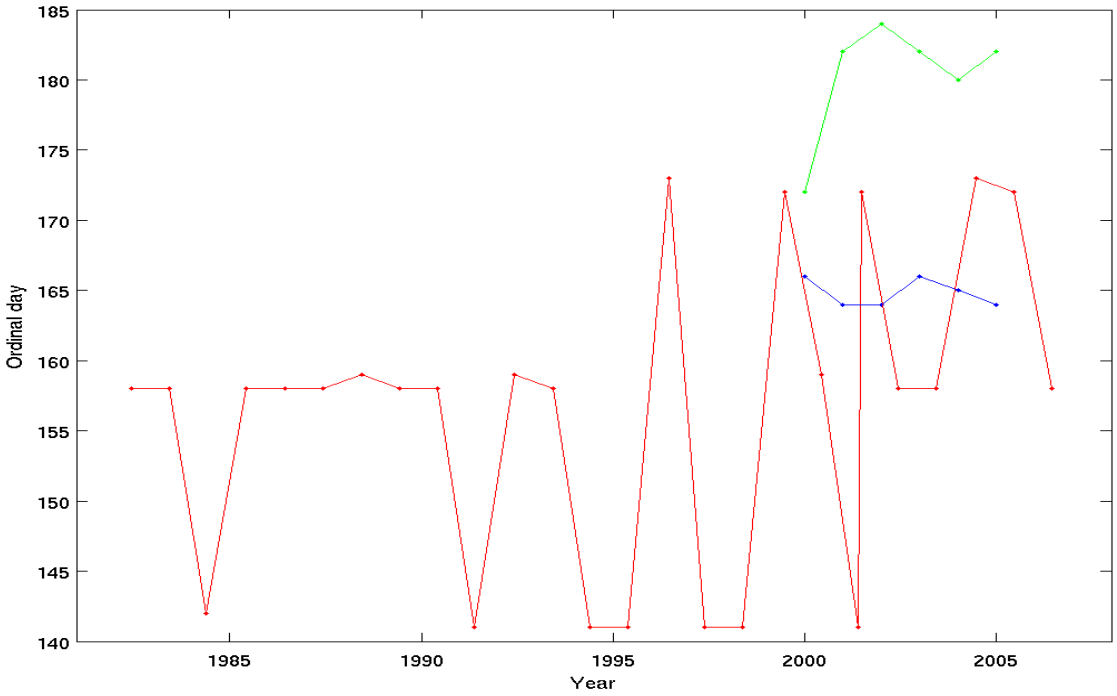

Figure 4.16: Spring phenology dates at Fosheim (red) estimated from GIMMS NDVI compared to (*Wang et al.*, 2008) snow melt onset (blue) and end (green) dates.

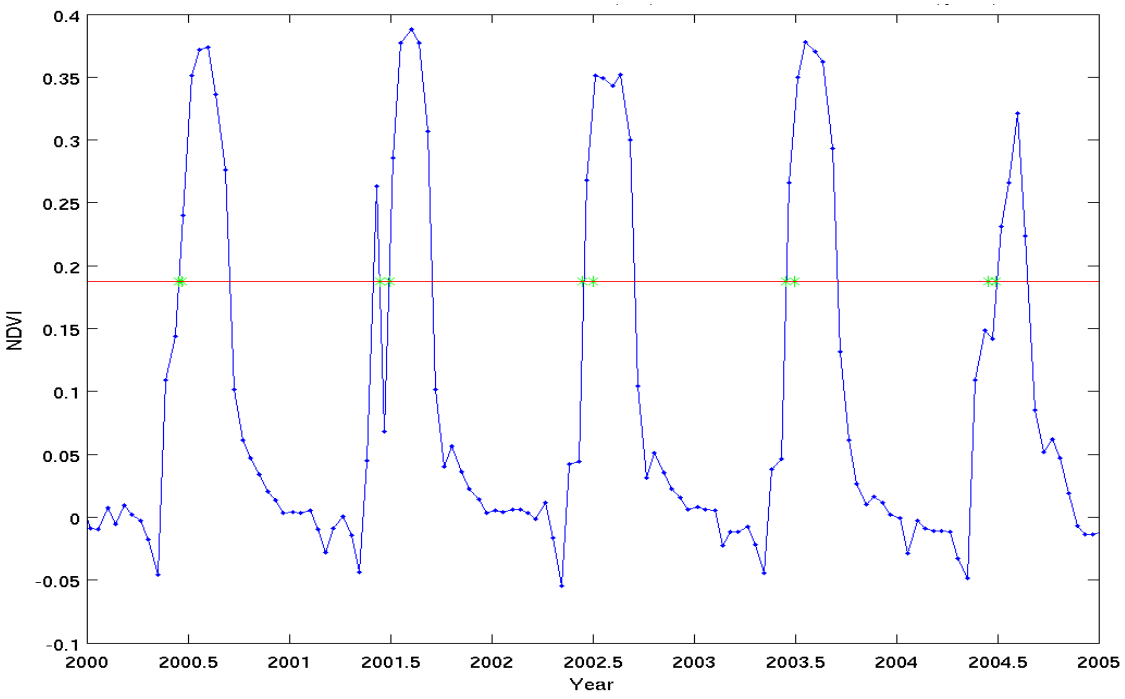

Figure 4.17: Spring phenology dates at Fosheim (blue) compared to (*Wang et al.*, 2008) snow melt onset/end dates (green). Threshold NDVI indicated in red.

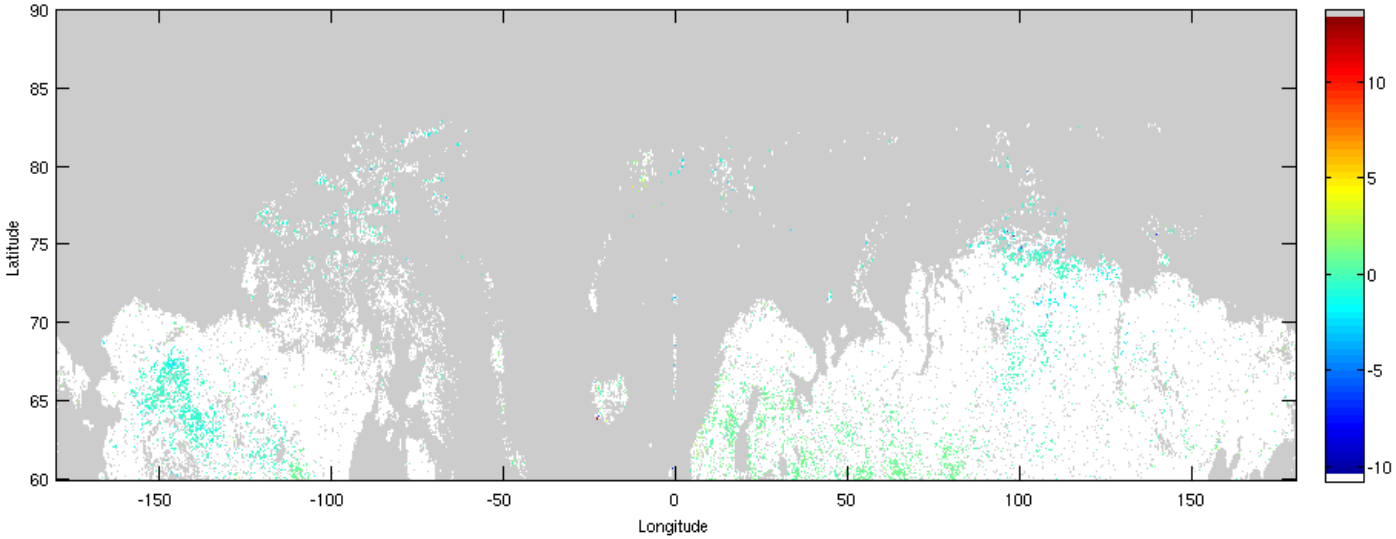

Figure 4.18: Pan-Arctic Sen's slope of significant changes in fall phenology (according to Mann-Kendall test)

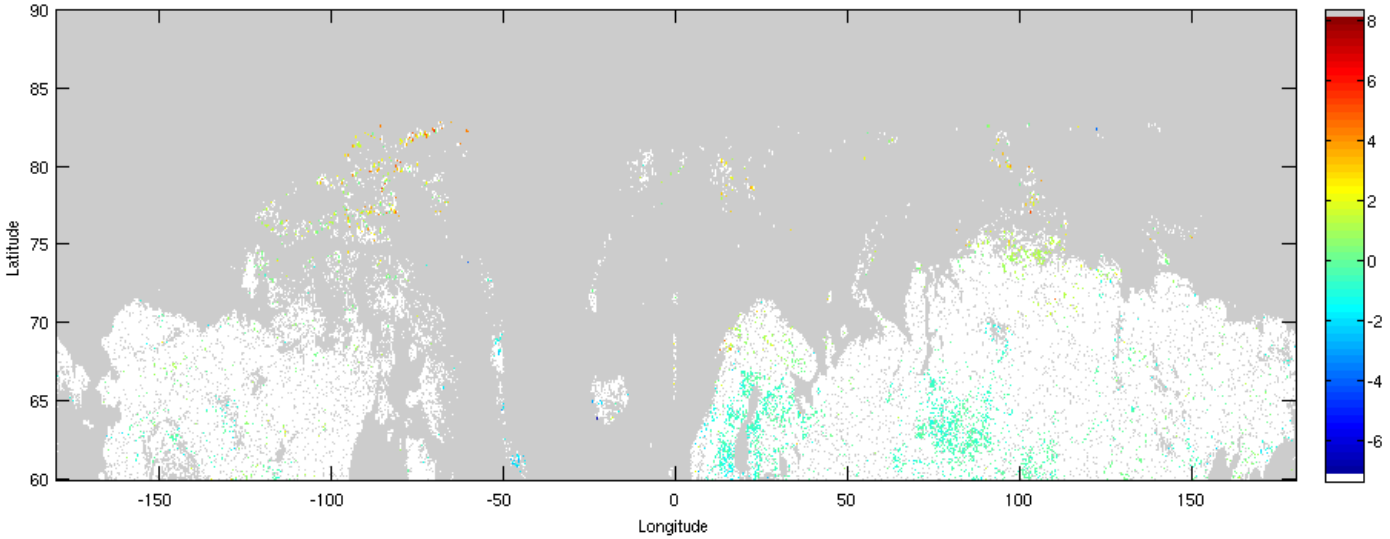

Figure 4.19: Pan-Arctic Sen's slope of significant changes in spring phenology (according to Mann-Kendall test)

4.3 Data product comparison

4.3.1 MODIS NDVI & EVI to GIMMS NDVI

GIMMS NDVI was compared to summertime (May to September, or MJJAS) MODIS NDVI and EVI readings for years 2002–2006. MODIS NDVI and EVI were not collected for winter readings because these are beyond the Arctic growing season, and thus beyond the scope of this study.

MODIS EVI gives a much lower estimate than MODIS NDVI, and gives lower readings over winter snow [Figure 4.20]. Although the GIMMS product filters water and clouds by producing the maximum NDVI value per fortnight and MODIS averages NDVI, MODIS NDVI appears to overestimate NDVI when comparing the maximum pixel value within MODIS NDVI to GIMMS NDVI. However, GIMMS appears to overestimate NDVI when compared to the pixel value of MODIS averaged over 8×8km. Overestimation is likely due to the difference in spatial resolution between the two products, which means that MODIS is a purer pixel value than GIMMS.

Overall, the timing of MODIS EVI, GIMMS NDVI and MODIS NDVI fit very closely, and it is impossible to determine which product best captures fluctuations in plant biomass without corresponding field measurements. The large drop in MODIS products in winter 2004 indicates a need for correction. Furthermore, MODIS does not appear to pick up on changes in vegeation below the scale of GIMMS [Figure4.20]. The observed discrepancy between in situ and remote sensing NDVI studies of ecology is therefore not due to processes which occur at the <500×500m resolution. Overall, the closeness of timing and fit of the two products, when considered in the context of the greater ease and better atmospheric correction of GIMMS compared to MODIS, confirm the decision to use GIMMS instead of

MODIS for estimating phenology and fit with NPP earlier in this thesis.

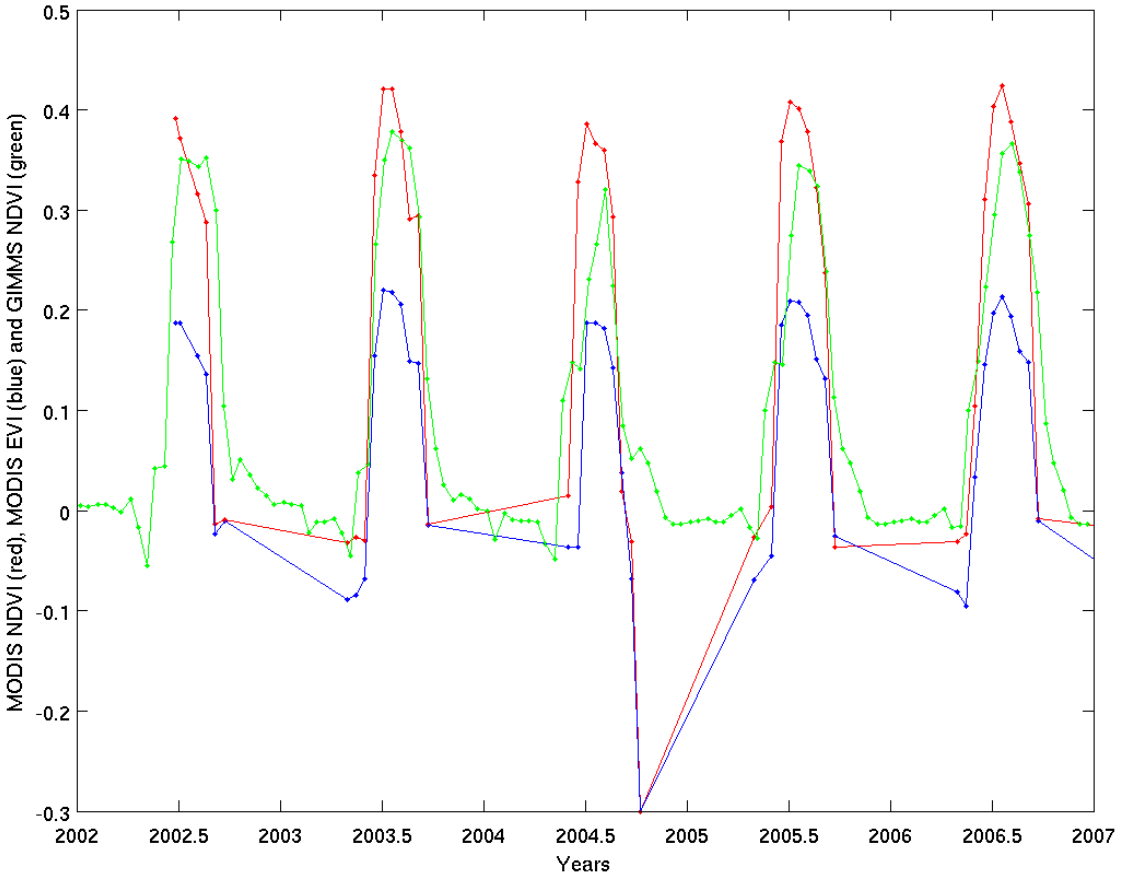

Figure 4.20: Comparison of mean MODIS NDVI (red) & EVI (blue) with GIMMS NDVI (green) near Fosheim (8×8km)

4.3.2 Landsat vs GIMMS NDVI

The following section examines fit between Landsat NDVI and GIMMS NDVI. Although the aforementioned section examined changes at the Fosheim site, Landsat images for this site were ordered in January 2009 and have yet to arrive. GIMMS NDVI was therefore compared to Landsat NDVI for an alternate study site, Herschel Island.

Moderate (Pearson r=0.74, root mean squared error=0.12) agreement exists between Landsat and GIMMS NDVI from 1985 to 2006 [Figure 4.23]. GIMMS appears to overestimate NDVI in comparison to Landsat, as seen in a scatterplot in Figure 4.21. Figure 4.22 examines the distribution of Landsat values for a single date (June 20, 2006) where GIMMS NDVI=0.34, and indicates a skewed distribution of Landsat readings with many low (NDVI<0.1) values. The date selected is representative of other single date examinations of the distribution of Landsat values. The low median estimates of NDVI by Landsat in comparison to GIMMS therefore likely arise from the fact that GIMMS uses the maximum NDVI value, whereas Landsat images selected have up to 20% cloud and high surface water percentages, both of which diminish NDVI.

This confirms the earlier hypothesis that GIMMS overestimates NDVI in comparison to Landsat because, unlike GIMMS, Landsat does not filter out surface water and clouds. Landsat therefore has many more low (NDVI<0.2) readings, although the mode values of Landsat NDVI (NDVI≈0.42) are higher than the GIMMS NDVI value (NDVI=0.34). Since the very low (NDVI< 0.2) readings are unlikely to be due to vegetation, it therefore appears that remote sensing at a 30×30m resolution does not pick up on any additional changes in vegetation not picked up by GIMMS. The discrepancy between field and remote sensing may therefore be either because in situ findings of rapid ecological change may not representative of

larger regions, or because even 30×30m resolution is too coarse to pick up on field scale changes in ecology.

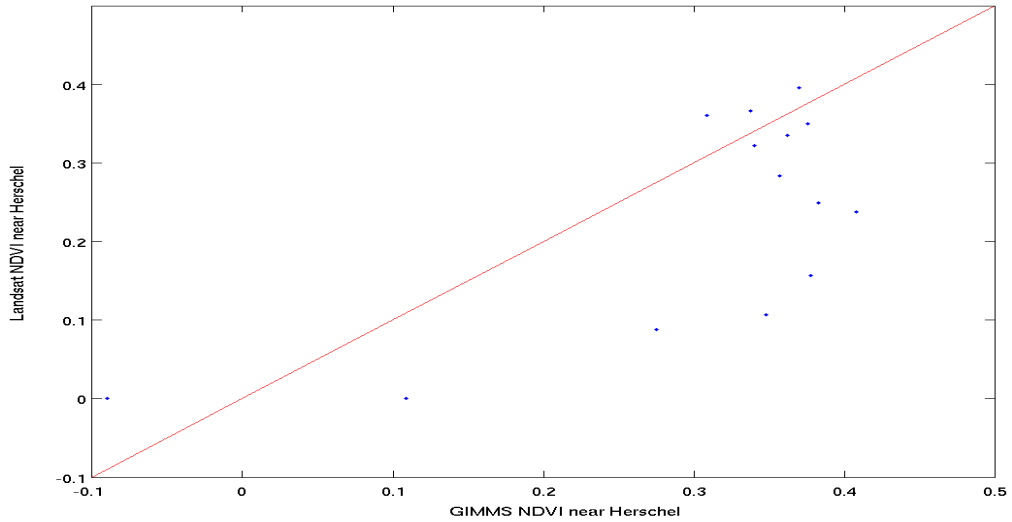

Figure 4.21: Scatterplot of GIMMS NDVI vs Landsat NDVI (Pearson r=0.74)

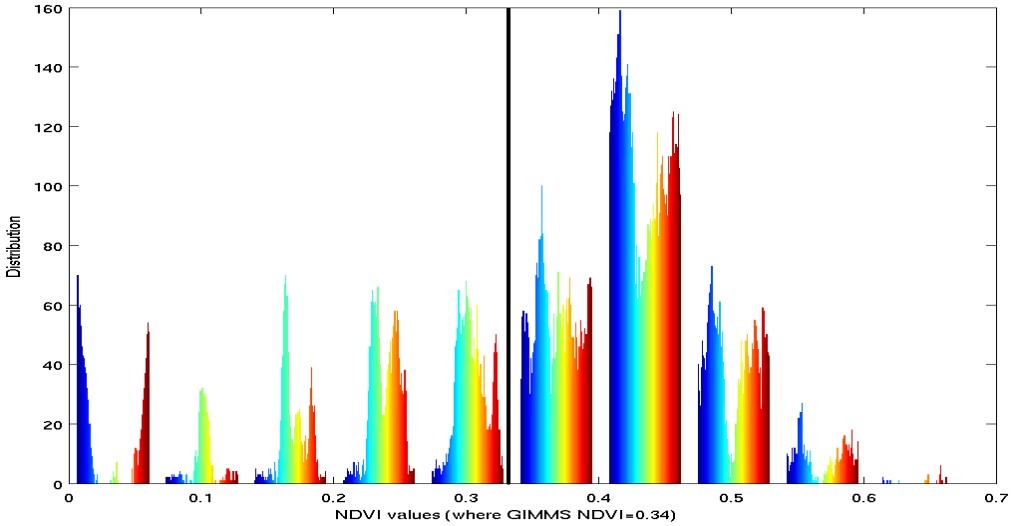

Figure 4.22: Histogram of Landsat pixels near Herschel Island, with vertical black line indicating GIMMS pixel value at this point in time (NDVI=0.34)

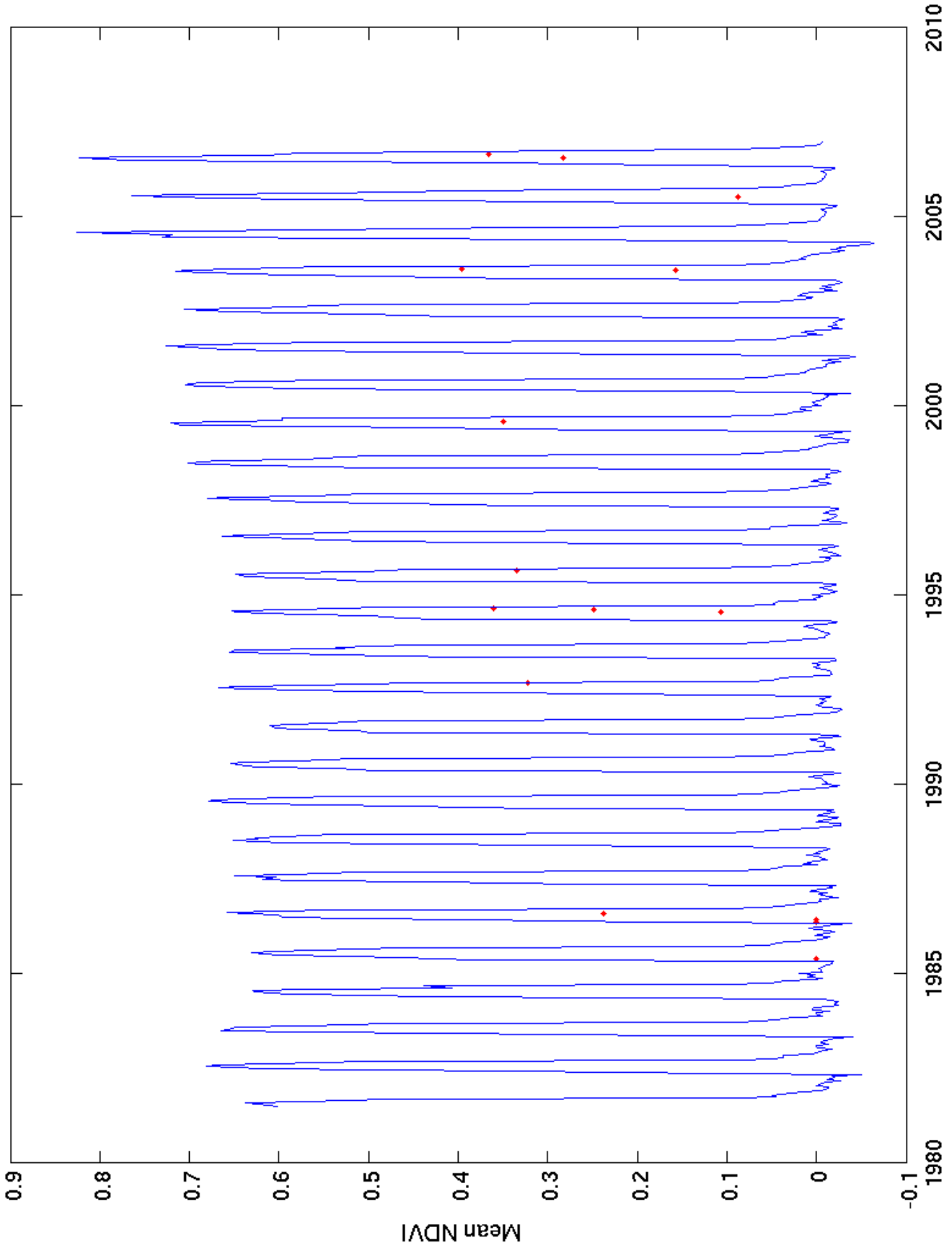

Figure 4.23: Comparison of GIMMS (blue) and mean Landsat (red) at Herschel 1982–2006

4.3.3 Comparison of GloPEM NPP with field NPP

Net primary productivity from satellite measurements was compared with field measurements, with both considered instantaneous measurements. Both field and remote sensing estimates of NPP are in gC/m^2, and are within the same 8×8km region. The time period 1989-2000 was selected for all comparisons based on availability of field data collected by Dr. Robert Jefferies (University of Toronto). GloPEM NPP is moderately correlated with field NPP for East Bay (r=0.50) [Figure 4.24] and not correlated with field NPP for Randy's Flat (r=0.10) [Figure 4.25].

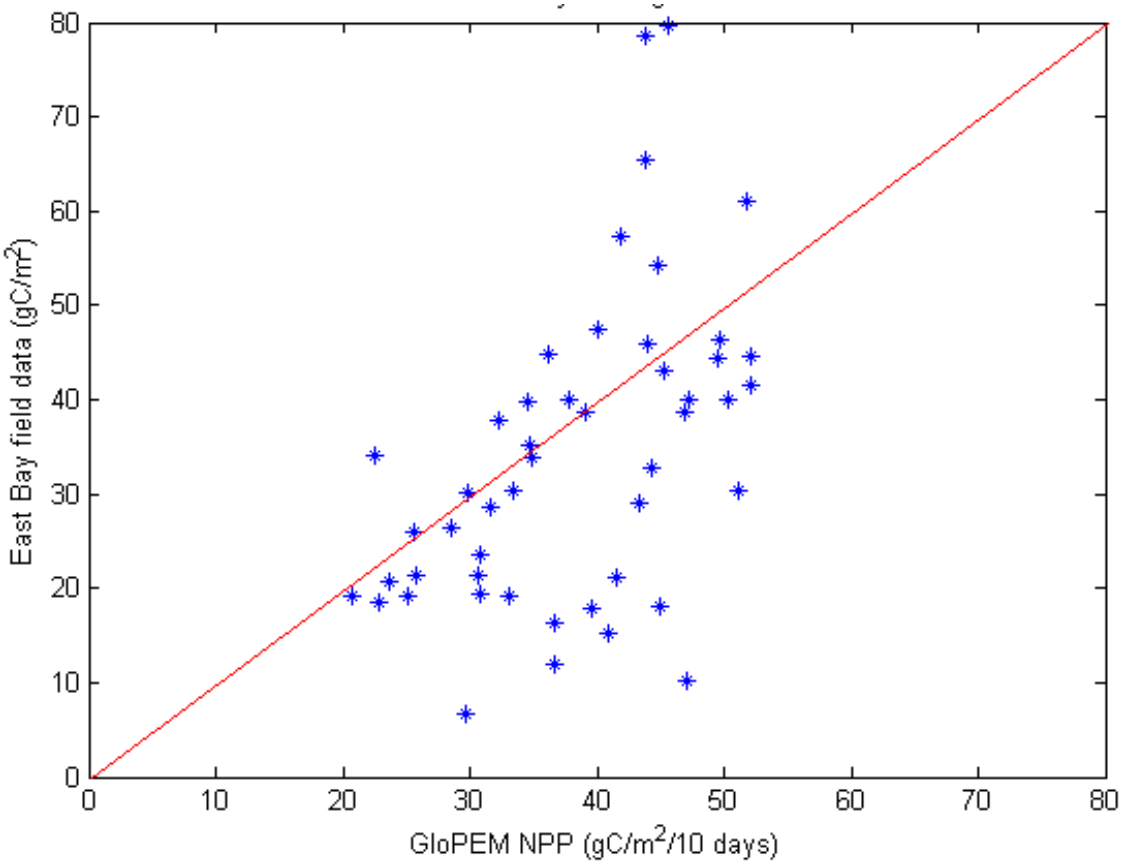

Figure 4.24: Correlation between East Bay and GloPEM NPP

However, field NPP from Randy's Flat and East Bay are moderately correlated (r=0.60). A comparison of GloPEM, Randy's Flat and East Bay NPP over time in Figure 4.26 indicates that GloPEM NPP tends to overestimate start of season NPP

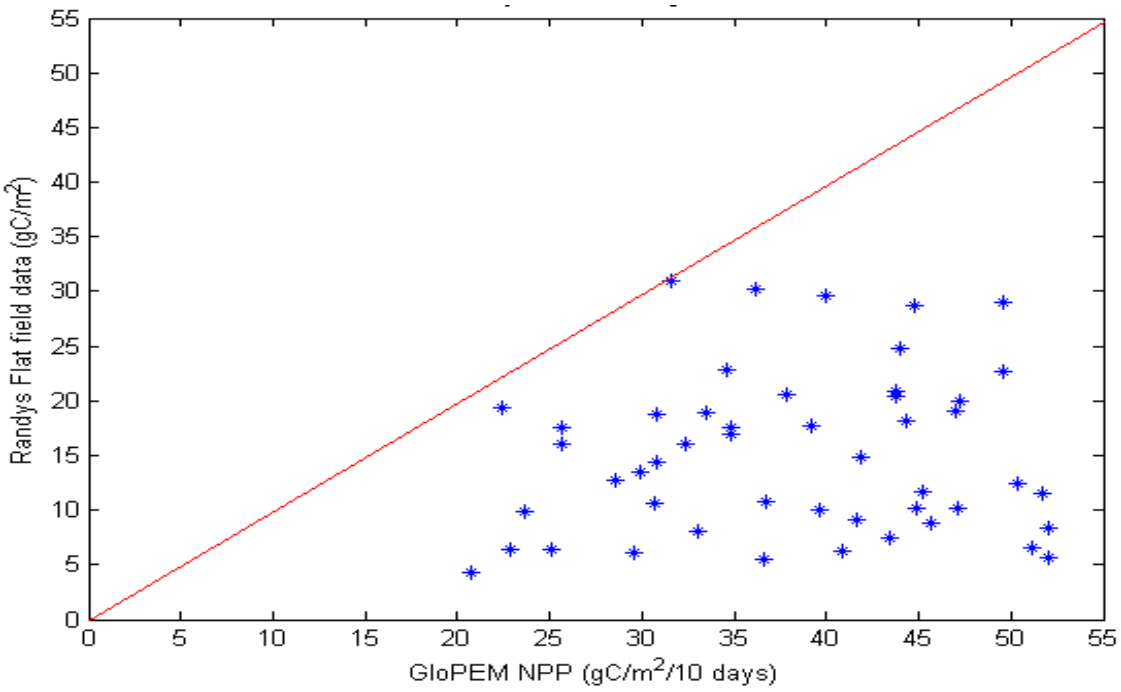

Figure 4.25: Correlation between Randy's Flat and GloPEM NPP

and underestimate peak NPP. This is especially interesting in light of the heavy summertime grazing of this region by snow geese (*Jefferies*, 2008), which would lead to the expected hypothesis that peak field NPP would be overestimated by GloPEM.

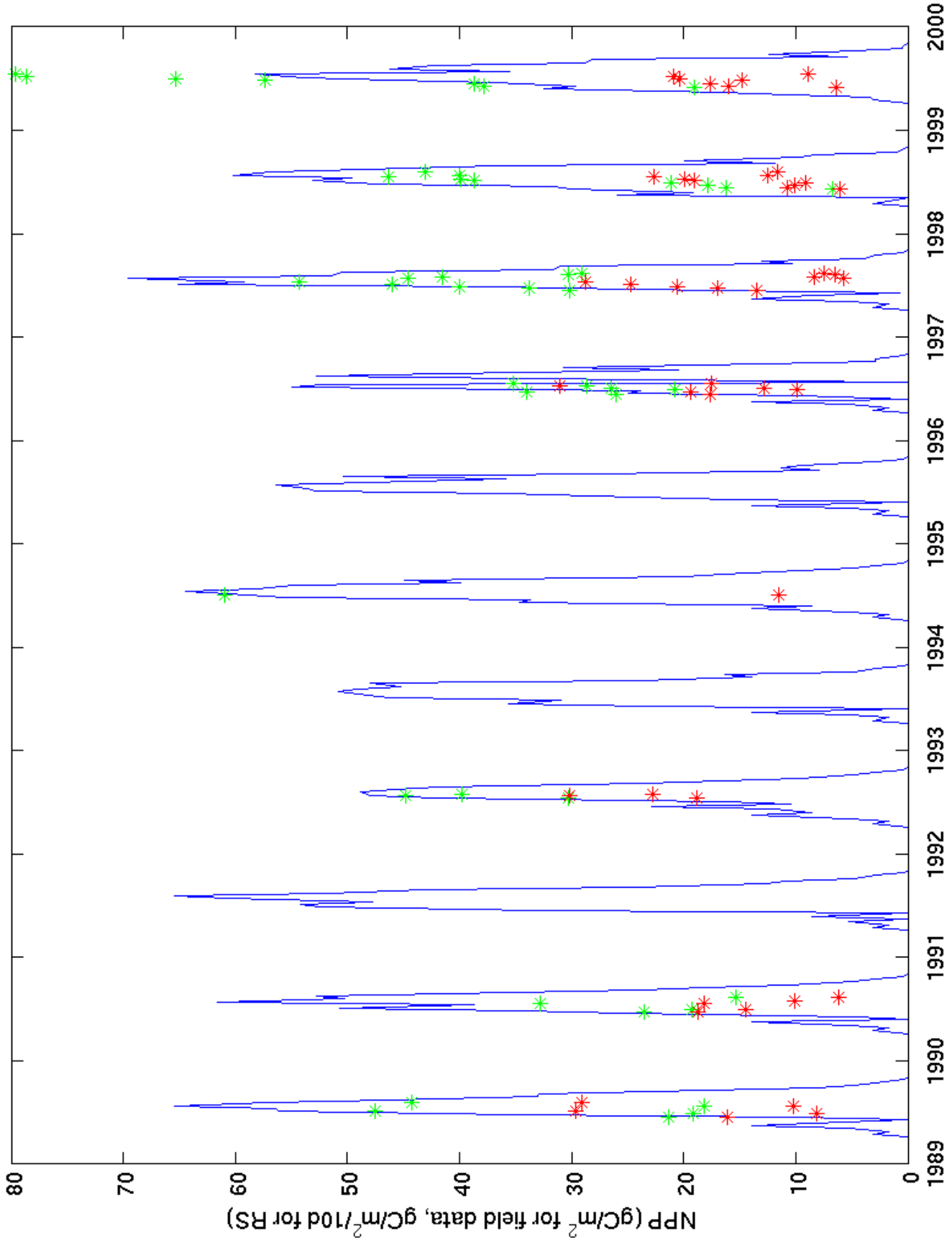

Figure 4.26: GloPEM (blue), Randy's Flat (red) and East Bay (green) NPP 1989–2000

4.4 Pan-Arctic changes in temperature bioclimatological indicators

The following section contains tables which compare the Sen's slope and Mann-Kendall test results for trend analysis in bioclimatological indicators and temperature over time [Table 4.8], followed by a similar analysis of trends in bioclimatological indicators relative to changes in mean annual growing season (May–September) temperatures [Table 4.4.2]. Figures indicating pixel-specific changes in each indicator are distributed across the previous sections.

4.4.1 Temporal trends

Pan-Arctic mean annual and growing season temperature increased significantly (1982–2004). Mean annual and annual growing season (May–September) temperature increased significantly 1982–2004 at all latitudes (except growing season temperature at 70-75^o N). However, these changes appear to have been focused in -60–180^o E for mean annual temperature, and -60–20^o E, 60–100^o E and 140–180^o E for mean summer temperature.

Changes in temperature are therefore focused in Europe and Russia, rather than Canada. Spring (March, April & May) temperatures did not increase significantly in any latitudinal band, but increased between -100– -60 and -20– 60 longitude. Summer (June, July & August) temperatures increased at longitudes -20–20, and latitudes 60–65, which corresponds to southern Scandinavia and the low latitudes of the Arctic. Overall, temperature increases were of a greater magnitude and significant over the greatest number of seasonal brackets in the low (60-65^{o}N) latitudes, which corresponds well with earlier findings in 4.2.2. of NPP increases being greatest at the low (60–65^o N) latitudes.

Total annual NPP increased across the pan-Arctic, and were largest at 60-70^o N, -20 – 20^o E (Scandinavia) and 100–140^o E (eastern Russia). NDVI and NPP were found to increase in different regions of the Arctic. Maximum annual NDVI increases at -100– -60^o E (eastern Nunavut) and 140–180^o E (eastern Russia). The discrepancy is interesting in light of the close theoretical and field correspondence between NPP and NDVI (*Raynolds et al.*, 2008). GloPEM NPP is furthermore calculated from AVHRR inputs that are very similar to NDVI, and NDVI and NPP are well correlated across the pan-Arctic [Figure 4.27]. Total annual NPP also shows a greater increase over time than maximum annual NDVI.

The ordinal date of spring onset increases at 80–85^o N, and the date of autumn onset similarly decreases at 75–85^o N (northern Canadian archipelago and northern Russia). Earlier spring and later autumn, indicative of a longer growing season, is inconsistent with what would be expected under warming conditions, and it is surprising that changes in spring and autumn onset are not significant at lower latitudinal bands, or across longitudinal bands.

In summary, significant pan-Arctic increases are observed in annual temperature, annual growing season temperature and total annual NPP. Increases in NPP and NDVI are observed for different regions of the Arctic. Diminishing growing season is observed at high latitudes (80–85^o N).

4.4.2 Trends according to temperature

The following subsection analyzes changes over time in bioclimatological indices with respect to changes in mean annual summer temperature over the same latitudinal or longitudinal bands [Table 4.4.2].

Across the pan-Arctic, increases in total annual NPP and maximum annual NDVI are significantly related to changes in mean annual summer temperature.

Increases in maximum annual NDVI are most closely related to rises in growing season temperature at the low (60–75^o N) latitudes as well as between -100– -60^o E (eastern Nunavut). Similarly, increases in total annual NPP are best explained by rises in growing season in low (60–75) latitudes, as well as between 60–100^o E (western Russia) and 140–180^o E (eastern Russia). It therefore appears that both maximum annual NDVI and total annual NPP are sensitive to changes in growing season temperature, and report changes at similar regions.

Shifts in spring and autumn onset are not significantly related to increasing growing season temperature across the pan-Arctic. However, later spring onset appears to be significantly related to rises in high Arctic (70–85^o N) growing season temperature, although the opposite would be expected. Similarly, earlier autumn onset is related to increasing growing season temperature at 70–75^o N, 60–100^o E and 140–180^o E.

Yet, because temperatures at the start and end of the growing season would be likely to have the greatest impact on spring and fall onset, it was believed that May temperatures would be positively related to spring onset, and September temperatures would be positively related to autumn onset. A comparison of these variables indicated no significant trends at any longitude or latitude [Table 4.4.2]. Further research therefore needs to be conducted into the dependence of temperature on Arctic phenology, and on the interpretation of these variables using remote sensing.

Latitude	60–65	65–70	70–75	75–80	80–85	Pan-Arctic
Mean annual temperature (^{o}C/year)	**0.0801**	**0.0454**	**0.0227**	**0.0193**	**0.0136**	**0.0158**
Mean summer temperature (^{o}C/year)	**0.0986**	**0.0539**	0.0217	**0.0242**	**0.0204**	**0.0175**
Mean March, April & May temperature (^{o}C/year)	**0.0564**	0.0196	-0.0005	0.0032	0.0025	0.0000
Mean June, July & August temperature (^{o}C/year)	**0.023**	0.0167	0.0059	0.005	0.0036	0.0044
Maximum annual NDVI (NDVI/year)	0.0001	0.0003	0.0001	0.0000	0.0000	0.0000
Ordinal date of spring onset (ordinal days/year)	-0.3203	-0.4061	-0.0528	0.0915	**0.0384**	0.0305
Ordinal date of fall onset (ordinal days/year)	0.0475	-0.0031	-0.0835	**-0.0877**	**-0.0122**	-0.0263
Total annual NPP (gC/m^2/year)	**2.2306**	**1.0159**	0.0444	0.0023	0.0089	**0.4361**

Longitude	-180– -140	-140– -100	-100– -60	-60– -20	-20–20	20–60	60–100	100–140	140–180
Mean annual temperature	0.014	0.0038	0.0097	**0.0122**	**0.0115**	**0.0152**	**0.0329**	**0.0232**	**0.1141**
Mean summer temperature	0.021	0.004	0.0281	**0.0146**	**0.0136**	0.0065	**0.0335**	0.0187	**0.1892**
Mean March, April & May temperature	0.0022	-0.0004	**0.0242**	0.0039	**0.0068**	**0.0068**	0.0037	0.0033	0.0612
Mean June, July & August temperature	0.0083	0.0034	0.0082	0.0048	**0.0038**	0.001	0.0075	0.0058	0.0417
Maximum annual NDVI	0.0000	0.0000	**0.0001**	0.0000	0.0000	0.0001	0.0002	0.0001	**0.0002**
Ordinal date of spring onset	0.0198	0.0514	0.2016	0.0514	0.0277	0.17	-0.1146	0.0593	0.0198
Ordinal date of spring onset	0.0071	0.0421	0.1054	0.0032	0.0059	0.059	-0.089	0.0602	0.0254
Ordinal date of fall onset	-0.039	-0.0347	0.0232	0.058	0.0224	0.0199	-0.1074	-0.1786	0.0001
Total annual NPP	0.3468	0.0293	0.2046	0.0576	**0.1519**	0.4056	0.5679	**1.1358**	1.5889

Table 4.8: Temporal trend in Sen's slope of temperature and bioclimatological variables (1982–2006). Results considered significant according to Mann-Kendall test (α <0.05) appear in bold.

Latitude	60–65	65–70	70–75	75–80	80–85	Pan-Arctic
Maximum annual NDVI (NDVI/^{o}C)	**0.002**	**0.0037**	**0.0031**	0.0004	0.0001	**0.0043**
Ordinal date of spring onset (day/^{o}C)	5.241	5.2671	**5.3803**	**3.0785**	**1.5161**	2.3024
Ordinal date of fall onset (day/^{o}C)	-0.1428	-0.5482	**-1.8777**	-1.2226	-0.1224	-1.4103
Total annual NPP (gC/m^2/^{o}C)	**13.7984**	**13.0771**	**7.2127**	**1.8672**	0.6404	**18.6423**

Longitude	-180– -140	-140– -100	-100– -60	-60– -20	-20–20	20–60	60–100	100–140	140–180
Maximum annual NDVI	0.0011	0.001	**0.0014**	0.0011	0.0021	0.001	0.0031	0.002	**0.0009**
Ordinal date of spring onset	-0.5114	1.4585	0.2628	-0.0385	0.6934	4.1654	-0.693	0.7317	0.0076
Ordinal date of fall onset	0.3951	-0.5457	-0.6253	1.6863	-1.308	-1.5844	**-2.0066**	0.5841	0.0009
Total annual NPP	5.7122	0.2553	3.3603	-0.4102	2.8098	-6.0987	**23.348**	21.3974	**9.0392**

Table 4.9: Sen's slope (with significant Mann-Kendall tests bolded) of pan-Arctic vegetation according to mean summer temperature over time (1982–2004)

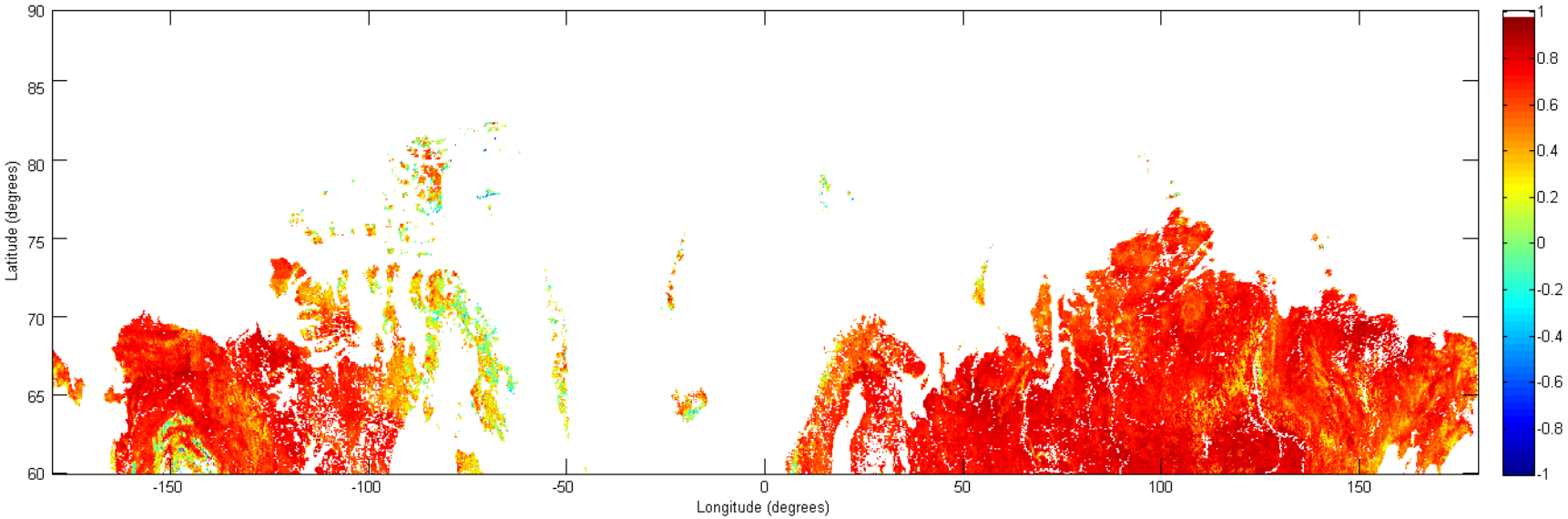

Figure 4.27: Pearson correlation (r) between summer GIMMS NDVI and GloPEM NPP (May, June, July, August and September, 1982-2000)

Longitude	-180– -140	-140– -100	-100– -60	-60– -20	-20–20	20–60	60–100	100–140	140–180
Spring (May)	0.0601	-0.5132	0.7415	-0.0040	0.4719	0.9049	1.9569	-0.3073	0.2775
Fall (Sept)	0.2958	-0.3786	-0.2790	0.2963	0.6064	-0.3111	-0.8076	0.0848	-0.0073

Table 4.10: Sen's slope of pan-Arctic spring and fall onset dates (1982–2004) according to mean May and September temperature respectively (ordinal days/^{o}C). No results are significant according to Mann-Kendall tests.

Chapter 5

Discussion

The following chapter discusses the main findings from this thesis in light of the major thesis aims relating to changes over time in bioclimatological indicators, warming induced changes in vegetation and a comparison of remote sensing, model and field data. However, the section begins with a discussion of limitations of the methodology applied in this study and how it may affect results.

5.1 Limitations

The primary limitation of using remote sensing and model outputs at an 8×8km resolution is that ecological observations at a finer resolution may be missed in their entirety. Results from this thesis indicate small but significant changes in ecology whereas field studies have indicated much more significant changes in species distribution, phenology and productivity, as described in Section 2.1. Poor fit between remote sensing NPP and field NPP further reinforce that coarse resolution remote sensing may not accurately assess Arctic ecosystem characteristics.

However, observed changes in NPP and NDVI have tended to be focused in regions of Alaska that coincide with the locations of field camps reporting significant

ecological changes (*Verbyla*, 2008; *Tape et al.*, 2006; *Jia et al.*, 2003). Further investigation will need to be conducted to determine whether the discrepancy between field studies and remote sensing is eliminated by very high resolution (<4×4m) imaging, or whether the discrepancy is in fact because of site selection in regions undergoing the greatest change.

Similarly, uncertainty regarding the sensitivity thresholds of the selected bioclimatological indicators, and how well these represent Arctic ecosystem change. Because these sensitivity thresholds are not well understood, it is possible that climatologically or ecologically significant trends do not appear as being statistically significant, or vice versa.

A data processing limitation has arisen regarding artefacts in several figures, as indicated by straight lines in Figures 3.8 and 4.2. The presence of these lines indicates a problem in processing that could not be resolved through different splicing of time series matrices, and it appears that the line in northern Russia seen in Figure 4.2 is present in the raw data provided by the Global Land Cover Facility. Questions regarding the reason for this line were not answered, and the artefact remains in the data set. The line appears to be consistent throughout the data set, which means that it would consistently underestimate NDVI in this region. It is therefore hoped that this artefact would thus not significantly affect analysis of change over time in NDVI and phenology.

Another limitation of this thesis methodology is the difficulty in downloading large batches of MODIS and Landsat data, which prevented pan-Arctic comparisons of data products. Also, cloud effects on MODIS and Landsat NDVI were dealt with through simple selection of <20% cloud cover images, whereas GIMMS is filtered for clouds using maximum two week NDVI. The difference between these data sets using the same type of filtering could therefore not be assessed. Snow and water also continue to act as confounders by creating low NDVI and NPP noise in pixels

that has not been filtered for. Most notably, this noise has led to a double peak in springtime NDVI which has led to false estimates of later spring onset, and has worsened the fit between snow melt end/onset and spring onset. Furthermore, field work would have provided greater insight into Arctic NPP but was not possible to conduct at this time.

A final significant limitation is that tests were conducted at nominal <0.05 level with no multiple testing corrections applied. Since there are 226 Mann-Kendall tests conducted, 11 of the positives detected may be false positives. 62 positive test results were found, which means that $\approx$18% of positives detected in this thesis may be false. This weakens confidence in all positive results, but could only be corrected through multiple testing corrections.

5.2 Bioclimatological indicators over time

Total annual NPP increased significantly across the Arctic, and was especially focused in low latitude regions that underwent the greatest increases in temperature. In terms of NDVI indicators, maximum annual NDVI showed the most significant change over time, followed by changes in timing of spring onset, autumn onset then peak NDVI.

The area (km^2) covered by each CAVM maximum annual NDVI classification over time showed very little change over time; however, small but significant circumpolar increases in maximum annual NDVI were observed throughout the Arctic. This observation is important in light of the close relationship between bioclimate subzones and NDVI classification described by *Walker et al.* (2005). It appears that recent increases in maximum annual NDVI are significant, but too small to be captured by *Walker et al.* (2005) classification bands ($\approx$ 0.05–0.1 NDVI). Overall, the finding of increases in NDVI is consistent with *Neigh et al.* (2007); *Jia et al.*

(2007).

The ordinal date of spring and autumn onset showed a great deal of variation from year to year. Spring onset occurred significantly earlier at Churchill; however, at the remaining study sites and the Arctic, very few significant changes occurred in spring and autumn phenology, and the observed significant changes were small ($\pm$3 days). Recent field findings of >30 day shifts in High Arctic ecology (*Høye et al.*, 2007) must therefore be considered in light of the lack of changes observed in remote sensing records.

It is possible that GIMMS NDVI is too coarse to pick up on regional ecological changes. Alternatively, because the response of various taxa and species to warming is highly divergent in the High Arctic (*Høye et al.*, 2007), it is possible that GIMMS NDVI is picking up strong signals from large and dominant species with phenological patterns that are less responsive to warming increases.

5.3 Response of vegetation to warming

Significant pan-Arctic increases in mean annual and mean growing season temperature were observed (1982–2004) (mean 1^{o}C/decade). Increases in pan-Arctic maximum annual NDVI and total annual NPP can be explained by these rises in mean growing season temperature. The spatial distribution of significant rises in mean annual temperature (focused in Alaska, Scandinavia, eastern Nunavut and eastern Russia) is also consistent with the pattern of rises in maximum annual NDVI and, to a lesser extent, total annual NPP. It is interesting that maximum annual NDVI shows significant increases in relation to temperature for the pan-Arctic, but that no relationship was found between these two variables for the three selected field sites. Both NPP and NDVI increase according to pan-Arctic warming, which is consistent with field level findings of a close correlation between NPP and NDVI

(*Laidler et al.*, 2008). However, the regions at which changes in NPP and NDVI increase, as well as the locations to which they increase significantly with growing season temperature, although they are closely correlated and GloPEM NPP uses AVHRR inputs similar to GIMMS NDVI. Further research is therefore required to elucidate the dependence of NPP and NDVI at the remote sensing scale.

Findings of warming-induced increases in productivity, as indicated by NDVI and NPP, are in line with predictions from field-scale experimental studies from ITEX (*Henry and Elmendorf*, 2008) as well as recent remote sensing studies (*Raynolds et al.*, 2008). The consequences of warming on greenhouse gas cycling therefore fall into uncertainty, and remain a central question in climate and biogeochemistry studies (*Heimann*, 2009). Uncertainty remains about the quantity of increased greenhouse gases being sequestered by the increased productivity of Arctic vegetation, especially in light of greenhouse gas emissions and sequestration by soils.

Another important finding was that delayed spring onset and earlier fall onset were related to increases in growing season temperature, although field studies have found opposite reactions to warming. Conversely, leaf phenology has been modeled by (*Delbart and Picard*, 2007) mainly as a positive function of air temperature. Comparisons of spring onset to May temperature, and autumn onset to September temperature indicated no relationship to growing season temperature. It is therefore likely that there must be confounding factors which are not properly identified which obscure the relationship between remote sensing NDVI estimates of phenology and remote sensing estimates of temperature.

5.4 Remote sensing, model and field data

Remote sensing and model outputs at >30×30m resolution do not relay significant changes in vegetation observed at the field scale at Churchill, Fosheim and Her-

schel. GIMMS and Landsat are correlated, although Landsat underestimates land vegetation by not filtering out low (NDVI<0.2) readings which are likely caused by cloud cover or surface water.

Comparisons of field and model NPP indicate that GloPEM underestimates peak annual NPP, even though GloPEM does not account for heavy grazing of the region by snow geese documented by *Jefferies* (2008). Furthermore, GloPEM is not correlated with Randy's Flat NPP and moderately correlated with East Bay NPP. Therefore, a clear need exists for better calibration and data collection of NPP models. GloPEM is heavily reliant on AVHRR inputs, and relies little on meteorological and field inputs, even though these appear to be important determinants of NPP.

Timing of snow melt end and onset from QuickScat data coincides very closely with GIMMS estimates of spring onset. Previous field studies have examined this linkage between snow melt-spring onset (*Buus-Hinkler et al.*, 2006; *Totland and Alatalo*, 2002), and the finding of a close fit in two remote sensing records lends credit to the validity of spring onset estimates. GIMMS NDVI, and MODIS EVI and NDVI, all share very similar timing of seasonal rises and falls, although EVI gives much lower readings than NDVI.

Chapter 6

Conclusions

The central finding from this thesis is small but significant pan-Arctic changes were observed in maximum annual NDVI and net primary productivity over time, and these changes can be explained as a function of increasing terrestrial circumpolar temperatures. The most significant findings from this thesis are that field and GloPEM NPP do not correspond closely, QuickScat and GIMMS estimates of snow melt and spring onset correspond well and that variations in autumn onset are significant at high (75-85^o N) latitudes, but shifts to earlier autumn onset cannot be explained by increases in temperature.

The major aim of this thesis was to provide insights into how bioclimatological indicators 1) vary over time; 2) are related to changes in temperature; 3) are represented in field, model and remote sensing records. This aim has been fulfilled through statistical investigations of pan-Arctic GIMMS NDVI, GloPEM NPP, Landsat TM, APP-x, MODIS EVI/NDVI and field NPP data sets, and analysis of the relationships between results and their context within recent literature. The research process has unfurled a number of new questions and potential directions for future studies, summarized in the section below.

6.1 Future work

Important research gaps remain regarding the relationship between MODIS and Landsat in the Arctic, the spectral response of various species of Arctic vegetation to warming, and which vegetation indices give the best estimates of Arctic plant health, biomass and field-scale productivity. One potential project could involve assessing the impact of site selection and scaling in recent field studies which have found dramatic changes in Arctic vegetation whereas this coarse resolution remote sensing study found few changes.

Estimating the current and future greenhouse gas balance of the Arctic under various warming scenarios is also a major research question (*Sitch et al.*, 2007), as is the assessment of feedbacks between soil, atmosphere and vegetation in the Arctic (*Heimann*, 2009). Insights into these feedbacks will require the use of NPP models which are well suited to the Arctic, and it appears that future work will be needed to calibrate GloPEM NPP, as well as to assess the reliability of various NPP models over heterogeneous Arctic ecosystems.

One potential idea would be to better understand the relationship between ground-based observations of phenology and productivity (from eddy flux flux towers and destructive sampling), and use this information to develop a model of Arctic vegetation growth which could be run under various IPCC scenarios. It will be very important in future for reliable estimates of productivity, phenology and NDVI to be gathered and analyzed if insights are to be gained about global greenhouse cycling and its response to climate change.

References

Baldocchi, D., et al. (2005), Predicting the onset of net carbon uptake by deciduous forests with soil temperature and climate data: a synthesis of FLUXNET data, *International Journal of Biometeorology*, *49*(6), 377–387. 16

Beerling, D. (2007), *The Emerald Planet: How Plants Changed Earth's History*, Oxford University Press, USA. 1, 21

Boelman, N., M. Stieglitz, H. Rueth, M. Sommerkorn, K. Griffin, G. Shaver, and J. Gamon (2003), Response of NDVI, biomass, and ecosystem gas exchange to long-term warming and fertilization in wet sedge tundra, *Oecologia*, *135*(3), 414–421. 19, 21, 27

Bunn, A., and S. Goetz (2006), Trends in satellite-observed circumpolar photosynthetic activity from 1982 to 2003: the influence of seasonality, cover type, and vegetation density, *Earth Interactions*, *10*(12), 1–19. 6, 10, 11

Buus-Hinkler, J., B. Hansen, M. Tamstorf, and S. Pedersen (2006), Snow-vegetation relations in a High Arctic ecosystem: Inter-annual variability inferred from new monitoring and modeling concepts, *Remote Sensing of Environment*, *105*(3), 237–247. 86

Cao, M., S. Prince, J. Small, and S. Goetz (2004), Remotely Sensed Interannual Variations and Trends in Terrestrial Net Primary Productivity 1981–2000, *Ecosystems*, *7*(3), 233–242. 19

Chapin III, F., G. Shaver, A. Giblin, K. Nadelhoffer, and J. Laundre (1995), Responses of Arctic Tundra to Experimental and Observed Changes in Climate, *Ecology*, *76*(3), 694–711. 13, 19

Christensen, J., et al. (2007), Regional Climate Projections, *Climate Change*, pp. 847–940. 1, 8, 24

Christensen, T., T. Johansson, H. Akerman, M. Mastepanov, N. Malmer, T. Friborg, P. Crill, and B. Svensson (2004), Thawing sub-arctic permafrost: Effects on vegetation and methane emissions, *Geophysical Research Letters*, *31*(4). 15

Cramer, W., and C. Field (1999), Comparing global models of terrestrial net primary productivity (NPP): introduction, *Global Change Biology*, *5*(Suppl. 1), iii–iv. 5

Delbart, N., and G. Picard (2007), Modeling the date of leaf appearance in low-arctic tundra, *Global Change Biology*, *13*, 2551–2562, doi:doi:10.1111/j.1365-2486.2007.01466.x. 5, 85

Duguay, C., T. Prowse, B. Bonsal, R. Brown, M. Lacroix, and P. Menard (2006), Recent trends in Canadian lake ice cover, *Hydrological Processes*, *20*(4), 781–801. 43

Eamer, J. (2009), *Global Outlook for Ice & Snow*, United Nations Environment Programme. xi, 2

Ebata, M., and R. Tateishi (2001), Phenological stage monitoring in Siberia by using NOAA/AVHRR data, in *Paper presented at the 22nd Asian Conference on Remote Sensing*, vol. 5, p. 9. 5

Fahey, T. J., and A. K. Knapp (2007), *Principles and Standards for Measuring Primary Production*, chap. Primary production: Guiding principles and standards for measurement, pp. 3–11, Oxford University Press. 18, 27, 28

Freedman, B. (2007), *Environmental Science: A Canadian Perspective*, Pearson Prentice Hall. 15

Global Land Cover Facility (), Landsat technical guide, Website, retrieved March 20, 2009. 27

Goetz, S. J., S. D. Prince, S. N. Goward, M. M. Thawley, and J. Small (1999), Satellite remote sensing of primary production: an improved production efficiency modeling approach, *Ecological Modelling*, *122*, 239–255, doi:10.1016/S0304-3800(99)00140-4. 20, 30

Gower, S. T., C. J. Kucharik, and J. M. Norman (1999), Direct and indirect estimation of Leaf Area Index, fAPAR, and Net Primary Production of terrestrial ecosystems, *Remote Sensing of Environment*, *70*, 29–51. 18, 29

Grace, J., F. Berninger, and L. Nagy (2002), Impacts of Climate Change on the Tree Line., *Annals of Botany*, *90*(4), 537. 1

Grogan, P. (2008), Birch shrubs in the Canadian low Arctic may respond relatively quickly to climate warming, in *Arctic Change*. 19, 20

Haboudane, D., J. Miller, E. Pattey, P. Zarco-Tejada, and I. Strachan (2004), Hyperspectral vegetation indices and novel algorithms for predicting green LAI of crop canopies: Modeling and validation in the context of precision agriculture, *Remote Sensing of Environment*, *90*(3), 337–352. 19

Hansen, M., R. DeFries, J. Townsend, R. Scholberg, C. Dimiceli, and M. Carroll (2002), Towards an operational MODIS continuous field of percent tree cover algorithm: examples using AVHRR and MODIS data, *Remote Sensing of Environment*, *83*(1-2), 303–319. 29

Heimann, M. (2009), On the use of atmospheric co2 observations to detect and quantify climate driven terrestrial carbon cycle feedbacks in the Earth system, in *MOCA 2009*. 85, 88

Henry, G., and S. Elmendorf (2008), Trends in tundra vegetation over the past 20 years: Analysis of long-term data sets from the International Tundra Experiment (ITEX), in *Arctic Change*. 3, 20, 85

Hobbie, S., J. Schimel, S. Trumbore, and J. Randerson (2000), Controls over carbon storage and turnover in high-latitude soils, *Global Change Biology*, *6*(S1), 196–210. 6

Hope, A. (1999), Response of the normalized difference vegetation index to varying cloud conditions in Arctic tundra environments, *International Journal of Remote Sensing*, *20*(1), 207–212. 23, 31

Høye, T., E. Post, H. Meltofte, N. Schmidt, and M. Forchhammer (2007), Rapid advancement of spring in the High Arctic, *Current Biology*, *17*(12), 449–451. 1, 9, 16, 24, 84

Huete, A., K. Didan, T. Miura, E. Rodriguez, X. Gao, and L. Ferreira (2002), Overview of the radiometric and biophysical performance of the MODIS vegetation indices, *Remote Sensing of Environment*, *83*, 195–213. 29

Jefferies, R. (1977), The vegetation of salt marshes at some coastal sites in arctic North America, *The Journal of Ecology*, pp. 661–672. 33

Jefferies, R., A. Jensen, and K. Abraham (1979), Vegetational development and the effect of geese on vegetation at La Perouse Bay, Manitoba, *Canadian Journal of Botany*, *57*(13), 1439–1450. 32

Jefferies, R. L. (2008), Personal e-mail communication. 32, 42, 72, 86

Jensen, J. R. (2005), *Introductory Digital Image Processing: a Remote Sensing Perspective*, 3rd ed., Pearson Prentice Hall Series in Geographic Information Science. 28

Jensen, J. R. (2007), *Remote Sensing of the Environment: An Earth Resource Perspective*, second ed., Pearson Prentice Hall. 23

Jia, G., H. Epstein, and D. Walker (2003), Greening of arctic Alaska, 1981–2001, *Geophysical Research Letters*, *30*(30), 2067. 39, 82

Jia, G., H. Epstein, and D. Walker (2007), Trends of Vegetation Greenness in the Arctic from 1982-2005, in *American Geophysical Union, Fall Meeting 2007, abstract# B21A-0041*. 4, 11, 12, 83

Juutinen, S., J. Bubier, P. Shrestha, R. Smith, and T. Moore (2008), Responses of bog vegetation and CO2 exchange to experimental N and PK addition, in *American Geophysical Union Fall Meeting*. 19

Karlsen, S., A. Elvebakk, K. Hogda, and B. Johansen (2006), Satellite-based mapping of the growing season and bioclimatic zones in Fennoscandia, *Global Ecology and Biogeography*, *15*(4), 416–430. 5

Laidler, G. J., P. M. Treitz, and D. M. Atkinson (2008), Remote sensing of Arctic vegetation: Relations between the NDVI, Spatial Resolution and Vegetation Cover on Boothia Peninsula, Nunavut, *Arctic*, *61*(1), 1–13. 5, 10, 12, 23, 85

Levesque, E., A. Cuerrier, S. Boudreau, J. Gerin-Lajoie, B. Tremblay, C. Lavallee, and C. Spiech (2008), Towards and understanding of the implications of shrub cover change in Nunavik, in *Arctic Change*. 3, 9

Liu, J., J. Chen, J. Cihlar, and W. Chen (2002), Net primary productivity mapped for Canada at 1-km resolution, *Global Ecology and Biogeography*, *11*(2), 115–129. 3

Loyarte, M., M. Menenti, and A. Diblasi (2008), Modelling bioclimate by means of Fourier analysis of NOAA-AVHRR NDVI time series in Western Argentina, *International Journal of Climatology*, *28*(9), 1175–1188. 17

Luus, K., and R. Kelly (2008), Assessing productivity of vegetation in the Amazon using remote sensing and modelling, *Progress in Physical Geography*, *32*(4), 363–377. 8, 29

Mack, M., E. Schuur, M. Bret-Harte, G. Shaver, and F. Chapin III (2004), Ecosystem carbon storage in arctic tundra reduced by long-term nutrient fertilization, *Nature*, *431*(7007), 440–443. 20

Mahadevan, P., et al. (2008), A satellite-based biosphere parameterization for net ecosystem CO 2 exchange: Vegetation Photosynthesis and Respiration Model (VPRM), *Global Biogeochem. Cyc*, *22*. 29

Mahey, B. F. (2008), *Statistics for environmental science and management*, second ed., CRC Press. 43

Maisongrande, P., A. Ruimy, G. Dedieu, and B. Saugier (1995), Monitoring seasonal and interannual variations of gross primary productivity and net ecosystem productivity using a diagnostic model and remotely-sensed data, *Tellus 47B*, pp. 178–190. 18

Menzel, A., et al. (2006), European phenological response to climate change matches the warming pattern, *Global Change Biology*, *12*(10), 1969–1976. 15

Migliavacca, M., M. Reichstein, R. Colombo, A. Richardson, G. Lasslop, and E. Tomelleri (2008), Semi-empirical modeling of biotic and abiotic factors controlling ecosystem respiration across eddy-covariance sites, in *American Geophysical Union Fall Meeting*. 6

Moritz, R., C. Bitz, and E. Steig (2002), Dynamics of Recent Climate Change in the Arctic, *Science*, *297*(5586), 1497–1502. xi, 32, 34

Myers-Smith, I. H., and D. S. Hik (2008), How do natural and artificial tall shrub canopies alter tundra soil temperatures?, in *Arctic Change*. 13

Myneni, R., S. Los, and G. Asrar (1995), Potential gross primary productivity of terrestrial vegetation from 1982-1990, *Geophysical Research Letters*, *22*, 2617–2617. 18

Nadelhoffer, K. J., G. R. Shaver, A. Giblin, and E. B. Ratstetter (1997), Potential impacts of climate change on nutrient cycling, decomposition, and productivity in the Arctic ecosystem, in *Global Change and Arctic terrestrial ecosystems*, edited by W. C. Oechel, T. Callaghan, T. Gilmanov, J. I. Holten, B. Maxwell, U. Molau, and B. Sveinbjornsson, no. 124 in Ecological Studies, pp. 349–364, Springer. 10, 13, 14, 20

NASA (2009), About MODIS, retrieved March 13, 2009. 14

Neigh, C. S., C. J. Tucker, and J. R. Townshend (2007), North American vegetation dynamics observed with multi-resolution satellite data, *Remote Sensing of Environment*, *112*(4), 1749–1772. xi, 1, 4, 10, 34, 83

Norby, R., J. Warren, C. Iversen, B. Medlyn, R. McMurtrie, and F. Hoffman (2008), Nitrogen limitation is reducing the enhancement of npp by elevated co2 in a deciduous forest, in *American Geophysical Union Fall Meeting*. 14, 19

Oechel, W., S. Hastings, G. Vourlitis, M. Jenkins, G. Riechers, and N. Grulke (1993), Recent change of Arctic tundra ecosystems from a net carbon dioxide sink to a source, *Nature*, *361*(6412), 520–523. 1

Oechel, W. C., and G. L. Vourlitis (1997), Climate change in Northern latitudes: alterations in ecosystem structure and function and effects on carbon sequestration, in *Global Change and Arctic terrestrial ecosystems*, edited by W. C. Oechel, T. Callaghan, T. Gilmanov, J. I. Holten, B. Maxwell, U. Molau, and B. Sveinbjornsson, no. 124 in Ecological Studies, pp. 381–401, Springer. 20, 21

Oelbermann, M., M. English, and S. Schiff (2008), Evaluating carbon dynamics and microbial activity in arctic soils under warmer temperatures, *Canadian Journal Of Soil Science*, *88*(1), 31. 20

Ollinger, S., A. Richardson, M. Martin, D. Hollinger, S. Frolking, L. Plourde, and P. Reich (2008a), Exploring carbon-nitrogen-albedo linkages in temperate and boreal forests., in *American Geophysical Union Fall Meeting*. 14

Ollinger, S., et al. (2008b), Canopy nitrogen, carbon assimilation, and albedo in temperate and boreal forests: Functional relations and potential climate feedbacks, *Proceedings of the National Academy of Sciences*, *105*(49), 19,336. 14

Olthof, I., R. Latifovic, and D. Pouliot (2008), Approaches to monitoring nothern vegetation change with satellite remote sensing, in *Arctic Change*. 5, 20, 40

Pan, Y., R. Birdsey, J. Hom, K. McCullough, and K. Clark (2006), Improved estimates of net primary productivity from modis satellite data at regional and local scales, *Ecological Applications*, *16*(1), 125–132. 30

Pettorelli, N., J. Vik, A. Mysterud, J. Gaillard, C. Tucker, and N. Stenseth (2005), Using the satellite-derived NDVI to assess ecological responses to environmental change, *Trends in Ecology & Evolution*, *20*(9), 503–510. 10, 48

Picard, G., S. Quegan, N. Delbart, M. Lomas, T. Toan, and F. Woodward (2005), Bud-burst modelling in Siberia and its impact on quantifying the carbon budget, *Global Change Biology*, *11*(12), 2164–2176. 5

Raynolds, M., D. Walker, and H. Maier (2006), NDVI patterns and phytomass distribution in the circumpolar Arctic, *Remote Sensing of Environment*, *102*(3-4), 271–281. 12, 27, 39

Raynolds, M., J. Comiso, D. Walker, and D. Verbyla (2008), Relationship between satellite-derived land surface temperatures, arctic vegetation types, and NDVI, *Remote Sensing of Environment*, *112*(4), 1884–1894. 3, 4, 10, 75, 85

Reed, B. (2006), Trend analysis of time-series phenology of North America derived from satellite data, *GIScience & Remote Sensing*, *43*(1), 24–38. 6, 27

Roerink, G., M. Menenti, W. Soepboer, and Z. Su (2003), Assessment of climate impact on vegetation dynamics by using remote sensing, *Physics and Chemistry of the Earth*, *28*(1-3), 103–109. 2, 5, 15

Schuur, E., J. Vogel, K. Crummer, H. Lee, J. Sickman, and T. Osterkamp (2008), Permafrost thaw stimulates old carbon release and alters net carbon exchange from tundra, in *American Geophysical Union Fall Meeting*. 15, 20

Sims, D., et al. (2006), On the use of MODIS EVI to assess gross primary productivity of North American ecosystems, *Journal of Geophysical Research*, *111*(G4), 4015. 29

Sitch, S., et al. (2007), Assessing the carbon balance of circumpolar Arctic tundra using remote sensing and process modeling, *Ecological Applications*, *17*(1), 213–234. 1, 12, 14, 20, 21, 23, 24, 88

Snyder, P. (2008), The hydrologic cycle response to rapid arctic vegetation change, in *American Geophysical Union Fall Meeting*. 3

Soil Classification Working Group (1998), *The Canadian System of Soil Classification*, 3rd ed., Agriculture and Agri-Food Canada. 32

Stieglitz, M., A. Giblin, J. Hobbie, M. Williams, and G. Kling (2000), Simulating the effects of climate change and climate variability on carbon dynamics in Arctic tundra, *Global Biogeochemical Cycles*, *14*(4), 1123–1136. 21

Stone, R., E. Dutton, J. Harris, and D. Longenecker (2002), Earlier spring snowmelt in northern Alaska as an indicator of climate change, *J. Geophys. Res*, *107*(4089), 10–1029. 1, 24

Stow, D., S. Daeschner, A. Hope, D. Douglas, and R. Myneni (2001), Spatial-temporal trend of seasonally-integrated normalized difference vegetation index as an indicator of changes in Arctic tundra vegetation in the early 1990s, *IEEE Geoscience and Remote Sensing Symposium*. 27

Stow, D., et al. (2004), Remote sensing of vegetation and land-cover change in Arctic Tundra Ecosystems, *Remote Sensing of Environment*, *89*(3), 281–308. 9, 13, 16, 19, 22, 23, 24

Sturm, M., J. Schimel, G. Michaelson, J. Welker, S. Oberbauer, G. Liston, J. Fahnestock, and V. Romanovsky (2005), Winter biological processes could help convert Arctic tundra to shrubland, *BioScience*, *55*(1), 17–26. 1

Tape, K., M. Sturm, and C. Racine (2006), The evidence for shrub expansion in Northern Alaska and the Pan-Arctic, *Global Change Biology*, *12*(4), 686–702. 3, 13, 82

Thompson, C., A. McGuire, J. Clein, F. Chapin, and J. Beringer (2006), Net Carbon Exchange Across the Arctic Tundra-Boreal Forest Transition in Alaska 1981–2000, *Mitigation and Adaptation Strategies for Global Change*, *11*(4), 805–827. 1, 12, 13, 14, 19, 21

Thornton, P. (2008), Disturbance history and nitrogen cycle controls on ecosystem response to increased CO2 and climate change, in *American Geophysical Union Fall Meeting*. 14

Thornton, P. (2009), Ecosystem modeling: Biome-bgc, retrieved 12 January 2009. 3

Totland, Ø., and J. Alatalo (2002), Effects of temperature and date of snowmelt on growth, reproduction, and flowering phenology in the arctic/alpine herb, Ranunculus glacialis, *Oecologia*, *133*(2), 168–175. 16, 86

Trishchenko, A., J. Cihlar, and Z. Li (2002), Effects of spectral response function on surface reflectance and NDVI measured with moderate resolution satellite sensors, *Remote Sensing of Environment*, *81*(1), 1–18. xi, 11

Tucker, C. (1979), Remote-sensing of lead water content in near-infrared, *Remote Sensing of Environment*, *10*, 23–32. 10, 26

Verbyla, D. (2008), The greening and browning of Alaska based on 1982-2003 satellite data, *Global Ecology and Biogeography*, *17*(4), 547–555. 16, 17, 23, 82

Vierling, L., D. Deering, and T. Eck (1997), Differences in Arctic Tundra Vegetation Type and Phenology as Seen Using Bidirectional Radiometry in the Early Growing Season, *Remote Sensing of Environment*, *60*(1), 71–82. 6

Vitt, D. H. (2007), *Principles and Standards for Measuring Primary Production*, chap. Estimating moss and lichen ground layer net primary production in tundra, peatlands, and forests, pp. 82–105, Oxford University Press. 9, 10, 18, 28

Walker, D., et al. (2005), The Circumpolar Arctic vegetation map, *Journal of Vegetation Science*, *16*(3), 267–282. xi, 3, 35, 51, 83

Wang, L., C. Derksen, and R. Brown (2008), Detection of pan-Arctic terrestrial snowmelt from QuikSCAT, 2000–2005, *Remote Sensing of Environment*, *112*(10), 3794–3805. xii, 58, 61, 62, 63

Wang, M., and J. Overland (2004), Detecting Arctic Climate Change Using KÖppen Climate Classification, *Climatic Change*, *67*(1), 43–62. 13

Wang, X., and J. Key (2003), Recent trends in Arctic surface, cloud, and radiation properties from space, *Science*, *299*(5613), 1725–1728. 26, 45

White, M., et al. (2008), Intercomparison, interpretation, and assessment of spring phenology in north america estimated from remote sensing for 1982 to 2006, in *American Geophysical Union Fall Meeting*. 6, 16, 17

White, M. A., P. E. Thornton, S. W. Running, and R. R. Nemani (2000), Parametrization and sensitivity analysis of the BIOME-BGC terrestrial ecosystem model: net primary production controls, *Earth Interactions*, *4*(3), 1–85. 3

Williams, M., and E. Ratsetter (1999), Vegetation characteristics and primary productivity along an arctic transect: implications for scaling-up, *Journal of Ecology*, *87*(885), 885–898. 13

Williams, M., R. Bell, L. Spadavecchia, L. Street, and M. van Wijk (2008), Upscaling leaf area index in an Arctic landscape through multi-scale observations, *Global Change Biology*. 19, 27

Wu, W., and A. Lynch (2000), Response of the seasonal carbon cycle in high latitudes to climate anomalies, *Journal of Geophysical Research*, *105*(D18), 22,897–22,908. 1, 21

Xiao, X., D. Hollinger, J. Aber, M. Goltz, E. A. Davidson, Q. Zhang, and B. Moore III (2004), Satellite-based modeling of gross primary production in an evergreen needleleaf forest, *Remote Sensing of Environment*, *89*(29), doi:10.1016/j.rse.2003.11.008. 29

Yoccoz, N. (2008), Personal communication at Arctic Change conference poster session. 27, 40

Young, D. R. (2007), *Principles and Standards for Measuring Primary Production*, chap. Estimating aboveground net primary production in shrub-dominated ecosystems, pp. 49–62, Oxford University Press. 18, 28

Young, K., M. Woo, and S. Edlund (1997), Influence of local topography, soils, and vegetation on microclimate and hydrology at a high Arctic site, Ellesmere Island, Canada, *Arctic and Alpine Research*, pp. 270–284. 33

Zhang, K., J. S. Kimball, K. C. McDonald, J. J. Cassano, and S. W. Running (2007), Impacts of large-scale oscillations on pan-Arctic terrestrial net primary production, *Geophysical Research Letters*, *34*, L21,403, doi:10.1029/2007GL031605,. 3

Zhang, X., M. Friedl, C. Schaaf, A. Strahler, J. Hodges, F. Gao, B. Reed, and A. Huete (2003), Monitoring vegetation phenology using MODIS, *Remote Sensing of Environment*, *84*(3), 471–475. 16

Appendices

Appendix A

Appendix- Publications and presentations completed during MSc

A.1 Refereed

- Luus, K.A. and R.E.J. Kelly. "Estimating transitions in pan-Arctic (N of 60N) bioclimate subzones and NDVI-derived biomass using Landsat and GIMMS (1982-2000)", MOCA Joint Assembly (19-29 July 2009). Oral presentation.
- Luus, K.A. and R.E.J. Kelly. "Response of pan-Arctic vegetation to recent climate change (1982–2007)", UW Graduate Student Research Conference (27-30 April 2009). Oral presentation.
- Luus, K.A. and R.E.J. Kelly. "Productivity of Canadian Arctic vegetation (1981-2000): Comparison of GIMMS NDVI and GloPEM NPP", American Geophysical Union (15-19 December 2008). Poster presentation.
- Luus, K.A. and R.E.J. Kelly. (2008) Estimating the biophysical impacts of land use change in the Amazon: A review of remote sensing and modeling approaches. Progress in Physical Geography, 32(4), 363–377.
- Luus, K.A. and L.J. Plug. "Modeling the emergent impacts of harvesting Acadian forests over 100+ years", Canadian Geophysical Union-Hydrological Section (7 - 8 December 2007). Oral presentation.

A.2 Non-Refereed

- Luus, K.A. and R.E.J. Kelly. "How is pan-Arctic vegetation affected by recent (1982-) climate change?", UW Graduate Student Seminar Series (19 March 2008). Oral presentation.

- Luus, K.A. and R.E.J. Kelly. "Response of pan-Arctic vegetation to recent (1982-2007) climate change", Interdisciplinary Centre on Climate Change Student Colloquium (4-5 March 2009). Oral Presentation.

- Luus, K.A. and R.E.J. Kelly. "Productivity of Canadian Arctic vegetation (1981-2000)", Arctic Change (7-9 December 2008). Poster presentation.

- Luus, K.A., A.R. Cabrera, P.J. Deadman, S. Hetrick, N. Vogt and E.S. Brondizio. "Biophysical parametrization of an Amazonian agent-based model using GIS and remotely sensed data", GIS Day (19 November 2008). Poster presentation.

- Luus, K.A., A.R. Cabrera, P.J. Deadman, S. Hetrick, N. Vogt and E.S. Brondizio. "Biophysical parametrization of an Amazonian agent-based model using GIS and remotely sensed data", Waterloo Unlimited graduate student poster presentations (14 November 2008). Poster presentation.

- Luus, K.A. and P.J. Deadman."Representing biophysical impacts of land use change in the Amazon using agent-based modeling", Ontario Division of the Canadian Association of Geographers Annual Meeting (October 17-19, 2008) . Oral presentation.

- Luus, K.A. and L.J. Plug. "Modeling the emergent impacts of harvesting Acadian forests over 100+ years", Canadian Association of Geographers of Ontario Annual Meeting (October 19-20, 2007). Oral presentation.

Appendix B

Appendix- Acronyms

Acronym	Definition
APP-x	Advanced Very High Resolution Radiometer Polar Pathfinder- Extended
AVHRR	Advanced Very High Resolution Radiometer
C	Carbon
CO_2	Carbon dioxide
EVI	Enhanced Vegetation Index
GEP	Gross Ecosystem Production
GIMMS	Global Inventory Modeling and Mapping Studies
GLCF	Global Land Cover Facility
GloPEM	Global Productivity Efficiency Model
GPP	Gross Primary Productivity
Landsat ETM	Landsat Enhanced Thematic Mapper
MODIS	Moderate Resolution Imaging Spectroradiometer
N	Nitrogen
NASA	National Aeronautics and Space Administration
NEP	Net Ecosystem Production
NDVI	Normalized Difference Vegetation Index
NPP	Net Primary Productivity
P	Phosphorous
QuickSCAT	Quick Scatterometer
USGS	United States Geological Survey

Table B.1: Acronym definitions

Appendix C

Appendix- Additional diagrams

For pan-Arctic time series videos of maximum annual NDVI, total annual NPP, and ordinal dates of spring and fall onset, please visit `http://www.fes.uwaterloo.ca/u/kaluus`. The following pages contain other additional thesis figures.

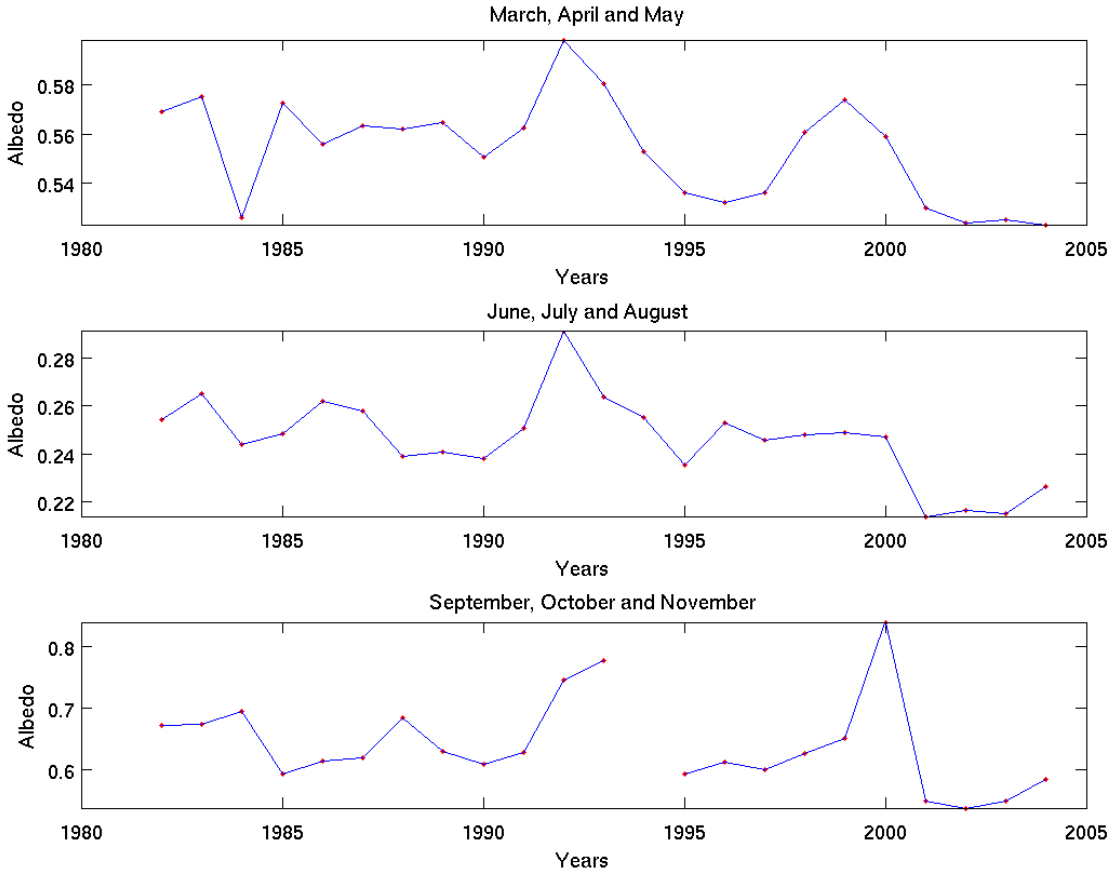

Figure C.1: Mean pan-Arctic albedo 1982–2000, as divided per season (spring- top, summer- middle, and fall- bottom)

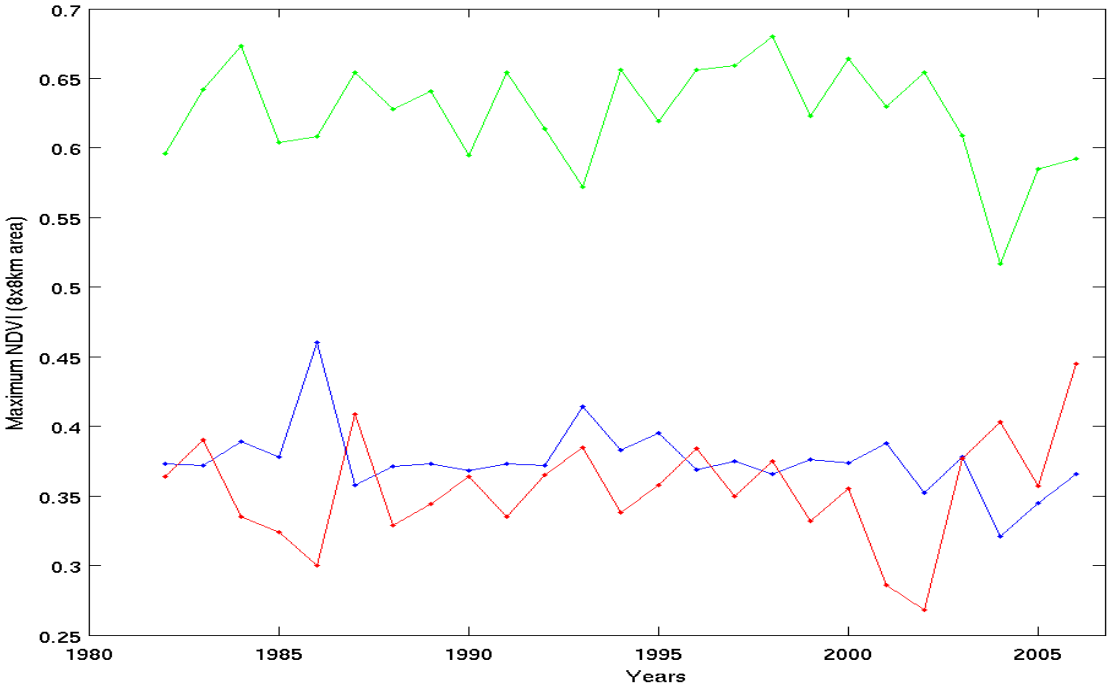

Figure C.2: Maximum annual NDVI at Fosheim (blue), Churchill (green) and Herschel (red)

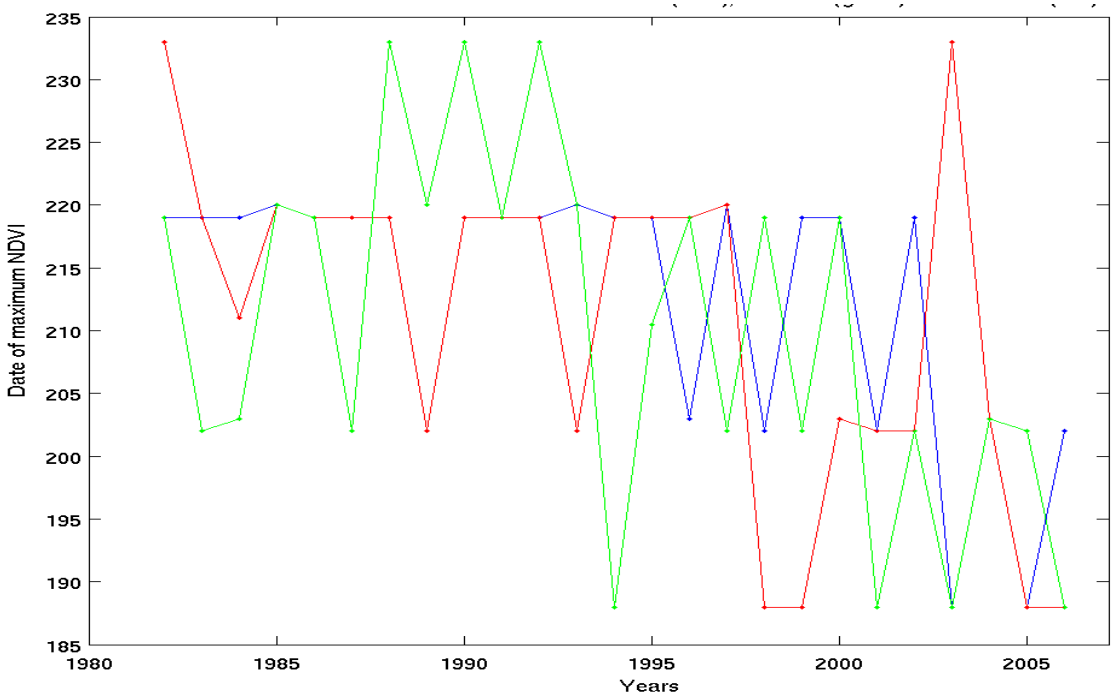

Figure C.3: Date of annual maximum NDVI at Fosheim (blue), Churchill (green) and Herschel (red)

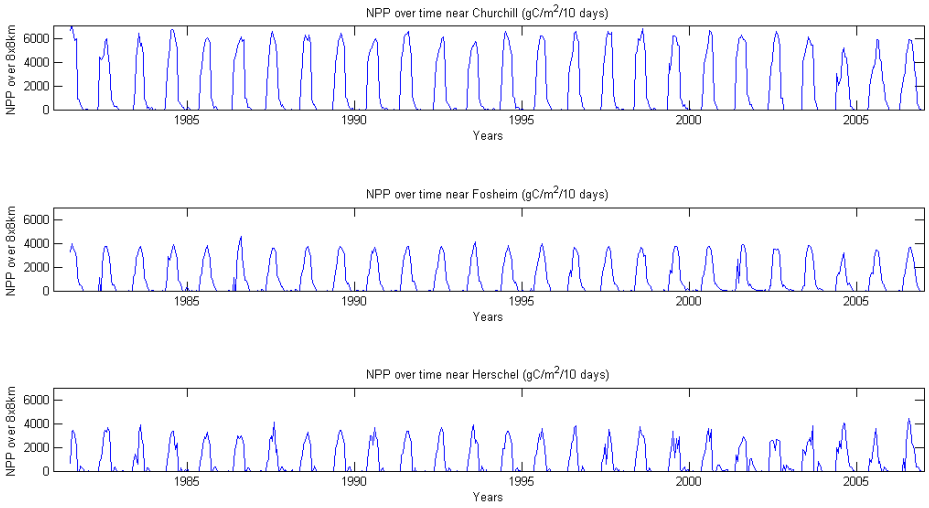

Figure C.4: GloPEM NPP 1982-2000

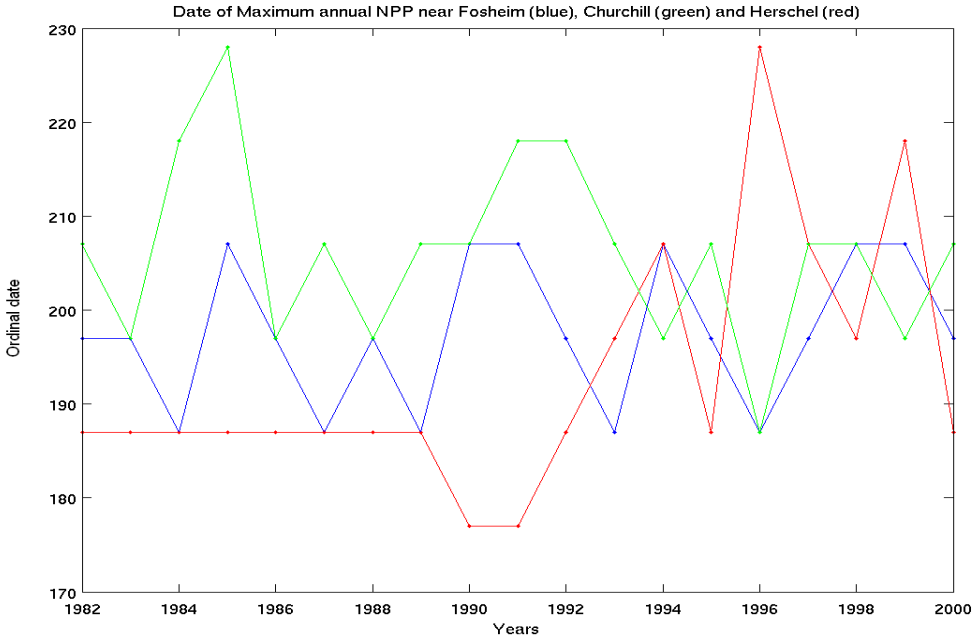

Figure C.5: Date of maximum annual NPP

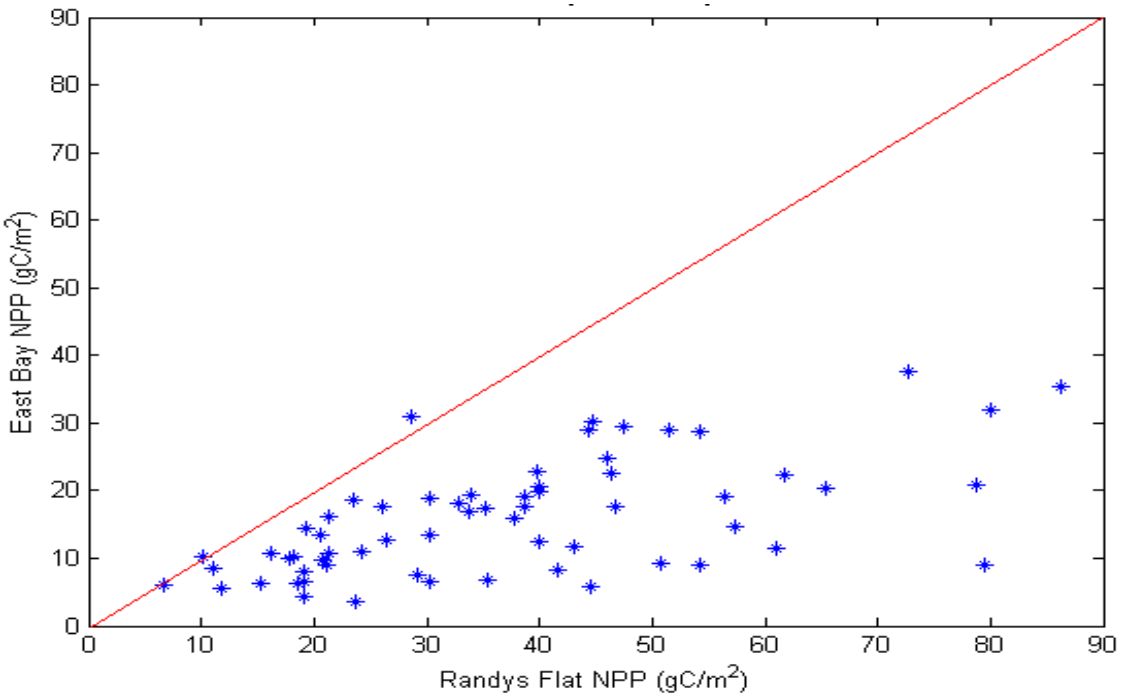

Figure C.6: Correlation between Randy's Flat and East Bay NPP

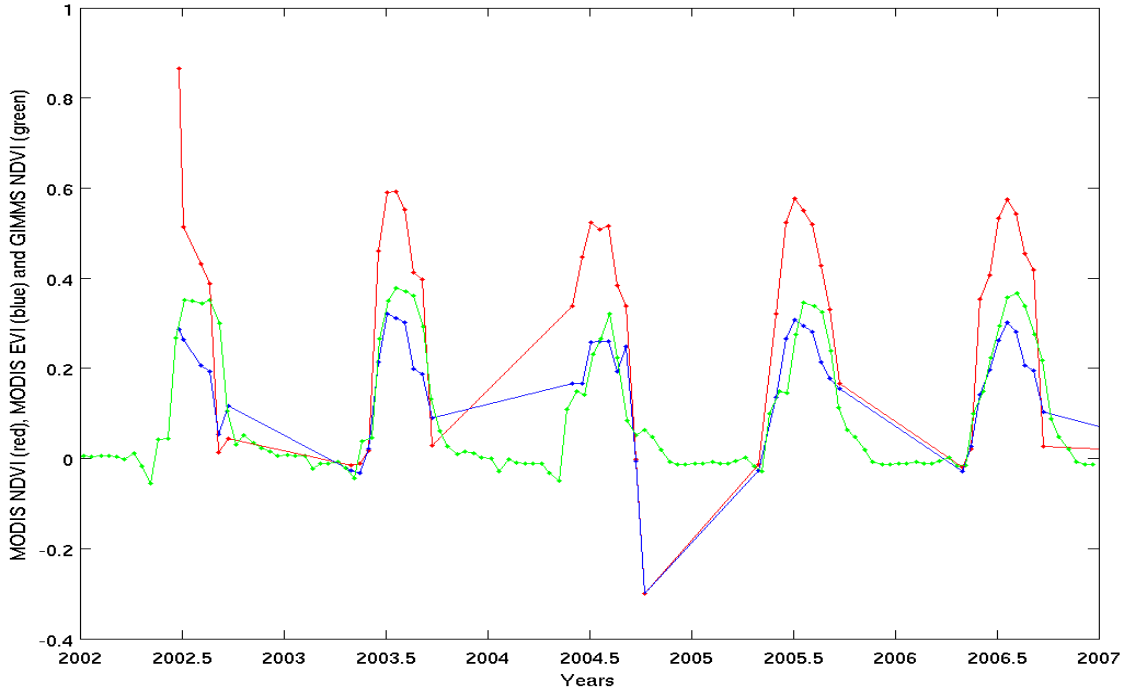

Figure C.7: Comparison of maximum MODIS NDVI (red) & EVI (blue) with GIMMS NDVI (green) near Fosheim (8×8km)